This is to certify that the
dissertation entitled

STRATEGIES FOR IMPROVING SYNTHESIS OF
QUINIC ACID AND SHIKIMIC ACID FROM D-GLUCOSE

presented by

JUSTAS JANCAUSKAS

has been accepted towards fulfillment
of the requirements for the

| Ph.D. | degree in | Chemistry |

_____
Major Professor's Signature

March 24, 2008
_____
Date

STRATEGIES FOR IMPROVING SYNTHESIS OF QUINIC ACID
AND SHIKIMIC ACID FROM D-GLUCOSE

By

Justas Jancauskas

A DISSERTATION

Submitted to
Michigan State University
in partial fulfillment of the requirements
for the degree of

DOCTOR OF PHILOSOPHY

Department of Chemistry

2008

ABSTRACT

STRATEGIES FOR IMPROVING SYNTHESIS OF QUINIC ACID AND SHIKIMIC ACID FROM D-GLUCOSE

By

Justas Jancauskas

Optimization of microbial synthesis of quinic acid by recombinant *E. coli* strains was performed. Overexpression of *E. coli* shikimate/quinate dehydrogenase YdiB resulted in lower quinic acid titer and yield under fed-batch conditions than when AroE was overexpressed. Increased levels of 3-dehydroquinic acid were also observed, which indicated that YdiB was not able to reduce 3-dehydroquinic acid at a sufficiently rapid rate. The use of *E. coli* B as a host for quinic acid production rather than *E. coli* K-12 was examined and revealed that overexpression of *tktA*-encoded transketolase was not necessary in *E. coli* B, since it synthesized the same concentration of quinic acid with or without plasmid-localized *tktA*. A decline in synthesis of quinic acid was observed as compared to the standard *E. coli* K-12 QP1.1/pKD12.138. The total synthesized hydroaromatics by the *E. coli* B producer harboring plasmid-localized *tktA* was 46 g/L while *E. coli* B without transketolase overexpression produced 65 g/L. Respectively, *E. coli* K-12 produced 72 g/L and 54 g/L of total hydroaromatics with or without transketolase overexpression. Optimum quinic acid production by *E. coli* K-12 QP1.1/pKD12.138 under fed-batch glucose-limited culture conditions was achieved with a total cultivation time of 78 h and a reduced phosphate concentration in the medium (35 mM instead of 43 mM). It was also demonstrated that 3-dehydroquinic acid is recaptured

by *E. coli* K-12 under glucose-limited culture conditions and further converted to quinic acid. However, glucose-rich fermentation conditions have to be avoided, especially during early stages of quinic acid production. A new quinic acid purification method was developed. It included aromatization of 3-dehydroquinic acid by 1 h reflux of cell-free and protein-free culture medium, followed by filtration through activated carbon. Salt precipitation was performed with 3 volumes of 100% ethanol. Quinic acid was recrystallized from salt-free ethanol with an 85% yield.

Quinic acid is a byproduct and contaminant during shikimic acid biosynthesis by *E. coli* SP1.1/pKD12.138. Historically, glucose-rich conditions were used to limit quinic acid levels in the culture medium. A new variant, JJ2.2, of *E. coli* SP1.1 was constructed by disrupting the genomic shikimate/quinate dehydrogenase *ydiB* gene. JJ2.2 showed no quinic acid accumulation during shikimic acid biosynthesis under fed-batch glucose-limited or glucose-rich culture conditions. *E. coli* JJ2.2/pKD12.138 produced 49 g/L of shikimic acid in 20% yield while SP1.1/pKD12.138 synthesized 30 g/L in 13% yield under glucose-limited culture conditions. However, SP1.1/pKD12.138 performed better under glucose-rich culture conditions and synthesized 60 g/L of shikimic acid in 26% yield, while JJ2.2/pKD12.138 produced 51 g/L in 20% yield, respectively. Another variant of SP1.1 was constructed where shikimate kinases AroK and AroL were inactivated using a scarless method rather than by transposon insertion as was done for SP1.1. Preliminary results showed that more carbon flowed into the shikimate pathway. An attempt to identify a hydroaromatics efflux system in *E. coli* was unsuccessful. Attempts were made to identify a shikimate dehydrogenase gene from *Gluconobacter oxydans* IFO 3244 and to overexpress it in *E. coli*.

To my parents

For their constant love and support

ACKNOWLEDGMENTS

Finally, I owe the sinceriest of thanks to my dear friends Dr. Konstantinos Rampalakos, Dr. Efthalia Kalliri, Dr. Nikoleta Theodoropoulou, Dr. Chrysoula Vasilieou, Kyoungsoo Lee and his family, Diana Gaidelyte and David Riess, Algirdas Baranauskas, Arunas Gaidelis, and Fei Yam for their understanding, help and support. I am also greatfull to all of my aunts, uncles cousins and their familys for so much needed support and understanding.

This thesis is dedicated to my parents, Alberta-Genovaite Jancauskiene and Zigmantas Jancauskas, my brother, Mindaugas Jancauskas and my sister-in-law Aukse Jancauskiene, my niece Agne Jancauskaite and my nephew Paulius Jancauskas.

TABLE OF CONTENTS

LIST OF TABLES

LIST OF FIGURES

LIST OF ABBREVIATIONS

Ac	acetyl
ADP	adenosine diphosphate
ATP	adenosine triphosphate
Ap	ampicillin
Ap^R	ampicillin resistance gene
bp	base pair
CIAP	calf intestinal alkaline phosphatase
Cm	chloramphenicol
Cm^R	chloramphenicol resistance gene
cat	chloramphenicol resistance gene
DAHP	3-deoxy-D-*arabino*-heptulosonic acid 7-phosphate
DCU	digital control unit
DHQ	3-dehydroquinic acid
DHS	3-dehydroshikimic acid
DO	dissolved oxygen
DTT	dithiothreitol
E4P	D-erythrose 4-phosphate
EMP	Embden-Meyerhof pathway
FBR	feedback resistant
FLP	flippase
FRT	flippase recognition targen
h	hour

IPTG	isopropyl β-D-thiogalactopyranoside
Kan	kanamycin
Kan^R	kanamycin resistance gene
kan	kanamycin resistance gene
kb	kilobase pair
k_{cat}	turnover number
kg	kilogram
K_m	Michaelis constant
LB	Luria broth
M	molar
M9	minimal salts
min	minute
mL	milliliter
μL	microliter
mM	millimolar
μM	micromolar
NAD	nicotinamide adenine dinucleotide, oxidized form
NADH	nicotinamide adenine dinucleotide, reduced form
NADP	nicotinamide adenine dinucleotide phosphate, oxidized form
NADPH	nicotinamide adenine dinucleotide phosphate, reduced form
NMR	nuclear magnetic resonance spectroscopy
OD	optical density
OTR	oxygen transfer rate

ORF	open reading frame
PEP	phosphoenolpyruvic acid
PID	proportional-integral-derivative
PCR	polymerase chain reaction
Phe	L-phenylalanine
psi	pounds per square inch
PTS	phosphotransferase system
QA	quinic acid
rpm	rotations per minute
SA	shikimic acid
SDS	sodium dodecyl sulfate
Tc	tetracycline
tet	tetracycline resistance gene
TCA	tricarboxylic acid
Trp	L-tryptophan
TSP	sodium 3-(trimethylsilyl)propionate-$2,2,3,3$-d_4
Tyr	L-tyrosine
UV	ultraviolet

CHAPTER ONE

Introduction

Much of the chemical industry is based on technologies where starting materials are derived from fossil fuels. As a nonrenewable natural resource, petroleum has several environmental and geopolitical problems associated with its use. The carcinogenicity of benzene, which is derived from fossil fuels, is additionally problematic.[1] Interest in using renewable starting materials has grown with the increasing demand for and cost of petroleum.[2] In addition to the actual cost of petroleum, the health costs[1] associated with fossil fuel-derived chemical building blocks such as benzene have to be considered.[2,3]

Carbohydrates derived from renewable feedstocks such as glucose, xylose and arabinose are abundant and can be used in biotic and abiotic processes to obtain products that are currently manufactured by the chemical industry using traditional technology.[4] Fermentation processes have existed for thousands of years to meet various human needs such as production of bread, wine, beer, vinegar and cheese.[5] However, the science behind these processes was not understood until French chemist Louis Pasteur discovered "germs". Discovery of the microorganisms and invention of the Pasteurization process laid the foundation for modern biotechnology.[6] Since then the discovery of DNA,[7] exploration of the plasmid,[8] development of sequencing techniques,[9] and application of polymerase chain reaction[10] (PCR) have revolutionized traditional microbiology and established a new global biotechnology industry. In the future, microbial synthesis alone

or combined with chemical synthesis will grow and replace many currently employed chemical syntheses.[11]

D-Glucose being renewable and the most abundant carbohydrate monomer holds great potential as a starting material for microbial synthesis. Today, the majority of glucose in the US used in microbial synthesis is derived from corn starch processed by wet milling operations. Another major source of glucose is cellulose. However, better technology for cellulose depolymerization must be developed in order to for cellulose to find use as a glucose source.[12]

To compete with chemical synthesis, microbial synthesis must produce value-added chemicals in high yield and high concentration. There are two general methods to increase the yield and concentration of desired products: Direct more carbon flow into the targeted biosynthetic pathway and eliminate byproduct formation. Chapter 2 of this dissertation will focus on increasing the yield and concentration of quinic acid synthesized by a recombinant *Escherichia coli* strain. Investigation of *E. coli ydiB*-encoded shikimate/quinate dehydrogenase YdiB as a substitute for currently employed *aroE*-encoded shikimate/quinate dehydrogenase for quinic acid production will be discussed. The use of *E. coli* B rather then *E. coli* K-12 as a host will be presented as well. Optimization of the microbial synthesis of quinic acid using *E. coli* QP1.1/pKD12.138 will be discussed in detail and will include the examination of such parameters as fermentation time, phosphate and aromatic amino acid levels in the production medium, together with a new method for purifying quinic acid.

Chapter 3 will focus on microbial synthesis of the shikimic acid. Quinic acid is an undesirable byproduct in shikimic acid biosynthesis, which lowers the yield of shikimic acid by channeling carbon flow away from biosynthesis of shikimic acid.

2

Secondly, if quinic acid accumulates at higher levels, it complicates shikimic acid purification.[13] A single genetic modification of shikimic acid producer SP1.1 afforded the first microbial synthesis of shikimic acid where accumulation of quinic acid as byproduct has been completely eliminated. Construction and preliminary investigation of the new shikimic acid producing *E. coli* JJ5 will be discussed as well as the use of heterologous shikimate dehydrogenase from *Gluconobacter oxydans* IFO3244. Hydroaromatics transport in *E. coli* was also investigated as an avenue to increase yields and concentrations of microbially synthesized shikimic acid or quinic acid.

The shikimate pathway

The shikimate pathway exists in plants, bacteria and fungi, and is involved in the transformation of carbohydrates into aromatics including the amino acids L-tyrosine, L-phenylalanine and L-tryptophan, and vitamin precursors such as 2, 3-dihydroxybenzoate, *p*-hydroxybenzoate and *p*-aminobenzoate.[14] Mammals are incapable of *de novo* biosynthesis of aromatics and must acquire these metabolites from their diet.

The first step of the shikimate pathway is the irreversible condensation of phosphoenolpyruvate (PEP) and D-erythrose 4-phosphate (E4P) to form 3-deoxy-D-*arabino*-heptulosonic acid 7-phosphate (DAHP), which is catalyzed by DAHP synthase (Figure 1). *E. coli* has three DAHP isozymes AroF, AroG and AroH, which are feedback inhibited, respectively, by L-tyrosine, L-phenylalanine and L-tryptophan.[15] DAHP is further converted to 3-dehydroquininc acid (DHQ) by *aroB*-encoded DHQ synthase.[16] A *syn* elimination of water from DHQ is catalyzed by 3-dehydroquinate dehydrogenase (AroD) and produces 3-dehydroshikimic acid.[17] Reduction of 3-dehydroshikimic acid by NADPH affords shikimic acid.

3
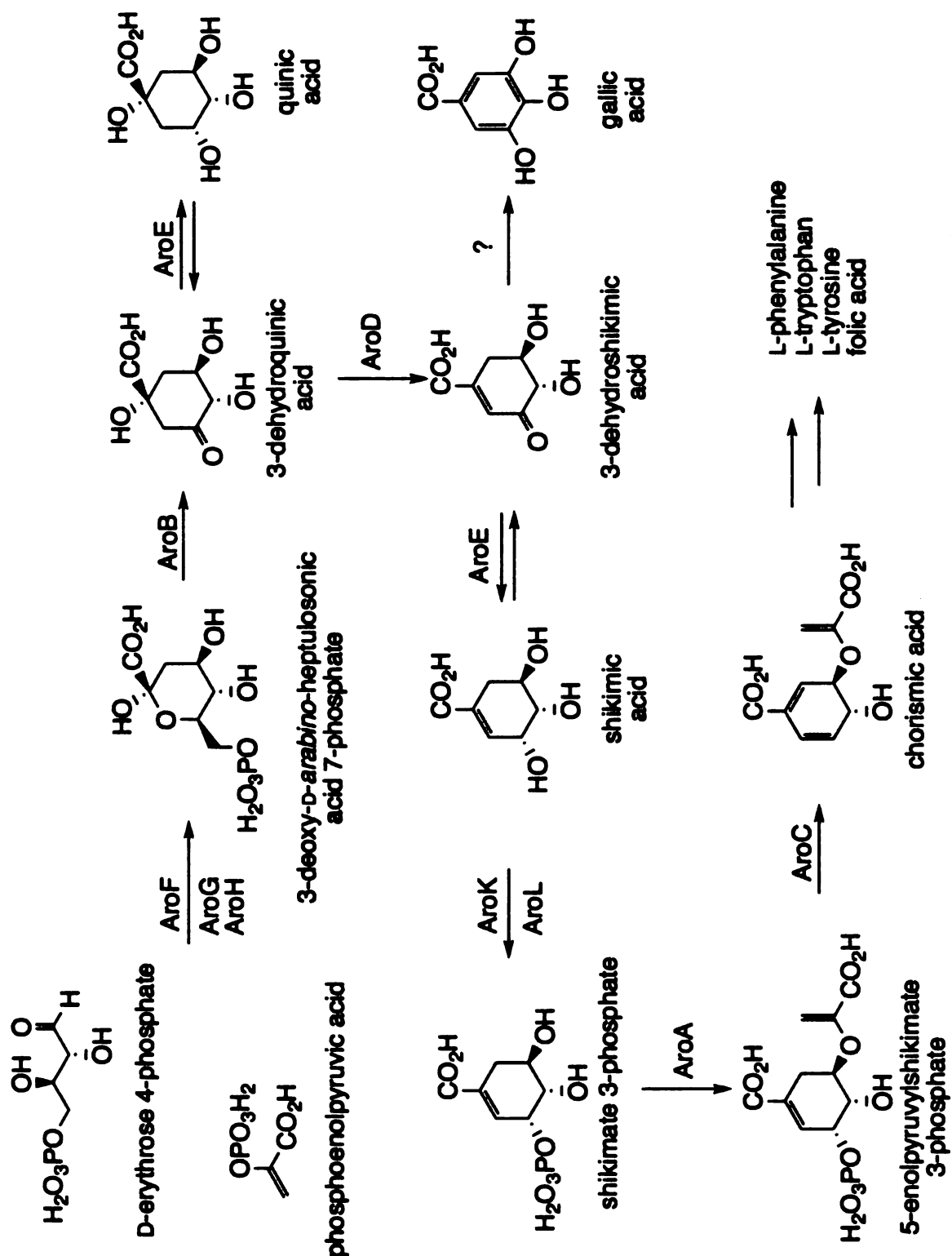
Figure 1. The shikimate pathway and biosynthesis of quinic acid and gallic acid.
Enzymes: DAHP synthase (AroF, AroG, AroH); 3-dehydroquinate synthase (AroB); 3-dehydroquinate dehydratase (AroD); shikimate dehydrogenase (AroE); shikimate kinase (AroK, AroL); 5-enolpyruvoylshikimate 3-phosphate synthase (AroA); chorismate synthase (AroC); unknown(?).

This reduction is catalyzed by *aroE*-encoded shikimate dehydrogenase,[18] which is feedback inhibited by shikimic acid.[19] A second putative shikimate/quinate dehydrogenase isozyme YdiB was recently identified in *E. coli*.[20] The next step requires ATP and is catalyzed by two shikimate kinase isozymes, AroK and AroL.[21] Phosphorylated shikimic acid is a substrate for 5-enolpyruvoylshikimate 3-phosphate synthase encoded by the *aroA* gene, which catalyzes enolpyruvoyl addition to the C-5 hydroxy using PEP as a substrate.[22] The last enzyme of the shikimate pathway is chorismate synthase (AroC).[23] It catalyzes 1,4-*trans* elimination of phosphate to form chorismic acid. Chorismic acid is the branching point for biosynthesis of aromatics. All three aromatic amino acids and aromatic vitamins are synthesized from this chorismic acid.

Regulation of the shikimate pathway in *E. coli* occurs at the protein level via feedback inhibition and at the transcriptional level. The transcription of L-tyrosine-sensitive AroF and L-phenylalanine-sensitive AroG isozymes is regulated by a transcriptional repressor encoded by the *tyrR* gene.[15] Transcription of L-tryptophan-sensitive AroH is regulated by the *trpR* gene product.[15] The same transcription regulators control shikimate kinase *aroL* transcription, while *aroK* is constitutively expressed in *E. coli*.[15]

3-Dehydroshikimic acid

3-Dehydroshikimic acid is an intermediate in the shikimate pathway and can be viewed as a branch point from which natural products can be biosynthesized without

intermediacy of chorismic acid (Figure 2). The aromatization of 3-dehydroshikimic acid

to protocatechuic acid is crucial to the value of 3-dehydroshikimic acid as an intermediate

for the synthesis of several commodity and fine chemicals. Protocatechuic acid is a

branch point in the biosynthesis of catechol,[24] cis, cis-muconic acid,[25] vanillin,[26] gallic

acid[27] and pyrogallol.[27] Hydrogenation of cis-cis-muconic acid affords adipic acid.[25]
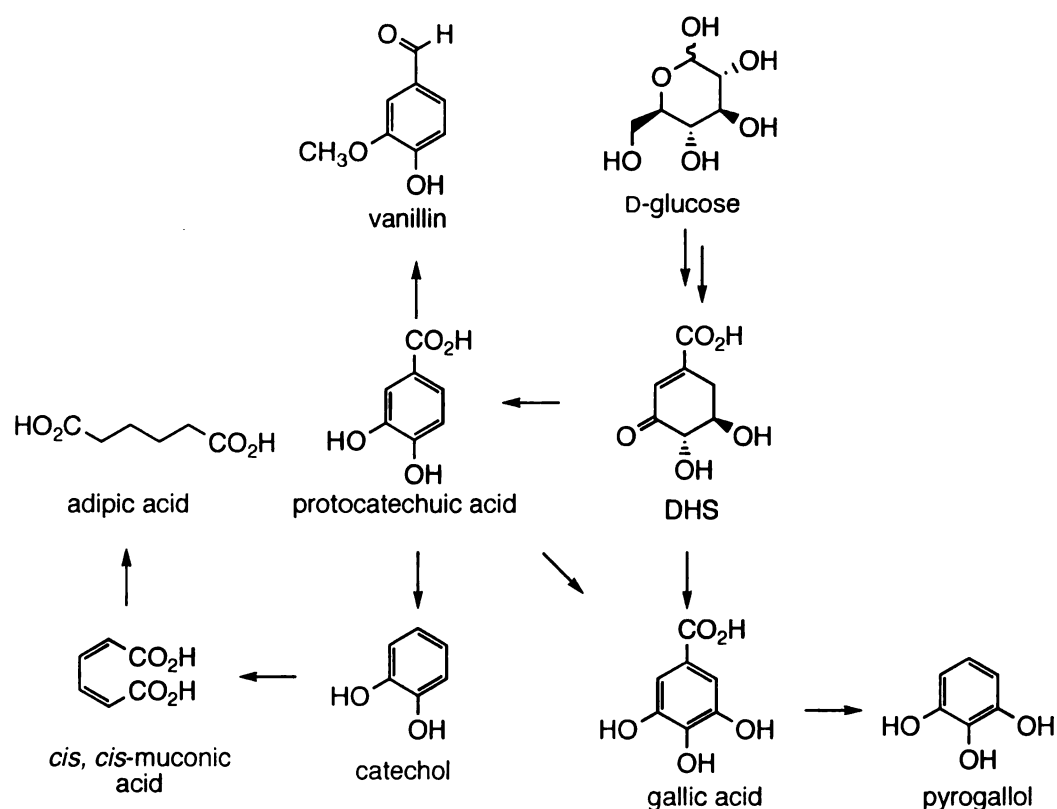
Figure 2. Value-added chemicals synthesized from glucose via 3-dehydroshikimic acid intermediacy.

The Frost group developed *E. coli* KL3/pJY1.216A as a construct capable of

converting glucose into 3-dehydroshikimic acid.[28] This 3-dehydroshikimic acid-

synthesizing biocatalyst was constructed by disruption of the genomic *aroE* locus (Figure

1) in *E. coli*, which resulted in accumulation of 3-dehydroshikimic acid in the culture

medium. Integration of a second *aroB* copy in the genome and plasmid-localized

6

expression of feedback-insensitive, *aroF*[FBR]-encoded DAHP synthase, *tktA*-encoded transketolase and *ppsA*-encoded PEP synthase increased the flow of carbon into the shikimate pathway and produced 69 g/L of 3-dehydroshikimic acid in 35% yield.

Shikimic acid

It has been demonstrated that shikimic acid is a useful chiral compound. It is a six-membered carboxylic ring with three stereogenic centers, and an endocyclic olefin. Schreiber and coworkers have exploited it as the core scaffold for a large combinatorial library synthesis (Figure 3).[29] Frost and coworkers reported that shikimic acid also serves as an environmentally-friendly precursor for phenol[30] and *p*-hydroxybenzoic acid (Figure 3).[31] The importance of shikimic acid increased with its use as the starting material for the manufacture of Tamiflu® (Figure 3), which is a potent inhibitor for Influenza A and Influenza B neuraminidases.[32] Tamiflu was approved by the FDA and is currently marketed by Roche as an orally administered antiinfluenza drug. Use of shikimic acid in Tamiflu synthesis and other synthetic applications was previously restricted by shikimic acid price and availability. Before a microbial synthesis of shikimic acid was developed by the Frost group, the only source of shikimic acid was isolation from the pericarps of Chinese star anise (*Illicium* sp. plants).[33]
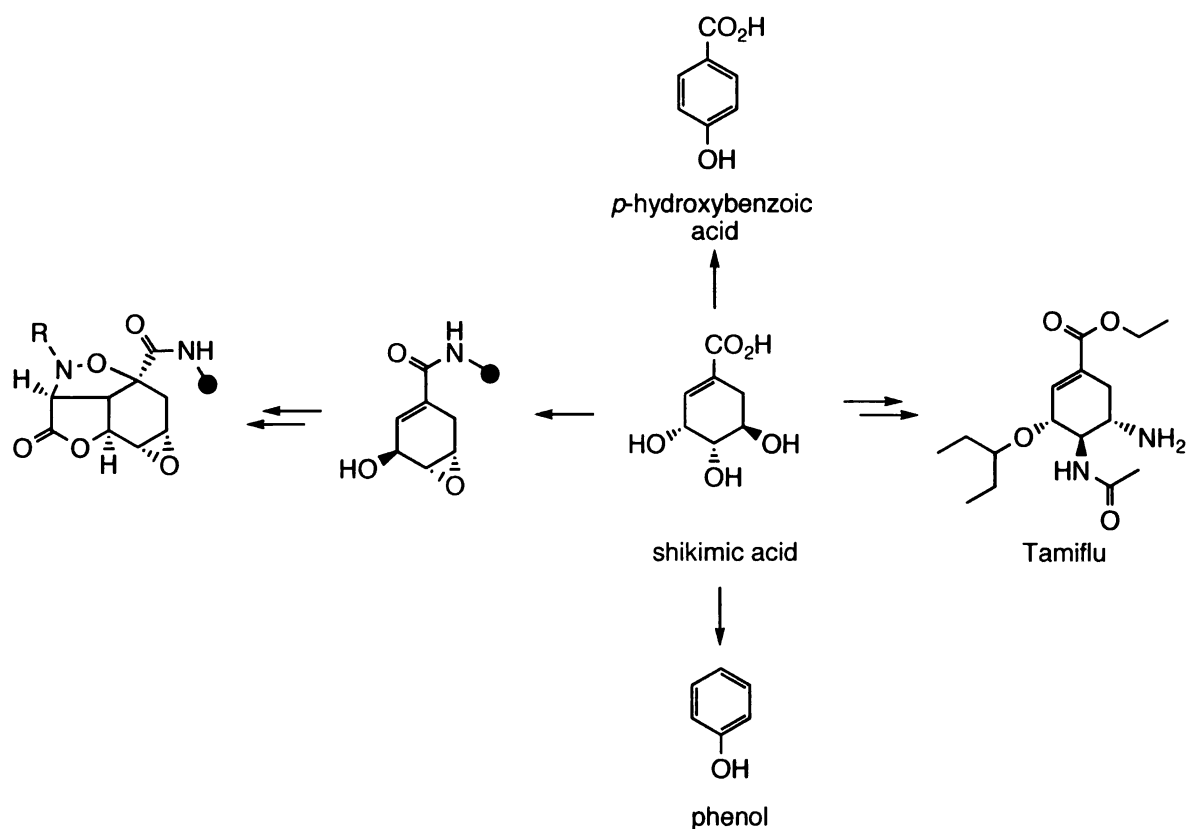
Figure 3. Use of shikimic acid in synthetic chemistry.

Genetically engineered *E. coli* SP1.1/pKD12.138 was constructed for microbial synthesis of shikimic acid.[34] This biocatalyst was created by disrupting the shikimate kinase-encoded *aroK* and *aroL* genomic loci in *E. coli*. Also integration of a second *aroB* copy in the genome and overexpression of plasmid-localized feedback insensitive *aroF*[FBR]-encoded DAHP synthase and *tktA*-encoded transketolase permitted an increase of carbon flow into the shikimate pathway, which ultimately translated into 52 g/L concentration of shikimic acid synthesized in 18% yield from glucose.[34] The SP1.1/pKD12.138 fermentation process has been scaled up and is licensed by Roche to provide a source of shikimic acid for the manufacture of Tamiflu.

Quinic acid

Quinic acid was first isolated from crude quinine (an anti-malaria drug isolated from *Cinchona* bark) in 1790.[35] The structure and stereochemistry of quinic acid was assigned only in 1932 by Fisher and Dangschat.[36] Quinic acid is an attractive molecule for combinatorial library or natural product synthesis due to its highly-functionalized six-membered carbocyclic ring and four asymmetric centers.[37] Quite a few biologically active natural products and natural product derivatives have been synthesized in whole, or in part, from quinic acid. The molecules include anti-influenza drug GS-4104-02 marketed by Roche as Tamiflu,[38] (-)-sugiresinol dimethyl ether (a derivative of (-)-sugiresinol isolated from *Cryptomeria japonica*),[39] the epoxycyclohexenone core of scyphostatin (a powerful inhibitor of neutral sphongomyelinase),[40] (+)-eutypoxide B (a secondary metabolite of fungus *Eutypa lata* responsible for pathogenic vineyard die-back disease)[41], the A ring of $1\alpha,25$-dihydroxyvitamin D_3 derivatives (potential drugs for treatment of osteoporosis and psoriasis),[42] the 2-iodocyclohexenone acetal portion of anticancer drug taxol,[43] and the bicyclic core structure of the potent enediyne antitumoral agent esperimicin-A_1[44] (Figure 4).

GS-4104

(-)-sugiresinol dimethyl ether

scyphostatin

(+)-eutypoxide B

1α,25-dihydroxy-19-norvitamin D₃

2-iodocyclohexenone acetal

1,5-dicaffeoylquinc acid

bicyclic core of esperamicin-A₁

1-caffeoyl-5-feruoylquinc acid

1,5-O-diferuoylquinc acid
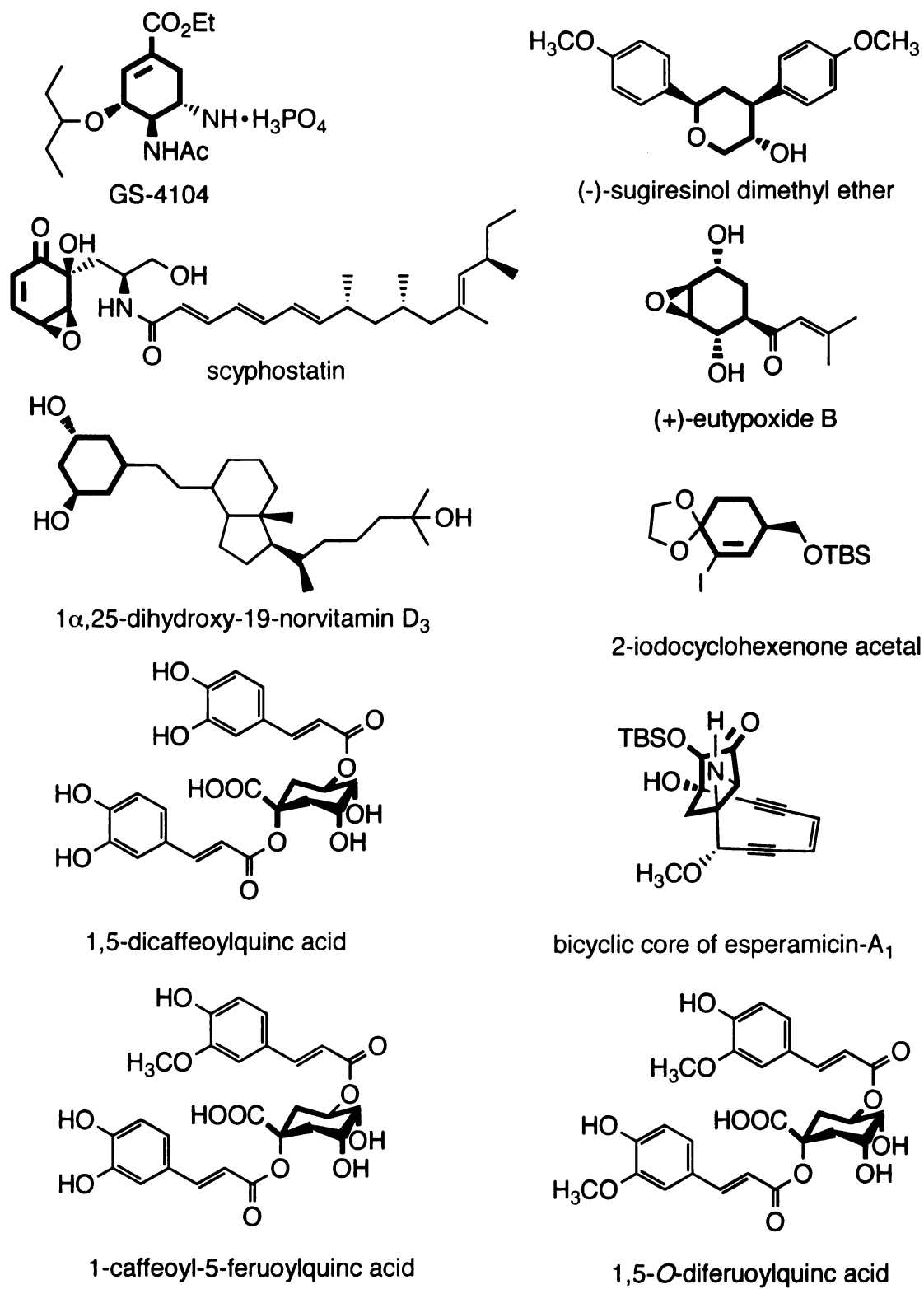
Figure 4. Biologically active quinic acid derivatives. The portions from quinic acid are indicated in bold.

10

Recently, dicaffeoylquinic acids have received attention as potent HIV-1 integrase inhibitor. Currently AIDS treatment consists of drug cocktails, which inhibit HIV-1 reverse transcriptase and protease. However, rapid mutation of HIV virus results in drug-resistant strains. Since HIV-1 is a retrovirus, it requires the integration of the proviral double-stranded DNA arising from the reverse transcription step into the host chromosome for its efficient replication, maintenance and productive infection. DNA integration is carried out by integrase, which thus constitutes another potential target in anti-retroviral drug design.[45] Robinson and coworkers were the first to report that dicaffeoylquinic acids were potent inhibitors of HIV-1 integrase in tissue culture.[46] More recent preclinical studies suggest, that 1,5-dicaffeoylquinic acid and its two metabolites, monomethylated 1-caffeoyl-5-feruoylquinic acid and dimethylated 1, 5-O-diferuoylquinic acid (Figure 4), show the highest inhibitory activity towards HIV-1 integrase.[47]

All biologically active natural products previously cited in this chapter had quinic acid as part of their structure. Does quinic acid by itself have any biological activity? In recent studies by Pero and coworkers it has been reported that ammonium salt of quinic acid is the active component in the *Uncaria tomentosa* (Cat's claw) extract C-Med 100®.[48a] The authors described that quinic acid inhibited transcriptional regulator NF-κB activity, and they postulate that this is the primary basis of the anti-inflammatory character of cat's claw extracts. The Pero group also reports that in human studies they have observed increased tryptophan and nicotinamide concentrations in subject's urine after ingestion of water supplemented with quinic acid.[48c] Additionally, no quinic acid or hippuric acid, a known metabolite derived from quinic acid in humans,[49] was observed in

blood serum. It was also shown that primates including humans have the greatest conversion of quinic acid to hippuric acid. This metabolism is apparently dependent on intestinal microflora, because there was no metabolism of quinic acid to hippuric acid when injected intraperitoneally.[49a] As a consequence of these observations, Pero and coworkers have postulated that the biological activity of quinic acid in humans could not be assigned directly to quinic acid. Instead, Pero has hypothesized that quinic acid is converted to biologically active metabolites by microorganisms in the human gastro-intestinal tract. The Pero group suggests that biological activity of quinic acid is arising from gastro-intestinal microbes catalyzing the conversion of quinic acid via the tryptophan-quinilinate-nicotinamide-NAD branch of the shikimate pathway. This is hypothesized to account for the observed elevated levels of tryptophan and nicotinamide in urine. Nicotinamide is a known NF-κB[50a] inhibitor and an antioxidant.[50m,n] High doses of nicotinamide have therapeutic value for treatment of lipid profiles,[50d,e] diabetes,[50f,h] depression,[50j] HIV,[50i,k] and migranes.[50l]

Increasing of carbon flow into the shikimate pathway

Modifications of central metabolism in *E. coli* to channel more carbon flow into the shikimate pathway has been the focus of considerable research activity.[51] The first strategy employed was overexpression[52] of feedback resistant AroF,[FBR] which helped to overcome feedback inhibition of DAHP synthase caused by aromatic amino acids.[53] Insensitivity to feedback inhibition by aromatic amino acids increases the *in vivo* catalytic activity of DAHP synthase. Because increased carbon flow into the shikimate pathway

results from increased DAHP synthase activity, increased accumulation of 3-dehydroshikimic acid and DAH level was observed during *E. coli* AB2834 cultivation.[54] The absence of catalytically-active shikimate dehydrogenase, which catalyzes conversion of 3-dehydroshikimic acid into the shikimic acid (Figure 1), in *E. coli* AB2834, resulted in the accumulation of 3-dehydroshikimic acid in the culture medium. Accumulation of DAH, which results from DAHP dephosphorylation, lowers 3-dehydroshikimic acid and shikimic acid concentration and yield. An approximately twofold increase in DHQ synthase specific activity is required[19] to eliminate DAH accumulation, which can be accomplished by introducing a second copy of *aroB* into the genome of *E. coli*.[55]

Table 1. Comparison of the impact of modification of the central metabolism in *E. coli* on synthesis of 3-dehydroshikimic acid and shikimic acid.

Entry	Construct[a]	Relevant characteristics[b]	Desired product			
			$[DHS]^c$, g/L	DHS yield,[d] %	[SA], g/L	SA yield, %
1	KL3/pKL4.33B	$aroF^{FBR}$, *serA*	20	17	-	-
2	KL3/pKL4.66B	$aroF^{FBR}$, *serA*, $aroF^{FBR}$	39	16	-	-
3	KL3/pKD12.291A	$aroF^{FBR}$, *serA*, P_{aroF}	41	18	-	-
4	KL3/pKL5.17A	$aroF^{FBR}$, *serA*, P_{aroF}, *tktA*	58	24	-	-
5	KL3/pJY1.216A	$aroF^{FBR}$, *serA*, P_{aroF}, *tktA*, *ppsA*	69	35	-	-
6	SP1.1/pKD12.112	$aroF^{FBR}$, *aroE*, *serA*	-	-	38	12
7	SP1.1/pKD12.138	$aroF^{FBR}$, *aroE*, *serA*, *tktA*	-	-	52	18
8	SP1.1/pKD15.071	$aroF^{FBR}$, *aroE*, *serA*, *tktA*, *ppsA*	-	-	66	23
9	SP1.1*pts*/pSC6.90B	$aroF^{FBR}$, *aroE*, *serA*, *tktA*, P_{tac} *glf glk*			71	27

[a] KL3: AB2834 *serA::aroB*; SP1.1: RB791 *serA::aroB aroL478::Tn10 aroK17::Cm^R*. [b] $aroF^{FBR}$: feed-back insensitive DAHP synthase; *serA*: 3-phosphoglycerate dehydrogenase P_{aroF}: promoter locus of *E. coli aroF* gene; tktA: transketolase; *ppsA*: phosphoenolpyruvate synthase; *glf*: glucose facilitator from *Z. mobilis*; *glk*: glucose kinase. [c] DHS: 3-dehydroshikimic acid; SA: shikimic acid. [d] (mol DHS)/(mol glucose consumed).

13

Several different routes were pursued for circumventing transcriptional repression of $aroF$.[51f] Use of two plasmid-localized copies of $aroF^{FBR}$ resulted in the synthesis of 39 g/L of 3-dehydroshikimic acid in 16% yield (Table 1, entry 2), while one plasmid-localized copy of $aroF^{FBR}$ afforded 20 g/L of 3-dehydroshikimic acid synthesized in 17% yield (Table 1, entry 1).[51f] A further improvement in 3-dehydroshikimic acid synthesis was achieved once $aroF^{FBR}$ was overexpressed together with unmodified native promoter P_{aroF}, which presumably helped to titrate away the cellular supply of TyrR repressor protein. Synthesis of 41 g/L of 3-dehydroshikimic acid in 18% yield was observed (Table 1, entry 3).[51f] These results indicated that the best configuration was to include in the plasmid one copy of P_{aroF} and $aroF^{FBR}$ under its native promoter. The same study also demonstrated that higher DAHP synthase activity did not necessarily translate into higher yields or concentrations of shikimate pathway products. This indicated that the substrates for DAHP synthase were limiting factors in increasing carbon flow directed into the shikimate pathway.
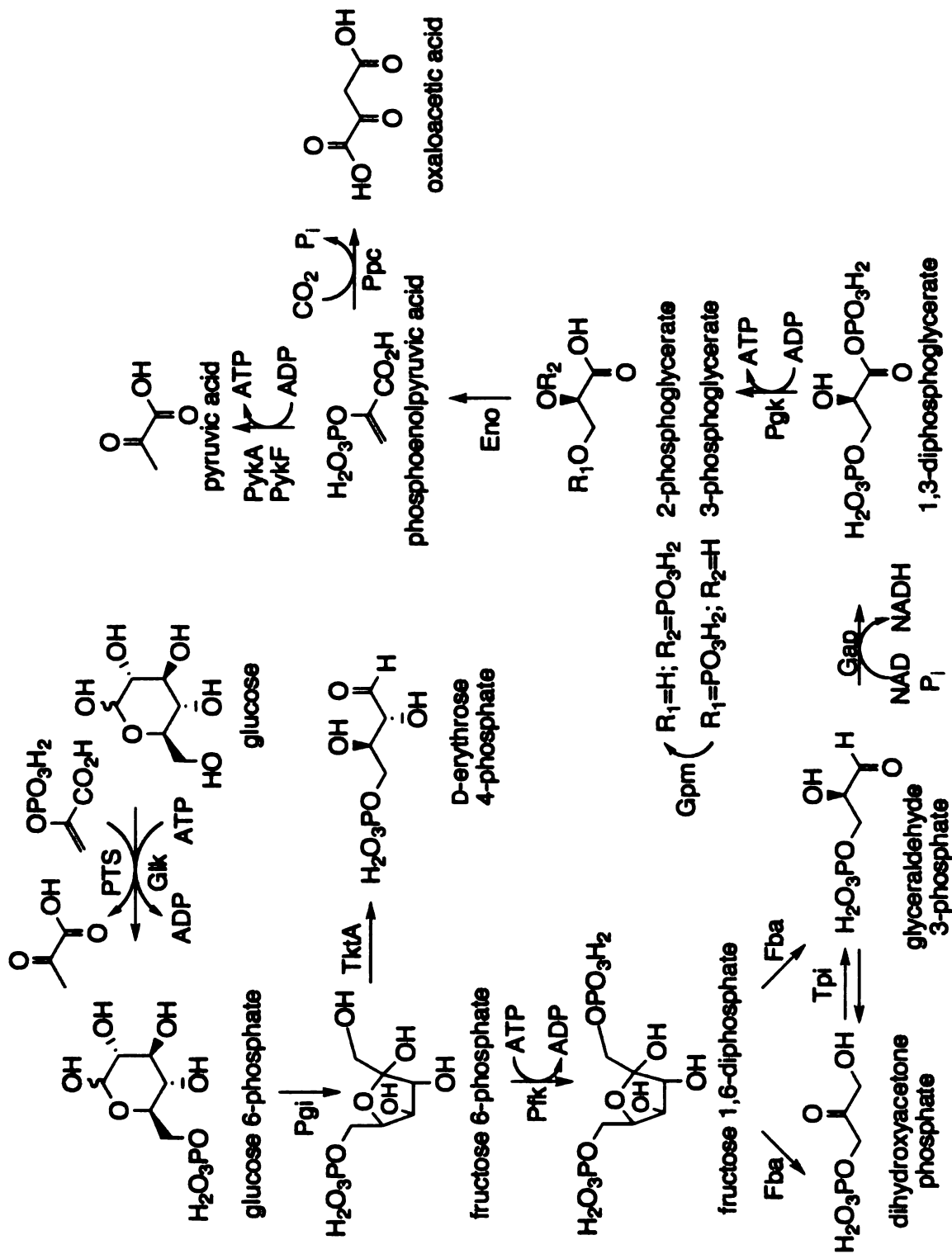
Figure 5. Glycolysis and biogenesis of D-erythrose 4-phosphate and phosphoenolpyruvic acid. Enzymes: phosphoenolpyruvate:carbohydrate phosphotransferase (PTS); glucokinase (Glk); phosphoglucose isomerase (Pgi); phosphofructose kinase (Pfk); fructose 1,6-diphosphate aldolase (Fba); glyceraldehyde 3-phosphate dehydrogenase (Gap); phosphoglycerate kinase (Pgk); enolase (Eno); pyruvate kinase (PykA, PykF); transketolase (TktA).

15

Frost and coworkers published the first work suggesting that D-erythrose 4-phosphate (E4P) availability was an important factor limiting *in vivo* DAHP synthase activity.[56] The reason for low E4P availability might be due to its tendency to polymerize in solution.[57] Dissociation back to the monomeric form of E4P is quite slow. This may be the reason why *E. coli* cells keep low steady-state concentrations of E4P. To increase the intracellular concentration of E4P, *tktA*-encoded transketolase was overexpressed, which led to an increased concentration and yield of 3-dehydroshikimic acid (Table 1, entry 4)[51f] and shikimic acid (Table 1, entry 7) relative to (Table 1, entry 6).[34]

With increased *in vivo* E4P availability, availability of phosphoenolpyruvate (PEP) became a limiting factor. A number of different cellular processes and enzymes compete with DAHP synthase for PEP including pyruvate kinase PykA and PykF (Figure 5), PEP carboxylase Ppc (Figure 5), and the PEP-dependent carbohydrate:phosphotransferase system (PTS) for transport of glucose and structurally related sugars into the cytoplasm. Efforts to improve intracellular PEP availability began with genomic inactivation of PEP carboxylase[51c,58] and pyruvate kinase,[59] but did not lead to significantly improved biosyntheses of aromatic amino acids. A better strategy was reported by Liao and coworkers.[51d, 51e] Liao used an *E. coli aroB* mutant (inactive 3-dehydroquinate synthase, Figure 1) with plasmid-localized *aroG*[FBR]-encoded feedback insensitive DAHP synthase, transketolase and overexpressed PEP synthase. This strategy was based on recycling pyruvic acid, which is generated by PTS-mediated glucose transport, back to PEP. The construction of *E. coli* strain KL3/pJY1.216A in the Frost

group afforded the best 3-dehydroshikimic acid producer constructed so far (Table 1, entry 5).[28] Plasmid pJY1.216A carried $aroF^{FBR}$-encoded feedback-insensitive DAHP synthase, $tktA$-encoded transketolase, $ppsA$-encoded PEP synthase and the P_{aroF} - encoded promoter region of DAHP synthase. The same approach was taken to create a better shikimic acid-producing biocatalyst in SP1.1/pKD15.071B (Table 1, entry 8).[60]

Another strategy was to use a non-PTS mechanism for glucose transport into the cell, thereby eliminating consumption of a mole of PEP for each mole of glucose transported into the cell. It was shown, that heterologous expression of *Zymomonas mobilis* plasmid-localized *glf* (glucose facilitator protein) and *glk* (glucose kinase) in a PTS-deficient *E. coli* strain reconstituted glucose transport and phosphorylation.[61] Increase in concentration and yield of microbe-synthesized shikimic acid was observed (Table 1, entry 9) when compared to SP1.1/pKD15.071B results (Table 1, entry 8).[60]

.

References

1   (a) Wong, O.; Raabe, G. K. Critical review of cancer epidemiology in petroleum industry employees, with a quantitative meta-analysis by cancer site. *Am. J. Ind. Med.* **1989**, *15*, 283-310. (b) Lewis, R. J. *Carcinogenically active chemicals*, Van Nostrand Reinhold, New York, **1991**, p. 68. (c) O'Connor, S. R.; Farmer, P. B.; Lauder, I. Benzene and non-hodgkin's lymphoma. *J. Pathol.* **1999**, *189*, 448-453. (d) Lan Q.; Zhang, L.; Li, G.; Vermeulen, R.; Weinberg, R. S.; Dosemeci, M.; Rappaport, S. M.; Shen, M.; Alter, B. P.; Wu, Y.; Kopp, K.; Waidyanatha, S.; Rabkin, Ch.; Guo, W.; Chanock, S.; Hayes, R. B.; Linet, M.; Kim, S.; Yin, S.; Rothman, N.; Smith, M. T. Hematotoxicity in workers exposed to low levels of benzene. *Science*, **2004**, *306*, 1774-1776.

2   (a) Tullo, A. Benzene costs hurt customers. *Chem. Eng. News* **2004**, *82*, 15-17. (b) http://www.eia.doe.gov/oiaf/aeo/index.html. *Annual energy outlook 2008 with projections to 2030.*

3   (a) Yoshida, J.; Inomata, M. Trends in developments of aromatics production technologies. *Aromatikkusu* **2002**, *54*, 123-135. (b) Tullo, A. H. A new source. *Chem. Eng. News* **2003**, *81*, 16-17.

4   (a) Frost, J. W.; Lievense, J. Prospects for biocatalytic synthesis of aromatics in the 21st- century. *New J. Chem.* **1994**, *18*, 341. (b) Bongaerts, J.; Kramer, M.; Muller, U.; Raeven, L.; Wubbolts, M. Metabolic engineering for microbial production of aromatic amino acids and derived compounds. *Metabol. Eng.* **2001**, *3*, 289-300.

5   Pannuri, S.; DiSanto, R.; Kamat, S. In *Kirk-Othmer encyclopedia of chemical technology online*; Biocatalysis, 2003, Wiley.

6   Junker, B. In *Kirk-Othmer encyclopedia of chemical technology online*; Fermentation, 2004, Wiley.

7   Watson, J.; Crick, F. A structure for deoxyribose nucleic acid. *Nature* **1953**, *171*, 737-738.

8   Cohen, S.; Chang, A. C. Y.; Boyer, H. W.; Helling, R. B. Construction of biologically functional bacterial plasmids *in vitro*. *Proc. Natl. Acad. Sci. U.S.A.* **1973**, *70*, 3240-3244.

9   (a) Sanger, F.; Coulson, A. R. A rapid method for determining sequences in DNA by primed synthesis with DNA polymerase. *J. Mol. Biol.* **1975**, *94*, 441-448. (b) Sanger, F.; Nicklen, S.; Coulson, A. R. DNA sequencing with chain-terminating inhibitors. *Proc. Natl. Acad. Sci. U.S.A.* **1977**, *74*, 5463-5467.

10   Saiki, R. K.; Scharf, S.; Faloona, F.; Mullis, K. B.; Horn, G. T.; Erlich, H. A.; Arnheim, N.   Enzymatic amplification of beta-globin genomic sequences and restriction site analysis for diagnosis of sickle cell anemia. *Science* **1985**, *230*, 1350-1354.

11   http://www.eere.energy.gov/industry/chemicals/visions_biocatalysis.html. *Chemical industry of the future*.

12   (a) Bozell, J. J.; Landucci, R. *Alternate feedstocks program technical and economic assessment*; U. S. Department of Energy, Office of Industrial Technologies, 1993. (b) Lynd, L. R.; Cushman, J. H.; Nichols, R. J.; Wyman, C. E. Fuel ethanol from cellulose biomass. *Science* **1991**, *251*, 1318-1323. (c) Zaldivar, J.; Nielson, J.; Olsson, L. Fuel ethanol production from lignocellulose: A challenge for metabolic engineering and process integration. *Appl. Microbiol. Biotechnol.* **2001**, *56*, 17-34.

13   Draths, K. M.; Knop, D. R.; Frost, K. M. Shikimic acid and quinic acid: replacing isolation from plant sources with recombinant biocatalysis. *J. Am Chem. Soc.* **1999**, *121*, 1603-1604.

14   (a) Haslam, E. In *Shikimic acid: Metabolism and metabolites*; Wiley: New York, 1993. (b) Bentley, R. The shikimate pathway - a metabolic tree with many branches. *Crit. Rev. Biochem. Mol. Biol.* **1990**, *25*, 307-384. (c) Herrmann, K. M. In *Amino acids: Biosynthesis and genetic regulation*; Herrmann, K. M., Somerville, R. L., Ed.; Addison-Wesley: Reading, 1983: p. 301.

15   Pittard, A. J. Biosynthesis of the aromatic amino acids. In *Escherichia coli and Salmonella typhimurium: cellular and molecular biology*. Neidhardt, F. C. ed. ASM Press (Washington, DC: American Society for Microbiology) 1996, p. 458-484.

16   (a) Frost, J. W.; Bender, J. L.; Kadonaga, J. T.; Knowles, J. R. Dehydroquinate synthase from *Escherichia coli*: purification, cloning, and construction of overproducers of the enzyme. *Biochemistry* **1984**, *23*, 4470-4475. (b) Carpenter, E. P.; Hawkins, A. R.; Frost, J. W.; Brown, K. A. Structure of dehydroquinate synthase reveals an active site capable of multistep catalysis. *Nature* **1998**, *394*, 299-302.

17   (a) Smith, B. W.; Turner, M. J.; Haslam, E.   Shikimate pathway. 4. Stereochemistry of 3-dehydroquinate dehydratase reaction and observations on 3-dehydroquinate synthetase. *J. Chem. Soc., Perkins Trans. 1* **1975**, *1*, 52-55. (b) Duncan, K.; Chaudhuri, S.; Campbell, M. S.; Coggins, J. R. The overexpression and complete amino acid sequence of *Escherichia coli* 3-dehydroquinase. *Biochem. J.* **1986**, *238*, 475-483.

18   (a) Anton, I. A.; Coggins, J. R. Sequencing and overexpression of the *Escherichia coli aroE* gene encoding shikimate dehydrogenase. *Biochem. J.* **1988**, *249*, 319-326. (b) Chaudhuri, S.; Coggins, J. R. The purification of shikimate dehydrogenase from *Escherichia coli*. *Biochem. J.* **1985**, *226*, 217-223.

19   Dell, K. A.; Frost, J. W. Identification and removal of impediments to biocatalytic synthesis of aromatics from D-glucose: rate-limiting enzymes in the common pathway of aromatic amino acid biosynthesis. *J. Am. Chem. Soc.* **1993**, *115*, 11581-11589.

20   (a) Michel, G.; Roszak, A. W.; Sauve, V.; Maclean, J.; Matte, A.; Coggins, J. R.; Cygler, M.; Lapthorn, A. J. Structures of shikimate dehydrogenase AroE and its paralog YdiB. *J. Biol. Chem.* **2003**, *278*, 19463-19472. (b) Benach, J.; Lee, I.; Edstorm, W.; Kuzin, A. P.; Chiang, Y.; Acton, T. B.; Montelione, G. T.; Hunt, J. F. The 2.3-Å crystal structure of the shikimate 5-dehydrogenase orthologue Ydib from *Escherichia coli* suggests a novel catalytic environment for an NAD-dependent dehydrogenase. *J. Biol. Chem.* **2003**, *278*, 19176-19182.

21   (a) DeFeyter, R. C.; Pittard, J. Genetic and molecular analysis of AroL, the gene for shikimate kinase-II in *Escherichia coli* K-12. *J. Bacteriol.* **1986**, *165*, 226-232. (b) DeFeyter, R. C.; Pittard, J. Purification and properties of shikimate kinase-II from *Escherichia coli* K-12. *J. Bacteriol.* **1986**, *165*, 331-333. (c) LØbner-Olesen, A.; Marinus, M. G. Identification of the gene (*aroK*) encoding shikimic acid kinase-I of *Escherichia coli*. *J. Bacteriol.* **1992**, *174*, 525-529.

22   Duncan, K.; Coggins, J. R. The SerC-AroA operon of *Escherichia coli*: a mixed function operon encoding enzymes from 2 different amino acid biosynthetic pathways. *Biochem. J.* **1986**, *234*, 49-57. (b) Duncan, K.; Lewendon, A.; Coggins. J. R. The purification of 5-enolpyruvylshikimate 3-phosphate synthase from an overproducing strain of *Escherichia coli*. *FEBS Lett.* **1984**, *165*, 121-127.

23   White, P. J.; Millar, G.; Coggins, J. The overexpression, purification and complete amino-acid sequence of chorismate synthase from *Escherichia coli* K12 and its comparison with the enzyme from *Neurospora crassa*. *Biochem. J.* **1988**, *251*, 313-322.

24   (a) Draths, K. M.; Frost, J. W. Environmentally compatible synthesis of catechol from D-Glucose. *J. Am. Chem. Soc.* **1995**, *117*, 2395-2400. (b) Li, W.; Xie, D.; Frost, J. W. Benzene-free synthesis of catechol: interfacing microbial and chemical catalysis. *J. Am. Chem. Soc.* **2005**, *127*, 2874-2882.

25   (a) Draths, K. M.; Frost, J. W. environmentally compatible synthesis of adipic acid from D-Glucose. *J. Am. Chem. Soc.* **1994**, *116*, 399-400. (b) Niu, W.; Draths, K. M.; Frost, J. W. Benzene-free synthesis of adipic acid. *Biotechnol. Prog.* **2002**, *18*, 201-211.

26   Li, K.; Frost, J. W. Synthesis of vanillin from glucose. *J. Am. Chem. Soc.* **1998**, *120*, 10545-10546.

27   Kambourakis, S.; Draths, K. M.; Frost, J. W. Synthesis of gallic acid and pyrogallol from glucose: replacing natural product isolation with microbial catalysis. *J. Am. Chem. Soc.* **2000**, *122*, 9042-9043.

28   Yi, J.; Li, K.; Draths, K. M.; Frost, J. W. Modulation of phosphoenolpyruvate synthase expression increases shikimate pathway product yields in *E. coli*. *Biotechnol. Prog.* **2002**, *18*, 1141-1148.

29   (a) Tan, D. S.; Foley, M. A.; Shair, M. D.; Schreiber, S. L. Stereoselective synthesis of over two million compounds having structural features both reminiscent of natural products and compatible with miniaturized cell-based assays. *J. Am. Chem. Soc.* **1998**, *120*, 8565-8566. (b) Tan, D. S.; Foley, M. A.; Stockwell, B. R.; Shair, M. D.; Schreiber, S. L. Synthesis and preliminary evaluation of a library of polycyclic small molecules for use in chemical genetic assays. *J. Am. Chem. Soc.* **1999**, *121*, 90073-90087.

30   Gibson, J. M.; Thomas, P. S.; Thomas, J. D.; Barker, J. L.; Chandran, S. S.; Harrup, M. K.; Draths, K. M.; Frost, J. W. Benzene-free synthesis of phenol. *Angew. Chem., Intl. Ed.* **2001**, *40*, 1945-1948.

31   Barker, J. L.; Frost, J. W. Microbial synthesis of *p*-hydroxybenzoic acid from glucose. *Biotechnol. Bioeng.* **2001**, *76*, 376-390.

32   Kim, C. U.; Lew, W.; Williams, M. A.; Liu, H.; Zhang, L.; Swaminathan, S.; Bischofberger, N.; Chen, M. S.; Mendel, D. B.; Tai, C. Y.; Laver, W. G.; Stevens, R. C. Influenza neuraminidase inhibitors possessing a novel hydrophobic interaction in the enzyme active site: design, synthesis, and structural analysis of carbocyclic sialic acid analogues with potent anti-influenza activity. *J. Am. Chem. Soc.* **1997**, *119*, 681-690.

33   Weber, W. F. Hoffmann-La Roche, Ltd., personal communication.

34   Knop, D. R.; Draths, K. M.; Chandran, S. S.; Barker, J. L.; von Daeniken, R.; Weber, W.; Frost, J. W. Hydroaromatic equilibration during biosynthesis of shikimic acid. *J. Am. Chem. Soc.* **2001**, *123*, 10173-10182.

35   Hofmann, F. C. *Crell's Chemische Annalen*, **1790**, *2* 314.

36   Fisher, H. O., L.; Dangschat, G. *Ber. Dtsch. Chem. Gas.* **1932**, *65*, 1009.

37   (a) Phoon, C. W.; Abell, C. Use of quinic acid as template in solid-phase combinatorial synthesis. *J. Comb. Chem.* **1999**, *1*, 485-492. (b) Gonzalez C.; Carballido, M.; Castedo, L. Synthesis of polyhydroxycyclohexanes and relatives from (-)- quinic acid. *J. Org. Chem.* **2003**, *68*, 2248-2255. (c) Kaila, N.; Somers,

W. S.; Thomas, B. E.; Thakker, P.; Janz, K.; DeBernardo, S.; Tam, S.; Moore, W. J.; Yang, R.; Wrona, W.; Bedard, P. W.; Crommie, D.; Keith, J. C.; Jr.; Tsao, D. H. H.; Alvarez, J. C.; Ni, H.; Marchese, E.; Patton, J. T.; Magnani, J. L.; Camphausen, R. T. Quinic acid derivatives as sialyl Lewis-Mimicking selectin inhibitors: Design, synthesis, and crystal structure in complex with E-selectin. *J. Med. Chem.* **2005**, *48*, 4346-4357. (d) Usami, Y.; Ueda, Y. Stereoselective syntheses of diastereomers of antitumor natural product pericosine A from (-)-quinic acid. *Synthesis*, **2007**, *20*, 3219-3225.

38   Federspiel, M.; Fischer, R.; Hennig, M.; Mair, H.-J.; Oberhauser, T.; Rimmler, G.; Albiez, T.; Bruhin, J.; Estermann, H.; Gandert, C.; Goeckel, V.; Goetzoe, S.; Hoffmann, U.; Huber, G.; Janatsch, G.; Lauper, S.; Roeckel-Staebler, O.; Trussardi, R.; Zwahlen, A. G. Industrial synthesis of the key precursor in the synthesis of the anti-influenza drug Oseltamivir phosphate (Ro 64-0796/002, GS-4104-02): Ethyl (3R,4S,5S)-4,5-epoxy-3-(1-ethyl-propoxy)-1-cyclohexene-1-carboxylate. *Org. Proc. Res. Develop.* **1999**, *3*, 266-274.

39   Matsuo, K.; Sugimura, W.; Shimizu, Y.; Nishiwaki, K.; Kuwajima, H. Synthesis of (-)-sugiresinol dimethyl ether utilizing (-)-quinic acid. *Heterocycles* **2000**, *53*, 1505-1513.

40   Murray, L. M.; O'Brien, P.; Taylor, R. J. K. Stereoselective reactions of a (-)-quinic acid-derived enone: application to the synthesis of the core of scyphostatin. *Org. Lett.* **2003**, *5*, 1943-1946.

41   Barros, M. T.; Maycock, C. D.; Ventura, M. R. Enantioselective total synthesis of (+)-Eutypoxide B. *J. Org. Chem.* **1997**, *62*, 3984-3988.

42   Ono, K.; Yoshida, A.; Saito, N.; Fujishima, T.; Honzawa, S.; Suhara, Y.; Kishimoto, S.; Sugiura, T.; Waku, K.; Takayama, H.; Kittaka, A. Efficient synthesis of 2-modified 1α,25-dihydroxy-19-norvitamin D3 with Julia olefination: high potency in induction of differentiation on HL-60 cells. *J. Org. Chem.* **2003**, *68*, 7407-7415.

43   Su, Z.; Paquette, L. A. Conversion of D-(-)-quinic acid into an enantiopure C-4 functionalized 2-iodocyclohexenone acetal. *J. Org. Chem.* **1995**, *60*, 764-766.

44   Ulibarri, G.; Nadler, W.; Skrydstrup, T.; Audrain, H.; Chiaroni, A.; Riche, C.; Grierison, D. S. Construction of the bicyclic core structure of the enediyne antibiotic esperamicin-A1 in either enantiomeric form from (-)-quinic acid. *J. Org. Chem.* **1995**, *60*, 2753-2761.

45   Tarrago-Livak, L.; Andreola, M. L.; Fournier, M.; Nevinsky, G.A.; Parissi, V.; de Soultrait, V.R.; Litvak, S. Inhibitors of HIV-1 reverse transcriptase and integrase: Classical and emerging therapeutical approaches. *Curr. Pharm. Des.* **2002**, *8*, 595-614.

46   Robinson, E. W., Jr.; Reinecke, M. G.; Abdel-Malek, S.; Jia, Q.; Chow, S.A. Inhibitors of HIV-1 replication that inhibit HIV integrase. *Proc. Natl. Acad. Sci. USA* **1996**, *93*, 6326-6331.

47   (a) Yang, B.; Meng, Z.; Dong, J.; Yan, L.; Zou, L.; Tang, Z.; Dou, G. Metabolic profile of 1,5-dicaffeoylquinic acid in rats, an *in vivo* and *in vitro* study. *Drug Metab. Dispos.* **2005**, *33*, 930-936. (b) Asres, K.; Seyoum, A.; Veeresham, C.; Bucar, F.; Gibbons, S. Naturally Derived Anti-HIV Agents. *Phytother. Res.* 2005, *19*, 557–581.

48   (a) Åkesson, Ch.; Lindgren, H.; Pero, R. W.; Leanderson, T.; Ivars, F. Quinic acid is a biologically active component of the Uncaria tomentosa extract C-Med 100®. *Int. Immunopharmacol.* **2005**, *5*, 219-229. (b) Mammone, Th.; Åkesson, Ch.; Gan, D.; Giampapa, V.; Pero, R. W. A water soluble extract from *Uncaria tomentosa* (cat's claw) is a potent enhancer of DNA repair in primary organ cultures of human skin. *Phytother. Res.* **2006**, *20*, 178–183. (c) Personal communication, manuscript in preparation, **2007**.

49   (a) Adamson, R. H.; Bridges, J. W.; Evans, M. E.; Williams, R. T. Species differences in the aromatization of quinic acid in vivo and the role of gut bacteria. *Biochem. J.* **1970**, *116*, 437-433. (b) Indahl, S. R.; Scheline, R. R. Quinic acid aromatization in the rat. Urinary hippuric acid and catechol excretion following the singular or repeated administration of quinic acid. *Xenobiotica* **1973**, *3*, 549-556.

50   (a) Pero, R.W.; Axelsson, B.; Siemann, D.; Chaplin, D.; Dougherty, G. Newly discovered anti-inflammatory properties of the benzamides and nicotinamides. *Mol. Cell. Biochem.* **1999**, *193*, 119-125. (b) Virag, L. Structure and function of poly (ADP-ribose) polymerase-1: role in oxidative stress-related pathologies. *Curr. Vasc. Pharmacol.* **2005**, *3*, 209-214. (c) Adams, J. D. Nicotinamdie and its pharmacological properties for clinic therapy. *Drug Des. Rev. Online* **2004**, *1*, 43-52. (d) Handfield-Jones, S.; Jones, S.; Peachey, R. High dose nicotinamide in the treatment of necroobiosis lipoidice. *Br. J. Dermatol.* **1988**, *118*, 693-696. (e) Takahashi, Y.; Tanaka, A.; Nakamura, T.; Fukuwatari, T.; Shibata, K.; Shimada, N.; Ebihhara, I.; Koide, H. Nicotinamide suppresses hyperphosphatemia in hemodiaylsis patients. *Kidney Int.* **2004**, *65*, 1099-1104. (f) Rakieten, N.; Gordon, B. S.; Beaty, A.; Cooney, D. A.; Schein, P. S.; Dixon, R. L. Modification of renal tumorgenic effect of streptozotocin by nicotinamide spontaneous reversability of streptozotocin diabetes. *Proc. Soc. Exp. Biol. Med.* **1976**, *151*, 356-361. (g) Yamada, K.; Nonaka, K.; Hanafusa, A.; Miyazaki, A.; Toyoshima, H.; Tarui, S. Preventive and theraeuitc effects of large-dose nicotinamide injections on diabetes associated with insulitis. An observation in nonobese diabetic (NOD) mice. *Diabetes* **1982**, *31*, 749-753. (h) Wilson, B. M.; Buckingham, B. Prevention of type 1a diabetes melitus. *Pediatr. Diabetes* **2001**, 2, 17-24. (j) Chouinard, G.; Young, S.N.; Annable, L.; Sourkes, T. L. Tryptophan-nicotinamide, imipramine and their combination in depression. A

controlled study. *Acta Psychiatr. Scand.* **1979**, *59*, 395-414. (i) Murray, M. F.; Langan, M.; MacGregor, R. R. Increased plasma tryptophan in HIV-infected patients treated with pharmacologic doses of nicotinamide. *Nutrition* **2001**, 17, 654-556. (k) Beales, P. E.; Burr, L. A.; Webb, G. P.; Mansfield, K. J.; Pozzilli, P. Diet can influence the ability of nicotinamide to prevent diabetes in the non-obese diabetic mouse. A preliminary study. *Diabetes Metab. Res. Rev.* **1999**, *15*, 21-28. (l) Gedye, A. Hypothesized treatment for migraines using low doses of tryptophan, niacin, calcium, caffeine, and acetylsalicyclic acid. *Med. Hypothesis* **2001**, *56*, 91-94. (m) Kamat, J. P.; Devasagayam, T. P. Nicotinamide (vitamin B3) as an effective antioxidant against oxidative damage in rat brain mitochrondria. *Redox Rep.* **1999**, *4*, 179-184. (n) Ungerstedt, J. S.; Blomback, M.; Soderstrom, T. Nicotinamide is a potent inhibitor of proinflammatory cytokines. *Clin. Exp. Immunol.* **2003**, *131*, 48-52.

51   (a) Draths, K. M.; Pompliano, D. L.; Conley, D. L.; Frost, J. W.; Berry, A.; Disbrow, G. L.; Staversky, R. J.; Lievense, J. C. Biocatalytic synthesis of aromatics from D-glucose: the role of transketolase. *J. Am. Chem. Soc.* **1992**, *114*, 3956-3962. (b) Gubler, M., Jetten, M., Lee, S. H., Sinskey, A. J. cloning of the pyruvate-kinase gene (Pyk) of *Corynebacterium glutamicum* and site-specific inactivation of Pyk in a lysine-producing *Corynebacterium lactofermentum* strain. *Appl. Env. Microbiol.* **1994**, *60*, 2494-2500. (c) Miller, J. E.; Backman, K.C.; O'Conner, M. J.; Hatch, R. T. Production of phenylalanine and organic-acids by phosphoenolpyruvate carboxylase-deficient mutants of *Escherichia coli*. *J. Ind. Microbiol.* **1987**, 2, 143-149. (d) Patnaik, R.; Liao, J. C. Engineering of *Escherichia coli* central metabolism for aromatic metabolite production with near theoretical yield. *Appl. Environ. Microbiol.* **1994**, *60*, 3903-3908. (e) Patnaik, R.; Spitzer, R. G.; Liao, J. C. Pathway engineering for production of aromatics in *Escherichia coli*: confirmation of stoichiometric analysis by independent modulation of AroG, TktA, and Pps activities. *Biotechnol. Bioeng.* **1995**, *46*, 361-370. (f) Li, K.; Mikola, M. R.; Draths, K. M.; Worden, R. M.; Frost, J. W. Fed-batch fermentor synthesis of 3-dehydroshikimic acid using recombinant *Escherichia coli*. *Biotechnol. Bioeng.* **1999**, *64*, 61-73.

52   (a) Weaver, L. M.; Herrmann, K. M. Cloning of an AroF allele encoding a tyrosine-insensitive 3-deoxy-D-*arabino*-heptulosonate 7-phosphate synthase. *J. Bacteriol.* **1990**, *172*, 6581. (b) Mikola, M. R.; Widman, M. T.; Worden, R. M. In situ mutagenesis and chemotactic selection of microorganisms in a diffusion gradient chamber. *Appl. Biochem. Biotechnol.* **1998**, *70-72*, 905-918.

53   Ogino, T.; Garner, C.; Markley, J. L.; Herrmann, K. M. Biosynthesis of aromatic-compounds - ^{13}C NMR-spectroscopy of whole *Escherichia coli* cells. *Proc. Natl. Acad. Sci. USA* **1982**, *79*, 5828-5832.

54   Draths, K. M.; Frost, J. W. Genomic direction of synthesis during plasmid-based biocatalysis. *J. Am. Chem. Soc.* **1990**, *112*, 9630-9632.

55 Snell, K. D.; Draths, K. M.; Frost, J. W. Synthetic modification of the *Escherichia coli* chromosome: enhancing the biocatalytic conversion of glucose into aromatic chemicals. *J. Am. Chem. Soc.* **1996**, *118*, 5605-5614.

56 (a) Draths, K. M.; Frost, J. W. Synthesis Using Plasmid-Based Biocatalysis: Plasmid Assembly and 3-Deoxy-D-*Arabino*-Heptulosonate Production. *J. Am. Chem. Soc.* **1990**, *112*, 1657-1659. (b) Frost, J. W. U.S. Patent 5,168,056, 1992.

57 Williams, J. F.; Blackmore, P. F.; Duke, C. C. MacLeod, J. K. Fact, uncertainty and speculation concerning the biochemistry of D-erythrose-4-phosphate and its metabolic roles. *Int. J. Biochem.* **1980**, *12*, 339-344.

58 Backman, K.C. U.S. Patent 5,169,768, 1992.

59 Mori, M.; Yokota, A. ; Sugitomo, S.; Kawamura, K. Patent JP 62,205,782, 1987.

60 Chandran, S. S.; Yi, J.; Draths, K. M.; von Daeniken, R.; Weber, W.; Frost, J. W. Phosphoenolpyruvate availability and the biosynthesis of shikimic acid. *Biotechnol. Prog.* **2003**, *19*, 808-814.

61 (a) Parker, C.; Barnell, W. O.; Snoep, J. L.; Ingram, L. O.; Conway, T. Characterization of the *Zymomonas mobilis* glucose facilitator gene product (*glf*) in recombinant *Escherichia coli*: examination of transport mechanism, kinetics and the role of glucokinase in glucose transport. *Mol. Microbiol.* **1995**, *15*, 795-802. (b) Snoep, J. L.; Arfman, N.; Yomano, L. P.; Fliege, R. K.; Conway, T.; Ingram, L. O. Reconstruction of glucose uptake and phosphorylation in a glucose-negative mutant of *Escherichia coli* by using *Zymomonas mobilis* genes encoding the glucose facilitator protein and glucokinase. *J. Bacteriol.* **1994**, *176*, 2133-2135. (c) Weisser, P.; Krämer, R.; Sahm, H.; Sprenger, G. A. Functional expression of the glucose transporter of *Zymomonas mobilis* leads to restoration of glucose and fructose uptake in *Escherichia coli* mutants and provides evidence for its facilitator action. *J. Bacteriol.* **1995**, *177*, 3551-3554.

CHAPTER TWO

Optimizing microbial synthesis of (-)-quinic acid

Introduction

Two stereospecific quinic acid syntheses are reported in the literature.[1] However,

commercially available quinic acid is isolated from *Cinchona* bark.[2] The first reported

microbial synthesis of quinic acid relied on heterologous expression in *E. coli* of the

Klebsiella pneumoniae qad gene that encodes quinate dehydrogenase.[3] Qad catalyzed

the reduction of 3-dehydroquinic acid to quinic acid. In *K. pneumoniae*, Qad oxidizes

quinic acid to 3-dehydroquinic acid in the presence of NAD^+, which is the first step in

quinic acid catabolism via the β-ketoadipate pathway.[4] The reduction of 3-dehydroquinic

acid by Qad in *E. coli* resulted in formation of quinic acid because *E. coli* does not have

the ability to catabolize 3-dehydroquinic acid. Quinic acid biosynthesis utilizing Qad

relied on maintenance in an *E. coli* host of two plasmids, which is problematic during

high density cultivation under fermentor-controlled conditions.[3] A subsequent microbial

synthesis of quinic acid developed by the Frost group utilized native *E. coli* shikimate

dehydrogenase, which was discovered to reduce 3-dehydroquinic acid to quinic acid.[5]

The resulting construct, *E. coli* QP1.1/pKD12.112, synthesized 40 g/L of quinic acid in

16% yield.[5]

Table 2. Comparison of the impact of modification of the central metabolism in *E. coli* on synthesis of 3-dehydroshikimic acid and quinic acid.

			Desired product			
			[DHS],	DHS	[QA],	QA yield,
Entry	Construct	Relevant characteristics	g/L	yiled, %	g/L	%
1	KL3/pKD12.291A	$aroF^{FBR}$, serA, P_{aroF}	41	18	-	-
2	KL3/pKL5.17A	$aroF^{FBR}$, serA, P_{aroF}, tktA	58	24	-	-
3	KL3/pJY1.216A	$aroF^{FBR}$, serA, P_{aroF}, tktA, ppsA	69	35	-	-
4	JY1/pJY2.183	$aroF^{FBR}$, serA, P_{aroF}, tktA, P_{tac} glf glk	60	34	-	-
5	QP1.1/pKD12.112	$aroF^{FBR}$, aroE, serA	-	-	40	16
6	QP1.1/pKD12.138	$aroF^{FBR}$, aroE, serA, tktA	-	-	49	20
7	QP1.1/pKD15.071	$aroF^{FBR}$, aroE, serA, tktA, ppsA	-	-	49	18
8	QP1.1/pNR4.230	$aroF^{FBR}$, P_{tac}aroE(ORF), serA, tktA	-	-	46	20

[a] KL3: AB2834 serA::aroB; QP1.1: AB2848 serA::aroB; JY1: KL3 ΔptsHptsIcrr::Kan^R.
[b] $aroF^{FBR}$: feed-back insensitive DAHP synthase; serA: 3-phosphoglycerate dehydrogenase P_{aroF}: promoter locus of *E. coli* aroF gene; tktA: transketolase; ppsA: phosphoenolpyruvate synthase; glf: glucose facilitator from *Z. mobilis*; glk: glucose kinase. [c] DHS: 3-dehydroshikimic acid; QA: quinic acid. [d] (mol DHS)/(mol glucose consumed).

A variety of strategies have been employed for improving the yields of shikimate pathway metabolites synthesized by *E. coli*.[6,7,8] These strategies have focused on expression of feedback-insensitive DAHP synthase as well as increasing the availability of D-erythrose 4-phosphate (E4P) and phosphoenolpyruvate (PEP). E4P and PEP are the substrates of DAHP synthase, which is the first enzyme in the shikimate pathway and catalyzes an irreversible condensation to form 3-deoxy-D-*arabino*-heptulosonic acid 7-phosphate (DAHP Figure 1). E4P is derived from the pentose phosphate pathway and PEP is formed in the Embden-Meyerhof pathway (glycolysis) as shown in Figure 5. Initial attempts to increase carbon flow into the shikimate pathway examined

overexpression of feedback-insensitive DAHP synthase isozymes.[9] Frost and coworkers used a 3-dehydroshikimate-synthesizing strain to demonstrate that the increases in overexpression of DAHP synthase leads to increased accumulation of 3-dehydroshikimic acid and byproducts in the culture supernatent.[6f] However, additional increases in DAHP synthase overexpression failed to have a positive impact, i.e. increased in synthesized 3-dehydroshikimic acid.[6f] Availability of E4P or PEP might be a limiting factor, since both molecules are used as the substrates for DAHP synthase. Overexpression of plasmid-localized *tktA*-encoding transketolase resulted in higher DAH production, which was attributed to increased E4P availability.[10] A 3-dehydroshikimic acid concentration of 41 g/L synthesized in 18% yield (Table 2, entry 1) increased to 58 g/L synthesized in 24% yield (Table 2, entry 2) once transketolase was overexpressed together with feedback-insensitive DAHP synthase in *E. coli* KL3/pKL5.17A.[6f] A similar trend was observed for microbial synthesis of quinic acid. *E. coli* QP1.1/pKD12.112 synthesized 40 g/L of quinic acid in 16% yield after 60 h cultivation without overexpression of transketolase (Table 2, entry 5).[5] However, when transketolase was overexpressed with plasmid-localized *tktA*, *E. coli* QP1.1/pKD12.138 produced 49 g/L of quinic acid in 20% yield after cultivation under fermentor-controlled conditions for 48h (Table 2, entry 6).[11]

In order to eliminate PEP limitation, a couple of strategies have been employed.[8,12,6d,e] Liao and co-workers demonstrated that a twofold increase in DAH production can be achieved by overexpression of phosphoenolpyruvate synthase, an enzyme that converts pyruvate to PEP with conversion of ATP to AMP.[6d] The combined

positive effect on synthesized DAH was observed once Liao and coworkers overexpressed transketolase and phosphoenolpyruvate synthase in the presence of feedback-insensitive DAHP synthase.[6e] Frost and co-workers demonstrated the combined effect of transketolase and phosphoenolpyruvate synthase overexpression using *E. coli* KL3/pJY1.216A, which synthesized 69 g/L of 3-dehydroshikimic acid under glucose-rich culture conditions in 35% yield (Table 2, entry 3).[8] The same strategy was explored for quinic acid synthesis. Overexpression of plasmid-localised *ppsA*-encoded phosphoenolpyruvate synthase in *E. coli* QP1.1/pKD15.071 resulted in synthesis of 49 g/L of quinic acid 48 h in 18% yield under fermentor-controlled conditions (Table 2, entry 7).[11]

Another strategy for increasing PEP availability employed a non phosphoenolpyruvate:carbohydrate phosphotransferase system (PTS) to phosphorylate and transport glucose across the cytoplasmic membrane. This strategy was based on the fact that during PTS-mediated glucose transport in *E. coli* one molecule of PEP is used to catalyze the phosphorylation and transport of one molecule of glucose, therefore limiting PEP *in vivo* availability. PEP used during PTS-mediated transport of glucose is converted to pyruvate, which is ultimately channeled to the tricarboxylic acid cycle (TCA). Therefore, *E. coli* lacking PTS-mediated glucose transport might possess increased *in vivo* PEP availability. Frost and coworkers showed that *E. coli* *pts*⁻ host strain JY1 with plasmid pJY2.183A-localized transketolase and feedback-insensitive DAHP synthase overexpression synthesized 60 g/L of 3-dehydroshikimic acid in 34% yield (Table 2, entry 7).[12] This showed an increase in 3-dehydroshikimic acid

concentration and yield when compared to KL3/pKL5.17A (Table 2, entry 2), which uses PTS for glucose transport (previously described). However, the increase was not as significant as for KL3/pJY1.216A (Table 2, entry 3), which employs phosphoenolpyruvate synthase for PEP recycling during PTS transport of glucose. Since JY1 had an inactivated PTS-mediated glucose transport system, plasmid pJY2.183A additionally carried the *glf* gene encoding the glucose facilitator protein from *Zymomonas mobilis* and the *E. coli glk* gene encoding the glucose kinase. Quinic acid producer host, lacking native PTS system QP1.1*pts* was constructed. Plasmid pKD12.138 was modified by inserting $P_{tac}glf,glk$ insert and resulted in pSC6.090 plasmid.[13] A new quinic acid producer QP1.1*pts*/pSC6.090 failed to grow well under fermentor-controlled conditions.[11]

3-Dehydroquinic acid accumulation was observed throughout the microbial synthesis of quinic acid. Therefore, another strategy was to increase shikimate dehydrogenase AroE activity. Ran reported that QP1.1/pNR4.230 had twofold higher shikimate dehydrogenase activity than QP1.1/pKD12.138.[11] above However, under the same conditions it produced 46 g/L of quinic acid in 20% yield (Table 2, entry 8), QP1.1/pKD12.138 synthesized 49 g/L of quinic acid in 20% yield (Table 2, entry 6).[11] Increase in shikimate dehydrogenase activity did not lead to increased quinic acid concentration and yield.

Biocatalytic synthesis of quinic acid by fed-batch fermentation

The quinic acid-synthesizing *E. coli* strains were cultivated under fed-batch glucose-limited fermentor-controled conditions at 33 °C, pH 7.0 and dissolved oxygen was maintained at 10% air saturation. Plasmid maintenance relied on nutritional pressure, since all *E. coli* hosts had disrupted *serA* genes and each carried plasmid with a *serA* insert. Glucose addition was controlled by dissolved oxygen concentration. Under aerobic conditions, O_2 is the best electron sink,[14] therefore a subtle change in metabolic rate can be detected immediately by dissolved oxygen concentration in the medium. When dissolved oxygen concentration (pO_2) decreased below a set point (10%) indicating an increased rate of metabolism due to ample concentrations of glucose, the rate of glucose addition decreased. Conversely, when pO_2 increased indicating a slower rate of metabolism due to inadequate concentration of glucose in the culture medium, the rate of glucose addition was increased. The glucose addition rate was controlled by a proportional-integral-derivative (PID) control loop. Overtime, the controller found the steady addition rate resulting in a steady state concentration of glucose of approximately 0.2 mM in the medium. A proportional gain (K_c) of 0.1 was used for glucose PID control. A concentration range of 55-170 mM glucose in the fermentation medium was maintained by manually adjusting the rate of glucose addition under glucose-rich conditions. Fermentations were run in duplicate and reported results represent the average of two runs unless otherwise stated. Metabolite concentrations were determined using ^1H NMR unless otherwise stated.

Host *E. coli* host QP1.1[5] was constructed by site-specific insertion of *aroB* into the *serA* locus of *E. coli* AB2848, which has inactive 3-dehydroquinate dehydratase due to a mutation in the *aroD* gene.[15] 3-Dehydroquinate dehydratase (AroD) is a shikimate pathway (Figure 1) enzyme. Without AroD, *E. coli* QP1.1 can not biosynthesize the aromatic amino acids and aromatic vitamins required for its growth and metabolism. Therefore, all QP1.1 cultures had to be supplemented with aromatic amino acids L-phenylalanine, L-tyrosine and L-tryptophan, and the precursors for aromatic vitamins *p*-hydroxybenzoic acid, *p*-aminobenzoic acid, and 2,3-dihydroxybenzoic acid, when grown in minimal salt medium. A second genomic copy of the *aroB* locus in *E. coli* QP1.1 increased the specific activity of 3-dehydroquinate synthase to a level where accumulation of 3-deoxy-D-*arabino*-heptulosonic acid (dephosphorylated DAHP Figure 1) was no longer observed.[16] Disruption of the *serA* locus in QP1.1 led to inactive 3-phosphoglycerate dehydrogenase, which is an enzyme required for L-serine biosynthesis in wild-type *E. coli*. A copy of the *serA* gene was inserted into plasmids and provided the basis for plasmid maintenance when cultures were cultivated on glucose in minimal salt medium.

The construction plasmid pKD12.112 was previously reported[5] as well as plasmid pKD12.138,[17] pNR4.230[11] and pJJ4.171.[19] The plasmid maps are shown in Figure 6. All plasmids shared genomic elements like *aroF*[FBR], $P_{tac}P_{aroE}$*aroE* and *serA*. To overcome feedback inhibition of DAHP synthase caused by the aromatic amino acid supplements, plasmid-localized feedback-insensitive DAHP synthase encoded by *aroF*[FBR] was required. Shikimate dehydrogenase encoded by *aroE* ensured reduction of

3-dehydroquinic acid to quinic acid. Plasmid pKD12.112 and pKD12.138 had *aroE* expression controlled by a native P_{aroE} promoter while *aroE* in pNR4.230 was expressed from a P_{tac} promoter. Plasmid pJJ4.171 was identical to pKD12.138 except it had *ydiB* ORF under control of P_{tac} promoter, rather than $P_{aroE}aroE$. Plasmid-encoded *serA* was required to maintain the plasmid under glucose-limited conditions and to restore 3-phosphoglycerate dehydrogenase activity after *aroB* was inserted into the *serA* locus of genomic DNA. Plasmids pKD12.138 and pNR4.230 also had transektolase encoding *tktA* locus.
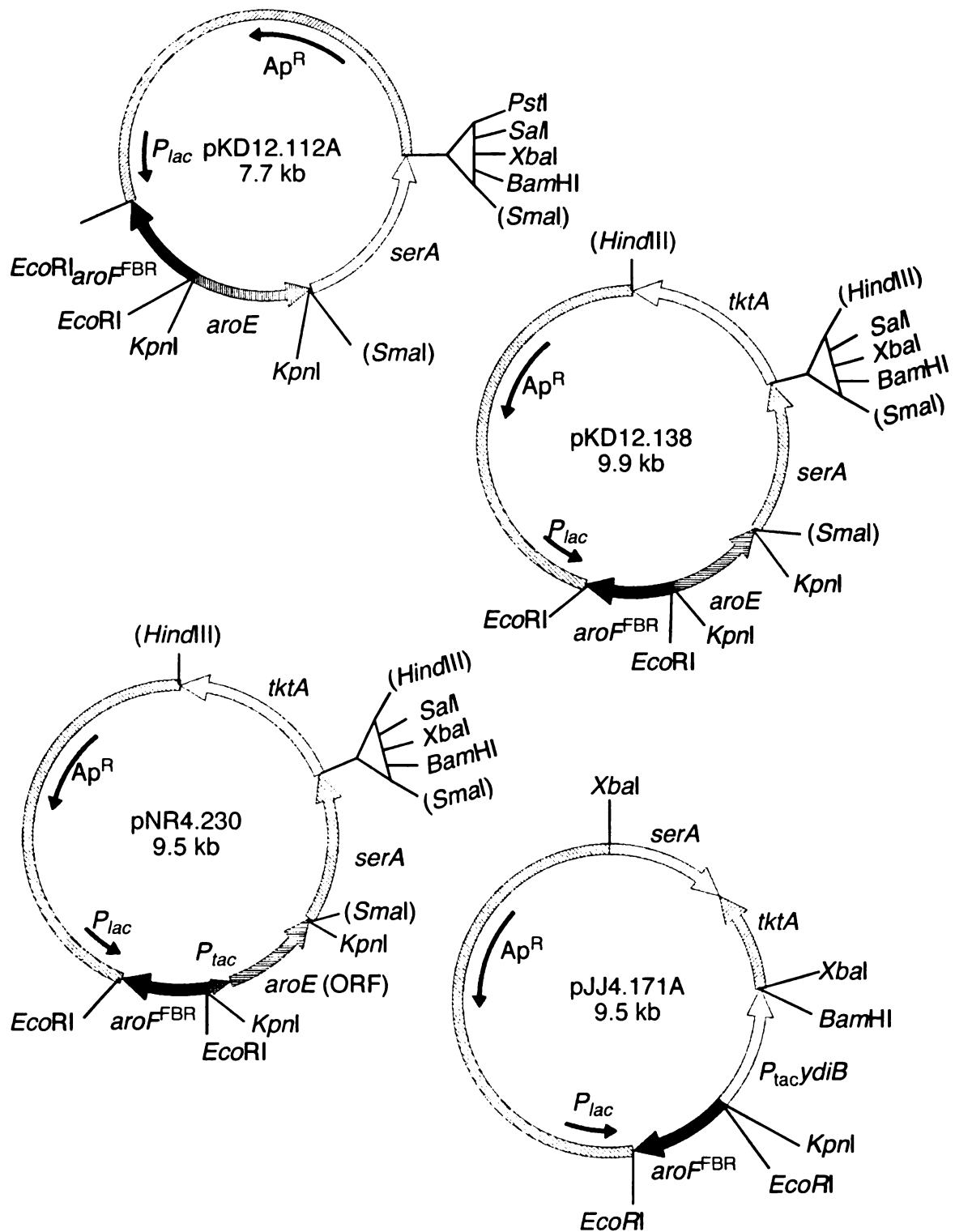
Figure 6. Plasmid maps of pKD12.112, pKD12.138, pNR4.230 and pJJ4.171.

A search for a better shikimate/quinate dehydrogenase

Previously in the literature, *E. coli* YdiB was named a putative shikimate dehydrogenase, because it showed activity towards shikimic acid,[18] and *E. coli ydiB* gene is in the same operon as another shikimate pathway enzyme *aroD*-encoded 3-dehydroquinate dehydratase. Crystal structures of YdiB and AroE were found to be very similar, even though *ydiB* share only 25% nucleotide sequence identity with *aroE*.[18a] It was also demonstrated that YdiB catalyzes shikimic acid conversion to 3-dehydroshikimic acid and quinic acid conversion to 3-dehdyroquinic acid in the presence of NADP⁺ and NAD⁺.[18a] Further evaluation of YdiB proved that it can function as a second shikimate dehydrogenase in *E. coli*.[19] First, it was shown that plasmid-localized *ydiB* restored *E. coli* AB2834 growth on glucose-minimal medium.[19] *E. coli* AB2834 lacks shikimate dehydrogenase activity due to a mutation in the *aroE* gene,[15] which results in an inability to grow on glucose-minimal medium lacking supplementation with shikimic acid or alternatively, supplementation with aromatic amino acids and aromatic vitamins.[15] The YdiB enzyme was also characterized as a feedback-insensetive shikimate dehydrogenase with shikimic acid, although based on K_m and k_{cat} determination YdiB was not as active of a shikimate dehydrogenase relative to AroE (Table 3).[19]

Table 3. Shikimate dehydrogenase AroE and YdiB kinetic parameters for 3-dehydroshikimic acid.

Enzyme	K_m (mM)	k_{cat}, s⁻¹
AroE	0.10	361
YdiB	10	83

An attempt was made to replace AroE with YdiB in microbial synthesis of quinic acid. *E. coli* QP1.1/pJJ4.171A did not produce any quinic acid under glucose-limited conditions in 48 h (Table 4, entry 3; Figure 8A). However, both control strains QP1.1/pKD12.138 (Table 4, entry 1; Figure 7A) and QP1.1/pNR4.230 (Table 4, entry 2; Figure 7B) produced 58 g/L in 22% yield and 57 g/L in 22% yield of quinic acid, respectively. *E. coli* QP1.1/pJJ4.171 did not produce any quinic acid (Table 4, entry 4; Figure 8B) when cultured glucose-rich fermentor-controlled conditions. The only hydroaromatic synthesized by QP1.1/pJJ4.171 was 3-dehydroquinic acid, which was synthesized at 52 g/L in 21% yield (Table 4, entry 3) under glucose-limited culture conditions and at 50 g/L in 21% yield (Table 4, entry 4) when cultivated under glucose-rich conditions. Since, 3-dehydroquinic acid is a substrate for shikimate dehydrogenase AroE and YdiB (Figure 1), accumulation of this metabolite instead of quinic acid suggested a lack of *ydiB* expression.
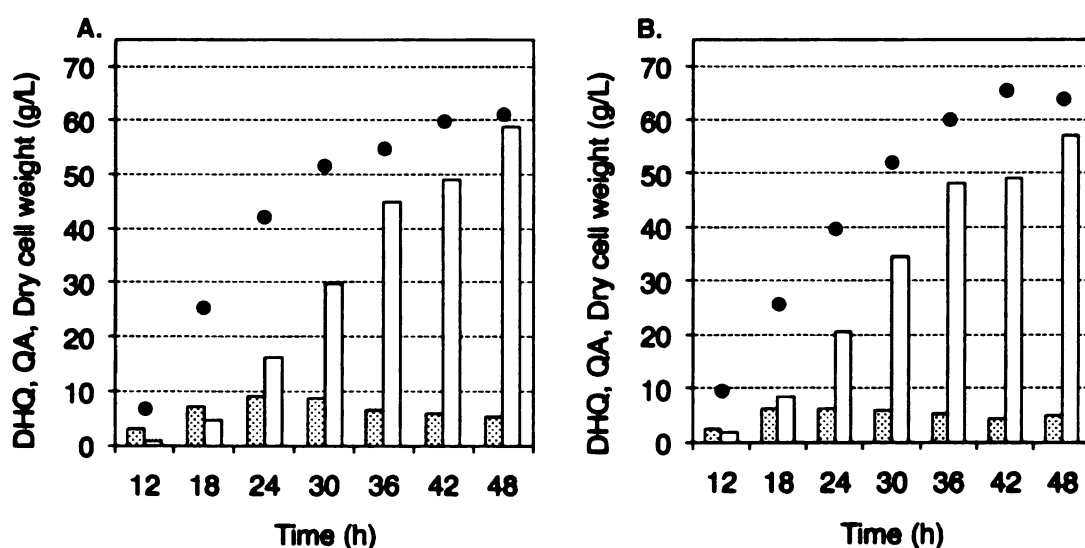
Figure 7. (A) *E. coli* QP1.1/pKD12.138 and (B) QP1.1/pNR4.230 cultured under glucose-limited conditions. Legend: (dotted bars) 3-dehydroquinic acid, (open bars) quinic acid, (black circles) dry cell weight.

Table 4. Concentrations and yields of products synthesized by quinic acid producing strains with plasmid-overexpression of *ydiB* or *aroE*.

Entry	Construct	[DHQ][c] g/L	[QA], g/L	QA[d] yield, %	Total yield,[e] %
1[a]	QP1.1/pKD12.138	5	58	21	22
2[a]	QP1.1/pNR4.230	5	57	22	22
3[a]*	QP1.1/pJJ4.171	52	0	0	21
4[b]*	QP1.1/pJJ4.171	50	0	0	21
5[a]*	QP1.1/pJJ5.069	62	11	4	26
6[b]*	QP1.1/pJJ5.069	48	8	3	19
7[a]*	QP1.1/pJJ5.073	12	20	5	12

[a]Glucose-limited conditions. [b]Glucose-rich conditions. * Single run fermentation. [c]Abbreviations: DHQ – 3-dehydroquinic acid, QA – quinic acid. [d](mol QA)/(mol glucose consumed). [e](mol DHQ + mol QA)/(mol glucose consumed).
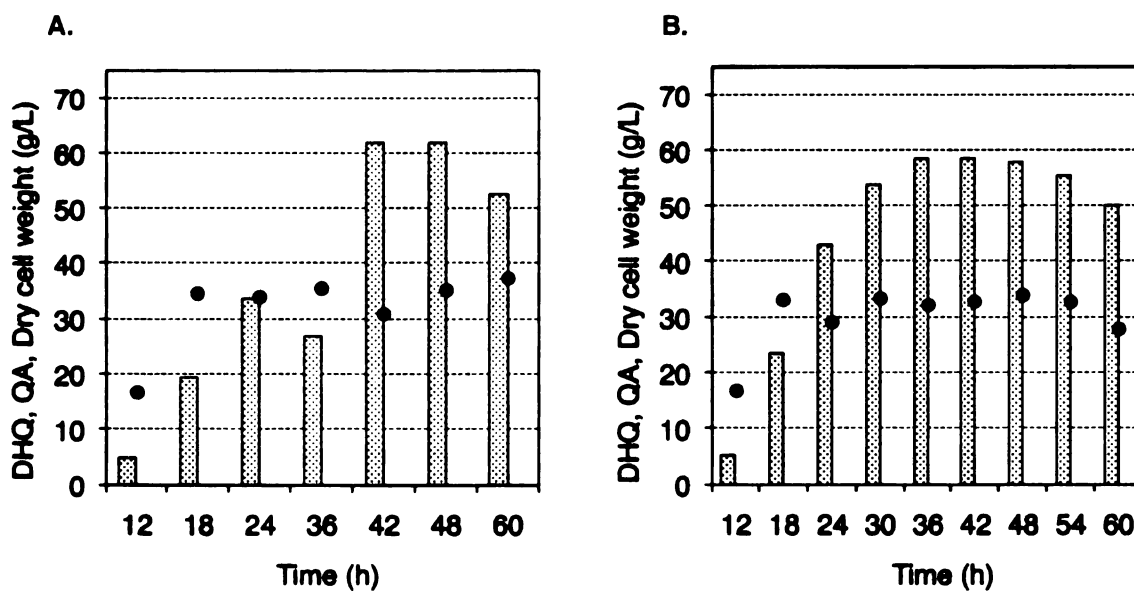
Figure 8. (A) *E. coli* QP1.1/pJJ4.171 cultured under glucose-limited culture conditions and (B) QP1.1/pJJ4.171 cultured under glucose-rich culture conditions. Legend: (dotted bars) 3-dehydroquinic acid, (open bars) quinic acid, (black circles) dry cell weight.

Similar gene overexpression problem were previously encountered when attempts to overexpress the ORF *adk*-encoded of adenylate kinase from a P_{tac} promoter did not yield assayable enzyme activity.[19] When 30 bp upstream from *E. coli* genomic *adk* were included with the *adk* ORF, successful overexpression of Adk was achieved.[20, 19] The same strategy was applied for *ydiB* cloning and expression. Two final plasmids were constructed in order to evaluate *ydiB* overexpression and quinic acid production under fermentor-controlled conditions. Plasmid pJJ5.069 was designed to be identical to pKD12.138 except $P_{aroE}aroE$ was replaced by $P_{tac}ydiB$ with 31 bp upstream genomic sequence included. Plasmid pJJ5.073 was constructed in the pKK223-3 cloning vector, rather than vector pSU18 as used for construction of plasmids pKD12.138 and pJJ5.069.

Construction of plasmid pJJ5.067 began with PCR amplification of a 0.9 kb *ydiB* fragment with a 31 bp upstream sequence (*ydiB*+31bp) from *E. coli* W3110 genomic DNA. The isolated PCR fragment was inserted into *Eco*RI and *Sma*I cloning site of the pKK223-3 vector (Figure 9). Since the target plasmid pJJ5.069 had to be as close as possible to pKD12.138, therefore plasmid pKD12.112 was chosen as the starting point for construction of the plasmid carrying the *ydiB* + 31 bp insert.

Digestion of plasmid pKD12.112 with *Kpn*I and *Bam*HI restriction endonucleases lead to loss of the 3.2 kb $P_{tac}aroE$ *serA* fragment. PCR amplified $P_{tac}ydiB$+31bp fragment from pJJ5.067 with *Kpn*I and *Bam*HI ends was inserted into linerized pKD12.112 yielding plasmid pJJ5.068 (Figure 10) after ligation. Digestion of plasmid pNR8.146A with *Xba*I restriction endonuclease liberated an intact 3.8 kb *tktA* *serA*

fragment, which was cloned into pJJ5.068 previously pretreated with XbaI to afforded

target plasmid pJJ5.069 (Figure 11).
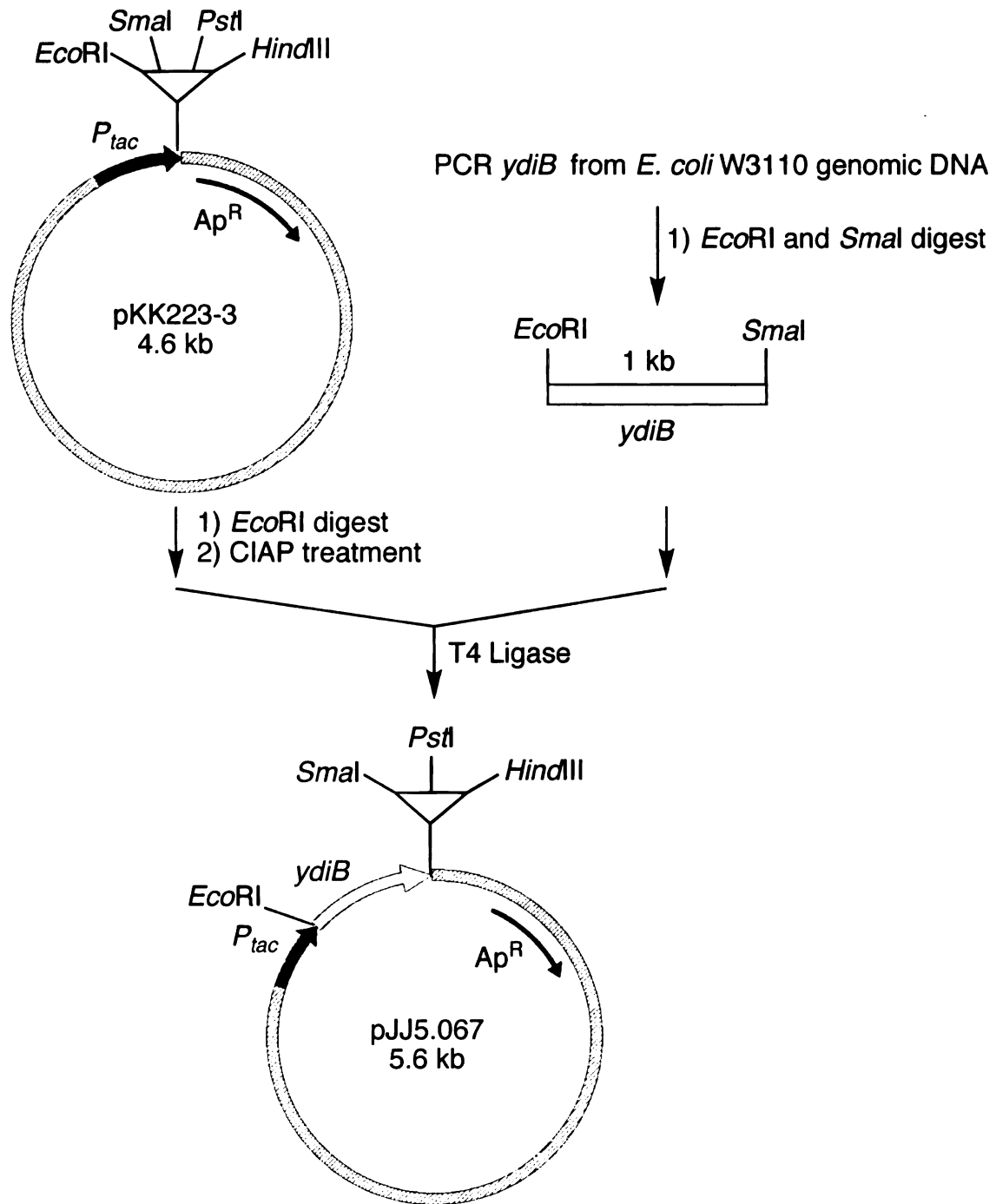
Figure 9. Construction of plasmid pJJ5.067.
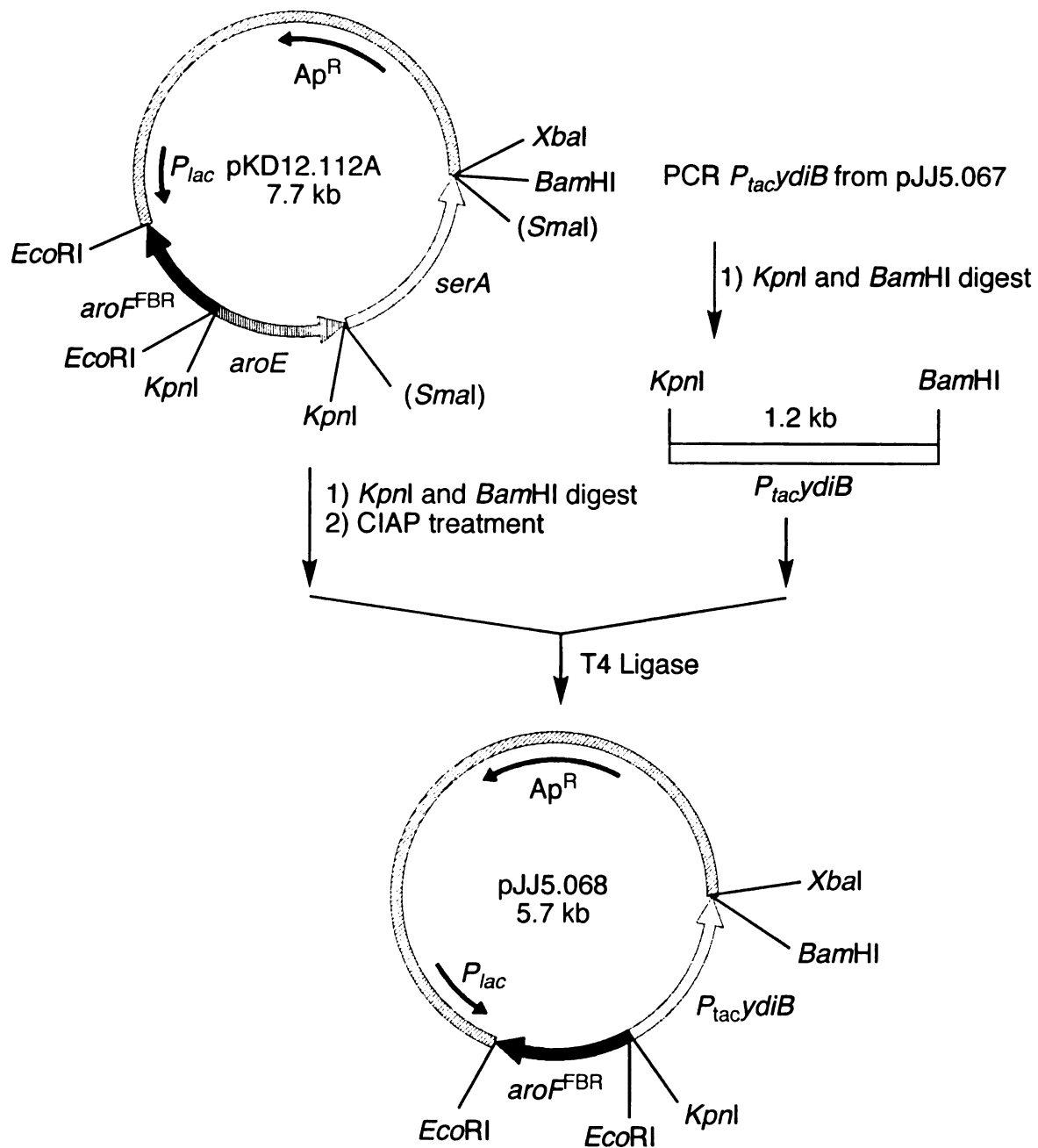
Figure 10. Construction of plasmid pJJ5.068.
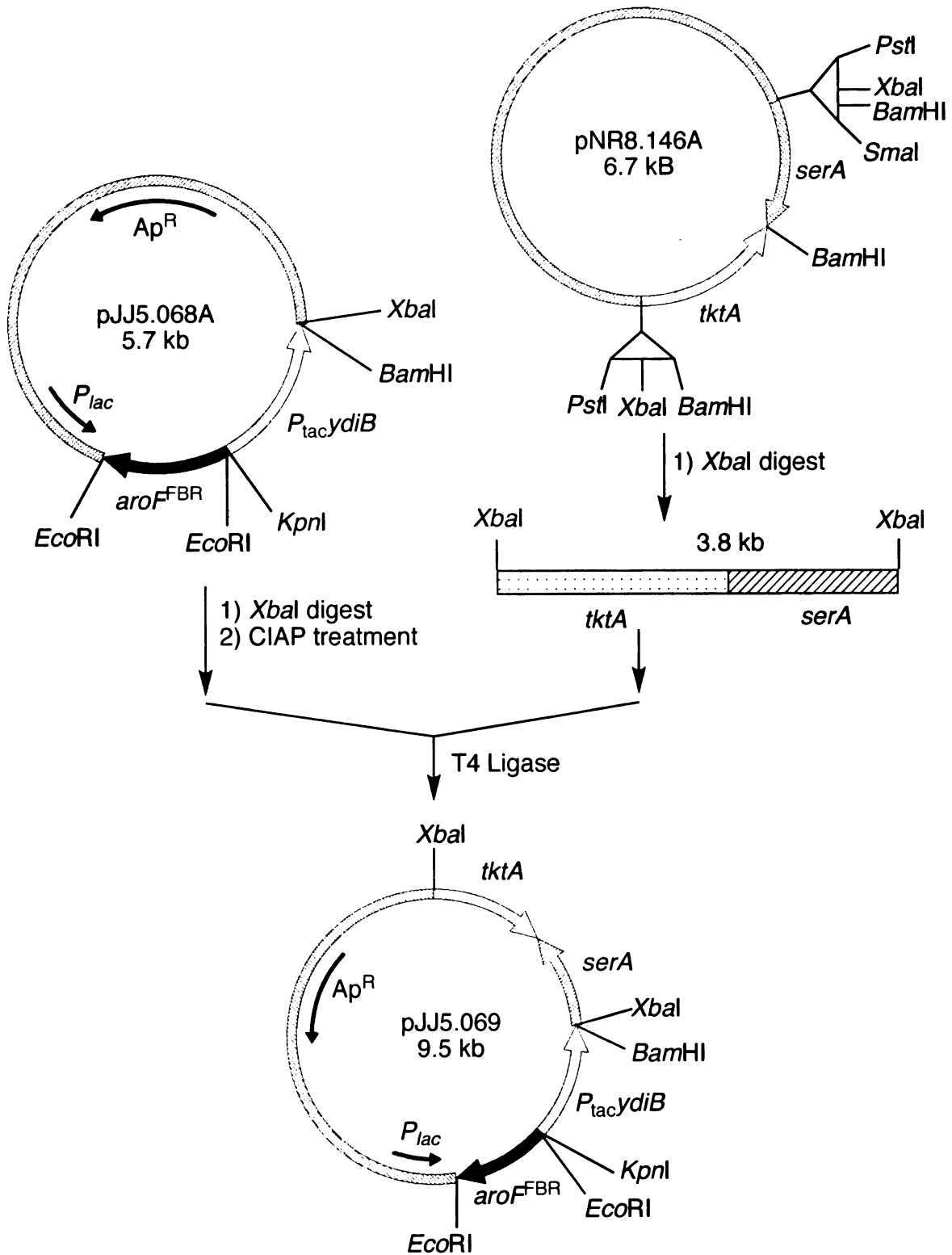
Figure 11. Construction of plasmid pJJ5.069
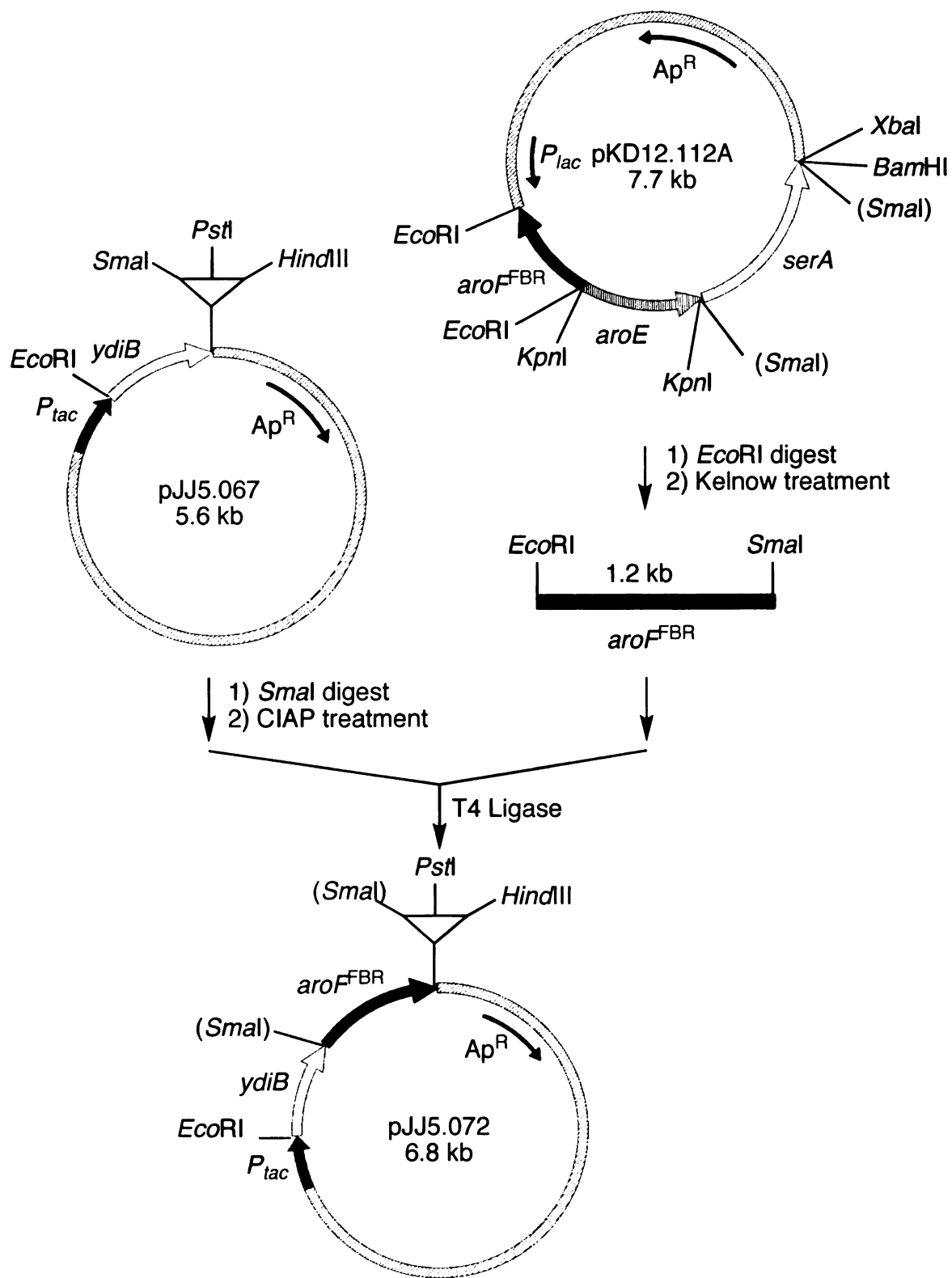
Figure 12. Construction of plasmid pJJ5.072.

42
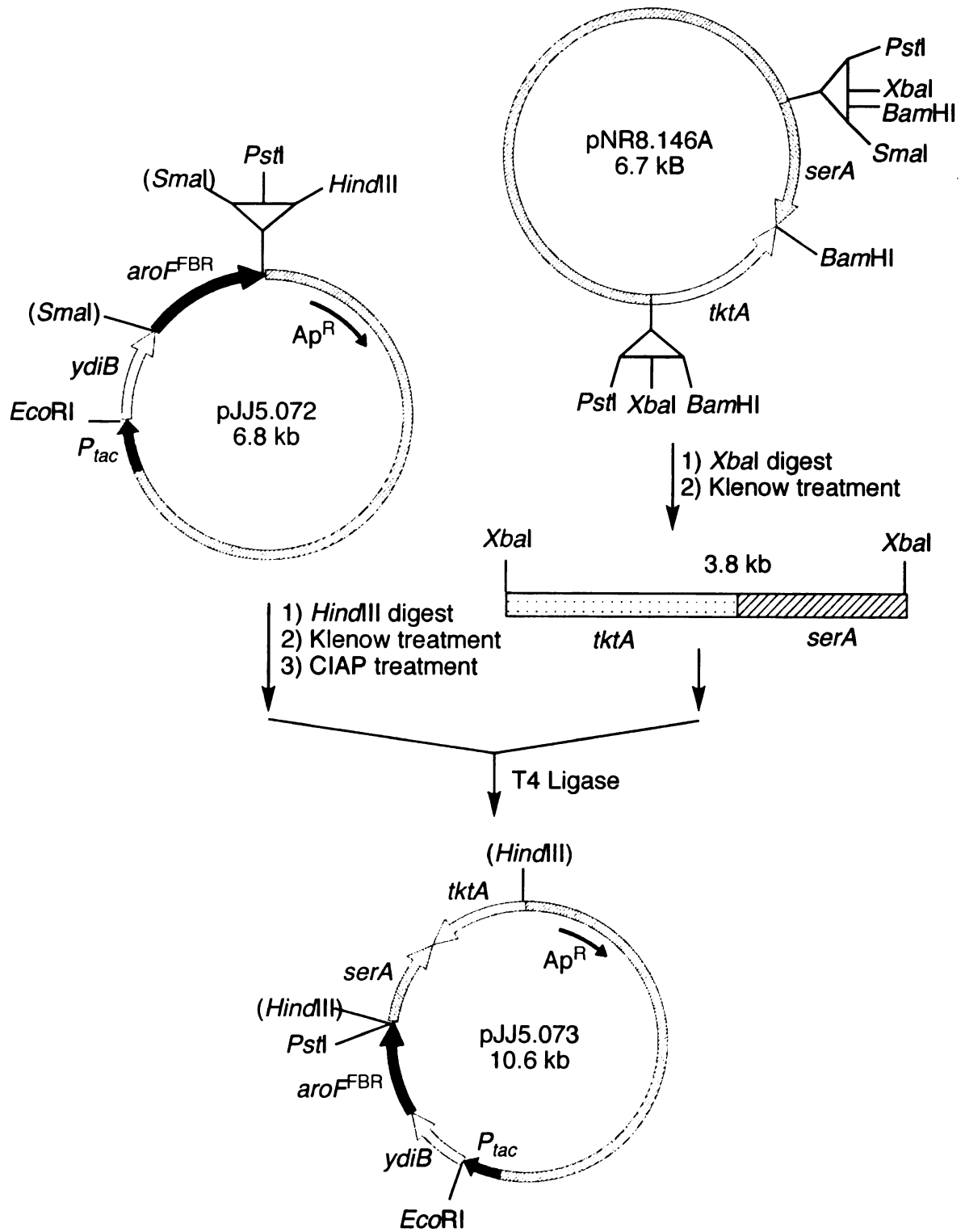
Figure 13. Construction of plasmid pJJ5.073.

Another plasmid pJJ5.073, had the same genomic elements as pJJ5.069, except that the parent vector was pKK223-3 rather than pSU18. The construction of pJJ5.073 started with digestion of pKD12.112 using $EcoRI$ restriction endonuclease followed by agarose gel isolation of a 1.2 kb $aroF^{FBR}$ fragment and Klenow treatment with dNTPs. The liberated $aroF^{FBR}$ fragment was inserted into previously $SmaI$ digested pJJ5.067, which resulted in pJJ5.072 (Figure 12). Digestion of plasmid pNR8.146A with $XbaI$ restriction endonuclease liberated an intact 3.8 kb $tktA$ $serA$ fragment, which was treated with Klenow. Insertion of this Klenow-treated $tktA$ $serA$ fragment into $HindIII$-digested and Klenow-treated pJJ5.072 afforded target plasmid pJJ5.073 (Figure 13).

Newly constructed plasmids were evaluated under fermentor-controlled conditions. $E.$ $coli$ QP1.1/pJJ5.069 produced 11 g/L of quinic in 4% yield under glucose-limited conditions (Table 4, entry 5; Figure 14A) and 8 g/L in 3% yield under glucose-rich conditions (Table 4, entry 6; Figure 14B). The major byproduct for both fermentations was 3-dehydroquinic acid, which accumulated to 62 g/L (Table 4, entry 5) and 48 g/L (Table 4, entry 6). The total yield of synthesized hydroaromatics (3-dehydroquinic acid + quinic acid) was 26% for QP1.1/pJJ5.069 cultivated under glucose-limited conditions and 19% for QP1.1/pJJ5.069 cultivated under glucose-rich conditions. These yields are close to the 22% observed for the control strains (Table 4, entry 1 and 2). This indicated that the carbon flow directed into the shikimate pathway was the same and only the last step, reduction of 3-dehydroquinic acid to quinic acid, was not as efficient for QP1.1/pJJ5.069 relative to QP1.1/pKD12.138.
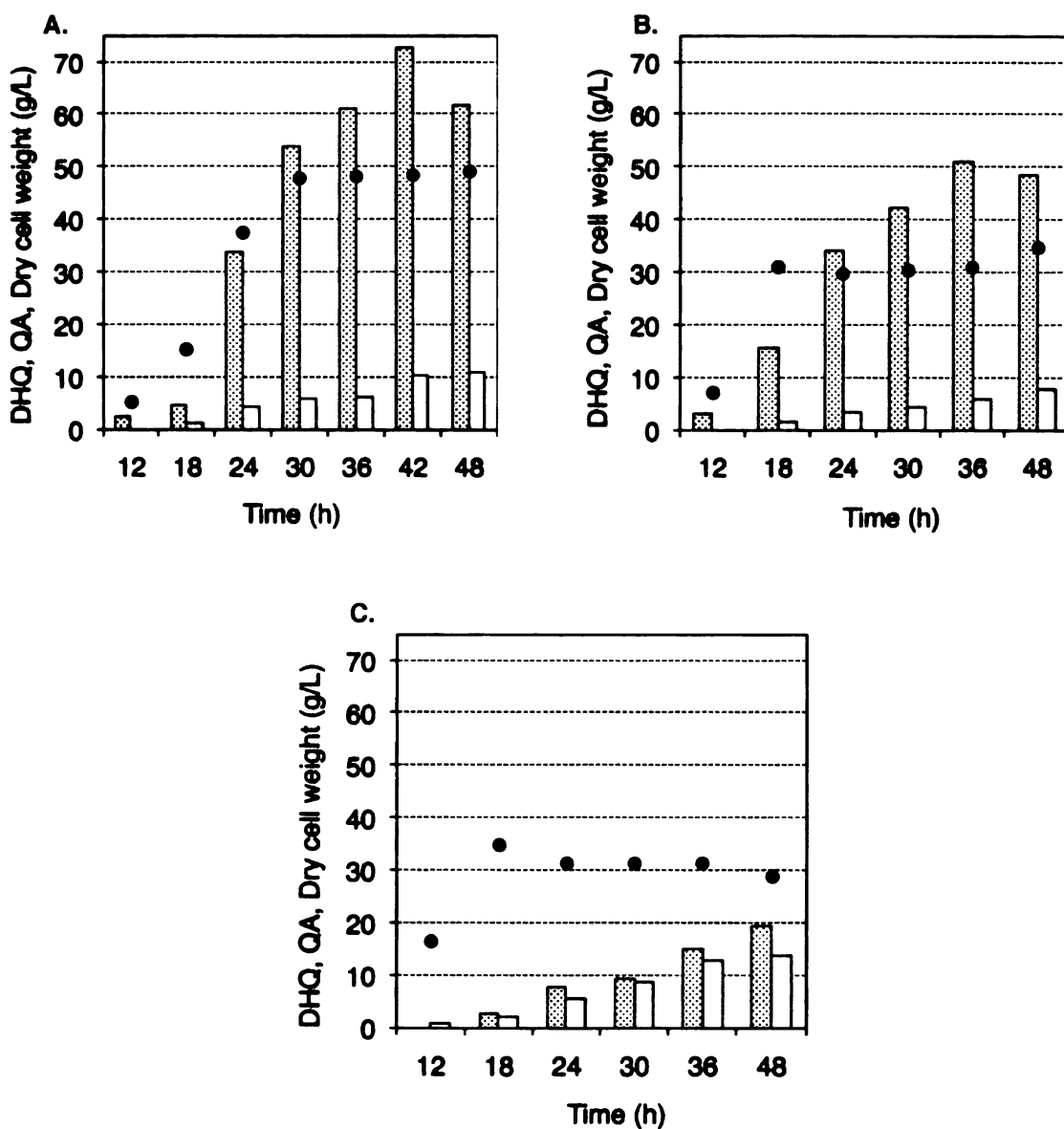
Figure 14. (A) *E. coli* QP1.1/pJJ5.069 cultured under glucose-limited conditions, (B) QP1.1/pJJ5.069 cultured under glucose-rich conditions and (C) QP1.1/pJJ5.073 under glucose-limited conditions. Legend: (dotted bars) 3-dehydroquinic acid, (open bars) quinic acid, (black circles) dry cell weight.

YdiB enzymatic activities were assayed in order to determine why 3-dehydroquinic acid reduction was deficient. Previously reported YdiB can utilize shikimic acid and quinic acid as substrates as well as NAD$^+$ and NADP$^+$ as cofactors. New constructs were assayed in the forward direction, *i.e.* reduction of 3-dehydroquinic

45

acid or 3-dehydroshikimic acid with NADH or NADPH. *E. coli* host QP1.1 showed

background shikimate/quinate dehydrogenase specific activity at around 0.1 U/mg (Table

5, entries 1-4). *E. coli* hosts DH5α and RB791*serA::aroB* had similar background

shikimate/quinate dehydrogenase activities relative to QP1.1. Based on the measured

quinate dehydrogenase specific activity with NADPH as the cofactor (Table 5, entry 6)

versus NADH as the cofactor (Table 5, entry 6), NADPH appears to be the preferred

cofactor for quinate dehydrogenase. YdiB with NADPH displayed a twofold higher

specific activity for reduction of 3-dehydroshikimic acid (Table 5, entry 7) relative to

reduction of 3-dehydroquinic acid (Table 5, entry 5). QP1.1/pJJ5.067 had approximately

tenfold higher quinate dehydrogenase activity (Table 5, entry 5) as compared to the

background quinate dehydrogenase activity in host *E. coli* QP1.1 (Table 5, entry 1). This

indicated that overexpression of *ydiB* was being achieved. *E. coli*

RB791*serA::aroB*/pJJ5.069 showed only background level quinate dehydrogenase

activity (Table 5, entry 10). This level of quinate dehydrogenase activity is consistent

with 3-dehydroquinic acid being the major product synthesized by QP1.1/pJJ5.069 under

fermentor-controled conditions. The discovery that final plasmid pJJ5.069 had no or

poor overexpression of plasmid-localized *ydiB*, served as the reason to construct a new

plasmid pJJ5.073 where *ydiB* in the final construct was not a PCR product as was the

ydiB insert in pJJ5.069. Even a high fidelity DNA polymerase can result in spontaneous

mutation during PCR.

Table 5. YdiB specific acitivities.

Entry	Construct	Substrate, Cofactor	Specific activity,[a] U/mg
1	QP1.1	DHQ, NADPH	0.14
2	QP1.1	DHQ, NADH	0.09
3	QP1.1	DHS, NADPH	0.14
4	QP1.1	DHS, NADH	0.01
5	QP1.1/pJJ5.067	DHQ, NADPH	1.29
6	QP1.1/pJJ5.067	DHQ, NADH	0.21
7	QP1.1/pJJ5.067	DHS, NADPH	2.34
8	QP1.1/pJJ5.067	DHS, NADH	0.20
9	DH5α/pJJ5.068	DHQ, NADPH	0.69
10	RB791serA::aroB/pJJ5.069	DHQ, NADPH	0.13
11	RB791serA::aroB/pJJ5.073	DHQ, NADPH	0.10

[a] One unit (U) of shikimate/quinate dehydrogenase corresponds to the formation of 1 μmole of NAD(P) in the presence of 3-dehydroshikimic or 3-dehydroquinic acid per min at 25 °C.

E. coli QP1.1/pJJ5.073 was evaluated under fermentor-controled glucose-limited conditions. This time it produced 14 g/L of quinic acid in 5% yield (Table 4, entry 7; Figure 14C). It was the best quinic acid producer with *ydiB* overexpression, but it produced fourfold less of quinic acid as compared to the control strains (Table 4, entry 1). Total hydroaromatics yield of 12% was also low as compared to the 22% produced by QP1.1/pKD12.138. 3-Dehydroquinic acid also accumulated at leaser (19 g/L, Table 4, entry 7) concentrations as compared to the 62 g/L produced by QP1.1/pJJ5.069 (Table 4, entry 5). This could indicate that *E. coli* QP1.1/pJJ5.073 had less carbon flow directed to the shikimate pathway. Quinate dehydrogenase activity for RB791serA::aroB/pJJ5.073 revealed 0.10 U/mg of specific activity which is at the same level as the background *E. coli* quinate dehydrogenase specific activity (Table 5, entry 1). Even though parent plasmid pJJ5.067 had twenty-fold higher quinate dehydrogenase activity, after inserting shared genomic elements, the final activity dropped down to the host levels, no matter how the quinate-synthesizing strains QP1.1/pJJ5.069 and QP1.1/pJJ5.073 were

constructed. Further pursuit of using YdiB to replace AroE as the shikimate/quinate dehydrogenase in quinate-synthesizing constructs was abandoned due to low YdiB activities in the final constructs.

E. coli B as a quinic acid producer

E. coli QP1.1 is a K-12 strain. Investigation of *E. coli* B as a host strain for the quinic acid production was pursued for a couple of reasons. From previous experiments in the Frost group, it was discovered that *E. coli* B has higher native transketolase specific activity than *E. coli* K-12.[21] Plasmid-localized transketolase overexpression might not be necessary for quinic acid production. Secondly, *E. coli* B is deficient in Lon proteases,[22] which are the major proteases catalyzing the endoproteolytic cleavage of proteins in the cell. High and more stable DAHP synthase and transketolase activity levels might therefore be in *E. coli* B, especially in the stationary phase, might therefore be realized in *E. coli* B.[22] Strains disrupted in the *lon* gene produce several phenotypic changes including increased sensitivity to UV and ionizing radiation, overproduction of mucopolysaccharide, reduced lysogenization of bacteriophages lambda and P1, and most importantly, reduced protein degradation.[22d]

Synthesis of quinic acid requires an inactive 3-dehydroquinate dehydratase encoded by *aroD* as well as a second copy of 3-dehydroquinate synthase encoded by *aroB*.[5] *E. coli* B *serA::aroB* was previously constructed.[21] Only *aroD* inactivation was required to afford an *E. coli* B host suitable for synthesis of quinic acid.

Wanner and coworkers have developed a method for gene deletion or disruption in *E. coli* (Figure 15).[23] The first step involves PCR of an antibiotic gene flanked by two FRT (flippase recognition target) sequences. Primers for this PCR step are designed in such a way that the first 40-50 bp sequence (H1 or H2) is homologous to the gene of interest that is going to be disrupted. The last 20 bp of the primer are homologous to the priming sequence (P1 and P2) before the FRT sites in the template plasmids. The template plasmids used in this work were pKD3, which encodes for chloramphenicol resistance, or pKD4, which encodes for kanamycin resistance. In the second step, a target *E. coli* host is transformed with the plasmid pKD46, which expressed bacteriophage λ Red recombinase from an inducible arabinose promoter. *E. coli* with λ Red recombinase is transformed with the PCR product from the first step, and the mutants are selected on antibiotic plates. The key factor of this step is the transformation efficiency. Since, transformation is performed with linear DNA from the PCR step, endogenous nucleases start degrading this linear DNA prior to completion of the recombination step. Therefore, a high transformation efficiency of 10^8-10^9 transformants per μg of DNA is required in order to obtain several mutants. Elimination of the antibiotic resistance marker is performed by transforming the mutant *E. coli* with plasmid-encoded FLP flippase pCP20,[24] which acts on the two FRT sites flanking the antibiotic gene. Flippase in pCP20 is transcribed from a temperature inducible promoter and the plasmid has a temperature-sensitive replicon, as well as ampicillin and chloramphenicol resistance genes. *E. coli* is transformed with pCP20 and ampicillin-resistant mutants are selected at 30 °C, after which a few single colonies are incubated at 43 °C in order to induce FLP synthesis and promote plasmid pCP20 loss. A mutant *E.*

coli strain with knocked-out gene is obtained with a small FRT scar (Figure 15, step 4.).

Helper plasmid encoding for λ Red recombinase pKD46, template plasmids pKD3 and

pKD4, and FLP-encoding plasmid pCP20 were purchased from *E. coli* Genetic Stock

Center at Yale University.

PCR amplify FRT-flanked resistance gene

1.

Transform strain expressing λ Red recombinase

2.

Select antibiotic-resistant transformants

3.

Eliminate resistance cassette using FLP expression plasmid

4.
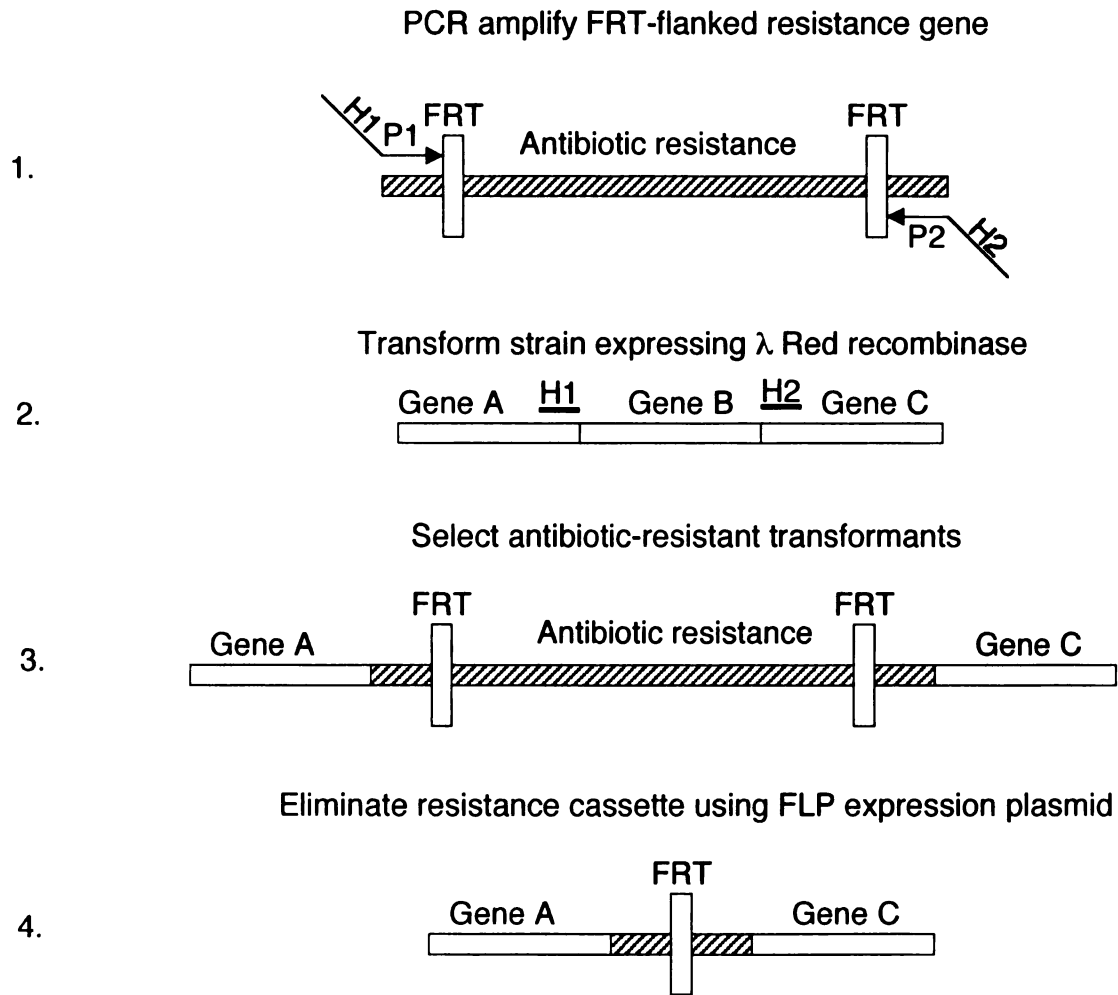
Figure 15. Gene deletion method in *E. coli*.

From previous experience in the Frost group, it was known that wild-type *E. coli*

B has very low transformation efficiency. Therefore, a strategy (Figure 16) was

employed to first delete the *aroD* gene in E. *coli* W3110 K-12 and then use P1 phage to transduce the mutation into E. *coli* B.[25] Construction of the E. *coli* W3110 *aroD*(-) mutant started with primer H1P1 and H2P2 design. The H1 sequence was chosen to be first 40 bp of *aroD* ORF (5'-ATGAAAACCGTAACTGTAAAAGATCTCGTCA-TTGGTACGG-3') and the H2 sequence was designed to be last 40 bp of *aroD* ORF (5'-TTATGCCTGGTGTAAAATAGTTAATACCGTGCGCAAATCA-3'). P1 (5'-GTGT-AGGCTGGAGCTGCTTC-3') and P2 (5'-CATATGAATATCCTCCTTAG-3') sequences were based on template pKD3.[23] A 1.1 kb PCR product was electroporated into E. *coli* W3110/pKD46 overexpressing λ Red recombinase. The mutants were selected on LB/Cm plates and the phenotype of obtained mutants screened by replication on selective plates. Since *aroD* is gene in the shikimate pathway, E. *coli* bearing inactive *aroD* will not be able to grow on glucose-minimal plates without aromatic amino acid and aromatic vitamin supplementation. Mutants also should grow on LB/Cm plates, due to FRT-*cat*-FRT insertion in the *aroD* gene. Sensitivity to ampicillin should indicate a loss of pKD46 or pCP20 plasmid. Several mutants were screened for the desired phenotype. E. *coli* W3110 showed sensitivity to the ampicillin and chloramphenicol but did not require aromatics or serine supplementation for growth on glucose-minimal plates (Table 6, entry 1). Mutant E. *coli* W3110 Δ*aroD*::FRT–*cat*–FRT required aromatic amino acid and aromatic vitamin supplementation while grown on glucose-minimal salts plates, and it was sensitive to ampicillin but not to chloramphenicol (Table 6, entry 4). The mutant was also confirmed by PCR. PCR primers V1 and V2 (Figure 16, Step 2) were designed to have homology outside H1 and H2 region. Therefore the PCR product for wild-type E. *coli* W3110 was expected to be approximately 1kb and for the mutant it

51

was expected to be 1.2 kb. PCR screening revealed a 1.2 kb size product on agarose gel for the mutant and a 1kb for the wild-type control. Both, phenotype screening and PCR verification suggested that obtained *E. coli* W3110 Δ*aroD*::FRT–*cat*–FRT was the correct mutant.

Table 6. Screening for *E. coli* mutant phenotype.

Entry	Strain	M9/Gluc [c]	M9/Gluc/Ser	M9/Gluc/Aros	M9/Gluc/Aros/Ser	LB/Ap	LB/Cm	LB
1	*E. coli* W3110	+	+	+	+	−	−	+
2	*E. coli* B	+	+	+	+	−	−	+
3	*E. coli* B *serA::aroB*	−	+	−	+	−	−	+
4	*E. coli* W3110 Δ*aroD*::FRT-*cat*-FRT	−	−	+	+	−	+	
5[a]	*E. coli* W3110 Δ*aroD*::FRT-*cat*-FRT	−	−	+	+	−	+	
6	*E. coli* B *serA::aroB* Δ*aroD*::FRT-*cat*-FRT	−	−	−	+	−	+	
7	*E. coli* W3110 Δ*aroD*::FRT- *cat* -FRT (new)	−	−	+	+	−	+	
8[b]	*E. coli* W3110 Δ*aroD*::FRT- *cat* -FRT (new)	−	−	+	+	−	+	
9	*E. coli* B *serA::aroB* Δ*aroD*::FRT- *cat* -FRT (new)	−	−	−	+	−	+	
10	*E. coli* B *serA::aroB* Δ*aroD*::FRT (new)	−	−	−	+	−	−	+

[a] *E. coli* W3110 was transduced with P1-W3110 Δ*aroD*::FRT-*cat*-FRT. [b] *E. coli* W3110 was transduced with P1-W3110 Δ*aroD*::FRT-*cat*-FRT (new). [c] Abbreviations: Gluc – glucose, Ser – L-serine, Aros – aromatic amino acids (L-phenylalanine, L-tyrosine and L-tryptophan) and aromatic vitamins (2,3-dihydroxybenzoic acid, *p*-aminobenzoic acid and *p*-hydroxybenzoic acid), Ap – ampicillin, Cm – chloramphenicol. Note: Five colonies of each strain were screened per selective plate.

1. PCR amplify insert with FRT-flanked resistance gene

pKD3 $\qquad$ H7P1 FRT $\qquad$ FRT $\qquad$

P2

Cm^R H2
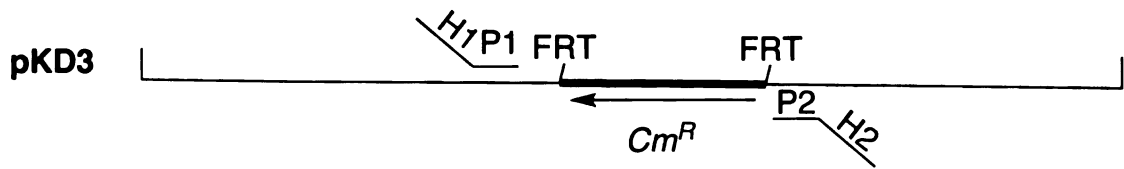
2. Transform fragment into W3110 expressing λ Red recombinase and select for chloramphenicol resistance

ydiB   V1   H1   P1FRT   FRT   ydiF

aroD   Cm^R P2 H2 V2
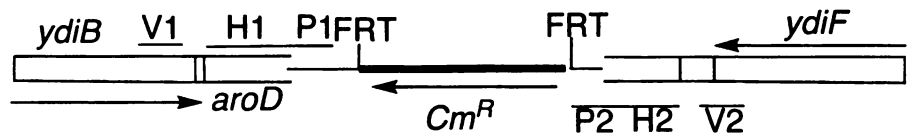
3. P1 phage-mediated transduction to *E. coli* B *serA::aroB*

4. Eliminate chloramphenicol resistance using FLP

ydiB   FRT   ydiF

E. coli B *serA::aroB* Δ*aroD::*FRT
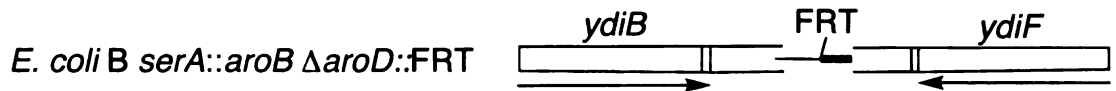
Figure 16. Construction of *E. coli* Δ*aroD*::FRT mutant.

P1 phage-mediated transduction was used to transfer the Δ*aroD*::FRT–*cat*–FRT mutation from *E. coli* W3110 Δ*aroD*::FRT–*cat*–FRT to *E. coli* B *serA::aroB*. Mutants were screened for the correct phenotype and were verified by PCR analysis. Wild-type *E. coli* W3110 also was used as a control strain for the P1 phage-mediated transduction. *E. coli* W3110 mutants obtained by plate after P1 transduction showed identical growth characteristics (Table 6, entry 5) as the donor strain (Table 6, entry 4). Candidate *E. coli* B *serA::aroB* Δ*aroD*::FRT–*cat*–FRT mutants also showed the correct growth pattern by requiring aromatics and serine supplementation for growth on glucose-minimal plates and displaying sensitivity towards ampicillin but not to chloramphenicol. Mutants required serine supplementation due to the *aroB* insertion into the *serA* locus in the parent *E. coli* B *serA::aroB* strain (Table 6, entry 3). Attempted PCR verification of the mutants

revealed quite unexpected results. PCR with *E. coli* B *serA::aroB* as a template afforded

a 1 kb sized DNA fragment on the agarose gel as was expected. However, the PCR

product from *E. coli* B *serA::aroB* Δ*aroD*::FRT–*cat*–FRT and an *E. coli* W3110

Δ*aroD*::FRT–*cat*–FRT (transduced) was 2.2 kb, in contrast to the 1.2 kb. This indicated

that there was an additional 1kb DNA fragment inserted together with the FRT–*cat*–FRT

cassette. Removal of the antibiotic resistance gene from the mutants (Table 6, entry 5

and 6) with plasmid pCP20-encoded flippase was unsuccessful as they still showed

resistance to chloramphenicol and a PCR product size of 2.2 kb. While a new strategy

was formulated and was executed, *E. coli* B *serA::aroB* Δ*aroD*::FRT–*cat*–FRT host was

evaluated under glucose-limited fermentor-controlled conditions.

E. coli B *serA::aroB* Δ*aroD*::FRT–*cat*–FRT/pKD12.112 produced 4 g/L of quinic

acid in 5% yield over 60 h of cultivation under fermentor-controlled conditions (Table 7,

entry 1). The major hydroaromatic metabolite was 3-dehydroquinic acid, which

accumulated to 43 g/L. The overall hydroaromatic yield was 22%. Very similar results

were obtained for the *E. coli* B *serA::aroB* Δ*aroD*::FRT–*cat*–FRT /pKD12.138, which

had plasmid localized-*tktA*, and synthesized 4 g/L of quinic acid together with 42 g/L of

3-dehydroquinic acid with an overall 18% yield of hydroaromatics in 60 h (Table 7, entry

2). The same concentrations of hydroaromatics indicated that transketolase

overexpression was not necessary in a *E. coli* B host, as had been anticipated. *E. coli* B

synthesis of quinic acid without transketolase overexpression showed even higher overall

yield relative to overexpression of transketolase. Interestingly, both fermentations

produced less biomass at about 22 g/L (Figure 17) relative to QP1.1/pKD12.138, which

produced approximately 60 g/L of dry cell weight (Figure 7A and Figure 25A).

Table 7. Concentrations and yields of products synthesized by quinic acid producing *E. coli* B strains under glucose-limited conditions.

Entry	Construct	Time, h	[DHQ]^a g/L	[QA], g/L	QA^b yield, %	Total^c yield, %
1	*E. coli* B *serA::aroB* Δ*aroD*::FRT–*cat*–FRT /pKD12.112	60	43	4	5	22
2	*E. coli* B *serA::aroB* Δ*aroD*::FRT–*cat*–FRT /pKD12.138	60	42	4	6	18
3*	*E. coli* B *serA::aroB* Δ*aroD* (new)::FRT–*cat*–FRT /pKD12.112	60	18	40	17	24
4*	*E. coli* B *serA::aroB* Δ*aroD* (new)::FRT–*cat*–FRT /pKD12.138	60	13	41	19	25
5*	*E. coli* B *serA::aroB* Δ*aroD* (new)::FRT–*cat*–FRT /pKD12.112	84	28	37	10	18
6*	*E. coli* B *serA::aroB* Δ*aroD* (new)::FRT–*cat*–FRT /pKD12.138	84	14	32	10	15
7	*E. coli* B *serA::aroB* Δ*aroD* (new)::FRT /pKD12.112	84	7	22	10	13
8*	*E. coli* B *serA::aroB* Δ*aroD* (new)::FRT /pKD12.138	84	11	42	17	21

* Single run fermentation. ^{a}Abbreviations: DHQ – 3-dehydroquinic acid, QA – quinic acid. ^{b}(mol QA)/(mol glucose consumed). ^{c}(mol DHQ + mol QA)/(mol glucose consumed).

Figure 17. (A) *E. coli* B *serA::aroB* Δ*aroD*::FRT–*cat*–FRT/pKD12.112 and (B) *E. coli* B *serA::aroB* Δ*aroD*::FRT–*cat*–FRT/pKD12.138 cultured under glucose-limited conditions. Legend: (dotted bars) 3-dehydroquinic acid, (open bars) quinic acid, (black circles) dry cell weight.

The same strategy was repeated multiple times in order to obtain an *E. coli* B

serA::aroB Δ*aroD*::FRT–*cat*–FRT mutant and every time the same 2.2kb sized DNA

fragment was obtained after PCR analyzis. This clearly indicated that it was not a

spontaneous mutation, and suggested a fundamental problem with the way *aroD* was

being deleted. The PCR product from a couple of different mutants was sequenced with

the same V1 and V2 primers in order to determine why the PCR product size was 2.2 kb

rather than 1.2 kb as had been expected. Sequencing was done at the Research

Technology Support Facility at Michigan State University.

```
  1 ctgacaggct gaccgcgtgc agaaagggta aaaaATGAAA ACCGTAACTG
 51 TAAAAGATCT CGTCATTGGT ACGGgtgtag gctggagctg cttcgaagtt
101 cctatacttt ctagagaata ggaacttcgg aataggaact tcATTTAAAT
151 GGCGCGCCTT ACGCCCCGCC CTGCCACTCA TCGCAGTACT GTTGTAATTC
201 ATTAAGCATT CTGCCGACAT GGAAGCCATC ACAAACGGCA TGATGAACCT
251 GAATCGCCAG CGGCATCAGC ACCTTGTCGC CTTGCGTATA ATATTTGCCC
301 ATGGTGAAAA CGGGGGCGAA GAAGTTGTCC ATATTGGCCA CGTTTAAATC
351 AAAACTGGTG AAACTCACCC AGGGATTGGC TGAGACGAAA AACATATTCT
401 CAATAAACCC TTTAGGGAAA TAGGCCAGGT TTTCACCGTA ACACGCCACA
451 TCTTGCGAAT ATATGTGTAG AAACTGCCGG AAATCGTCGT GGTATTCACT
501 CCAGAGCGAT GAANACGTTT CAGTTTGCTC ATGGAAAACG GTGTAACAAG
551 GGTGAACACT ATCCCATATC ACCAGCTCAC CGTCTTTCAT TGCCATACGT
601 AATTCCGGAT GAGCATTCAT CAGGCGGGCA
```

Figure 18. Sequencing of the 5' end of PCR product with V1 primer of *E. coli* B
serA::aroB Δ*aroD*::FRT–*cat*–FRT **2.2 kb PCR product.** Legend: atgc – *aroD*
upstream sequence; ATGC – *aroD*; atgc – P1 or P2 on pKD3; *atgc* – FRT; *ATGC*
– *cat*.

Sequencing results of the 5' end of PCR product did not show any unexpected

sequence. Small letters in Figure 18 represents *E. coli* DNA sequence upstream of *aroD*

gene with a 100% identity. This sequence is followed by 40 bp H1 sequence of *aroD*

(ATGC) and 20 bp of P1 sequence from pKD3 template (atgc). The entire 48 bp FRT

sequence (*atgc*) was also present. The rest of the sequence (*ATGC*) corresponded to *cat*
gene sequence responsible for the chloramphenicol resistance.

Sequencing of the 2.2 kb 3' end PCR product revealed different result (Figure
19). It had the *aroD* downstream sequence (atgc) followed by the 40 bp H2 sequence of
aroD (ATGC) and 20 bp of P2 sequence from the pKD3 template (at**g**c). However, only
28 bp of the FRT (*atgc*) sequence was found and it was followed by an *E. coli* IS5
transposase and transactivator seguence (*nmpC*), which was determined using BLSAT
analysis. *E. coli* genomic sequence revealed that *aroD* and *nmpC* sequences are 1.2 x 10⁶
bp apart. Three mutants from different cloning attempts were submitted for sequencing
analysis and all of them revealed identical results. Even though *aroD* and *nmpC* share
only 3% sequence identity, it was postulated that deletion of the entire *aroD* ORF was
problematic.

```
  1 ttttttagtt cggcggggag ggtgttcccg ccgaaatatt attgcTTATG
 51 CCTGGTGTAA AATAGTTAAT ACCGTGCGCA AATCAcatat gaatatcctc
101 cttagttcct attccgaagt tcctattctc tagGGAAGGT GCGAATAAGC
151 GGGGAAATTC TTCTCGGCTG ACTCAGTCAT TTCATTTCTT CATGTTTGAG
201 CCGATTTTTT CTCCCGTAAA TGCCTTGAAT CAGCCTATTT AGACCGTTTC
251 TTCGCCATTT AAGGCGTTAT CCCCAGTTTT TAGTGAGATC TCTCCCACTG
301 ACGTATCATT TGGTCCGCCC GAAACAGGTT GGCCAGCGTG AATAACATCG
351 CCAGTTGGTT ATCGTTTTTC AGCAACCCCT TGTATCTGGC TTTCACGAAG
401 CCGAACTGTC GCTTGATGAT GCGAAATGGG TGCTCCACCC TGGCCCGGAT
451 GCTGGCTTTC ATGTATTCGA TGTTGATGGC CGTTTTGTTC TTGCGTGGAT
501 GCTGTTTCAA GGTTCTTACC TTGCCGGGGC GCTCGGCGAT CAGCCAGTCC
551 ACATCCACCT CGGCCAGCTC CTCGCGCTGT GGCGCCCCTT GGTAGCCGGC
```

Figure 19. Sequencing of the 3' end of PCR product with V2 primer of *E. coli* B
serA::aroB Δ*aroD*::FRT–*cat*–FRT 2.2 kb PCR product. Legend: atgc – *aroD*
upstream sequence; ATGC – *aroD*; at**g**c – P1 or P2 on pKD3; *atgc* – FRT; ATGC
– IS5 transposase and trans-activator, DLP12 prophage, truncated outer membrane porin.

A new strategy was pursued were only half of the *aroD* ORF was to be deleted. The same H1P1 primer was used in the first step (Figure 16). The H2 sequence was chosen to start at the 439 nucleotide of the *aroD* sequence (5'-CCGGTAAATAACT-CCAGATCGATCATATCAACCAGGCCGC-3'). *E. coli* W3110 Δ*aroD*(new)::FRT–*cat*–FRT was obtained successfully, and it was verified by correct growth characteristics on selective plates (Table 6, entry 7) and PCR. The newly constructed mutant required aromatics substitution to grow on glucose-minimal salts plates and it was sensitive to ampicillin but not to chloramphenicol. PCR analysis revealed the 1.6 kb sized DNA fragment on agarose gel. A successive P1 phage-mediated transduction of *aroD*(new)::FRT-*cat*-FRT from *E. coli* W3110 Δ*aroD*(new)::FRT-*cat*-FRT to *E. coli* B *serA::aroB* afforded the desired mutant of *E. coli* B *serA::aroB aroD*(new)::FRT-*cat*-FRT. Growth characteristics of the new *E. coli* B mutant revealed the correct phenotype, requiring aromatics and serine supplementation when grown on glucose-minimal salts plates and sensistivity to ampicillin but not to chloramphenicol (Table 6, entry 9). However, elimination of FRT-*cat*-FRT cassette using pCP20 was unsuccessful after multiple trials. A solution to the removing the insert's drug resistance was provided by Ingram's group successful use of FLP flippase encoded by the pFT-A plasmid in *E. coli* B.[26] The key difference between pFT-A and pCP20 is that in pFT-A FLP expression is controlled by a chlorotetracycline inducible promoter rather than by a temperature inducible promoter as in pCP20. Plasmid pFT-A has a temperature sensitive replicon. Therefore it can be eliminated from the host by growing at 43 °C. *E. coli* B *serA::aroB aroD*(new)::FRT-*cat*-FRT/pFT-A were induced with chlorotetracycline and incubated for 6 h at 30 °C. This 30 °C, 6 h culture was then used to inoculate a culture incubated at 43 °C overnight.

58

Single colonies were obtained by the streaking overnight culture on LB plates. Phenotype screening of *E. coli* B *serA::aroB aroD*(new)::FRT revealed the correct growth pattern, with mutants requiring aromatics and serine supplementation when grown on glucose-minimal salts plates and sensitivity to chloramphenicol and ampicillin. PCR analysis with V1 and V2 primers revealed 0.5 kb sized DNA fragment indicating a truncated *aroD* gene. The wild-type *aroD* gene size is 0.8 kb.

Newly constructed *E. coli* B mutants were evaluated under glucose-limited fermentor-controlled conditions. The results were obtained after a single fermentor run for each mutant. *E. coli* B *serA::aroB aroD*(new)::FRT-*cat*-FRT/pKD12.112 and *E. coli* B *serA::aroB aroD*(new)::FRT-*cat*-FRT/pKD12.138 showed very similar cellular growth and metabolite accumulation (Figure 20A and Figure 20B). Quinic acid was the major product and it accumulated to 40 g/L in 17% yield (Table 7, entry 3) and 41 g/L in 19% yield (Table 7, entry 4) over 60 h cultivation. *E. coli* B *serA::aroB aroD*(new)::FRT-*cat*-FRT/pKD12.112 without transketolase overexpression (Table 7, entry 3) and with transketolase overexpression *E. coli* B *serA::aroB aroD*(new)::FRT-*cat*-FRT/pKD12.138 (Table 7, entry 4) produced the same amounts of quinic acid in the same overall total hydroaromatics yield. This indicated that transketolase overexpression in *E. coli* B had a negligible impact on hydroaromatics biosynthesis. The biomass accumulation remained low at approximately 20 g/L for both fermentations. 3-Dehydroquinic acid accumulated to a 13 and 18 g/L concentration, which was higher relative to *E. coli* K-12 synthesis of quinic acid. The molar ratio between quinic acid and 3-dehydroquinic acid decreased from 11.5 for QP1.1/pKD12.138 to 3.1 for *E. coli* B *serA::aroB aroD*(new)::FRT-*cat*-FRT/pKD12.138. As shown in Figure 20A and Figure 20B, quinic acid concentration

kept increasing until the end of fermentor run and 3-dehydroquinic acid concentration stopped increasing. Therefore, quinic acid biosynthesis by newly constructed *E. coli* B strains was prolonged to 84 h (Figure 21).
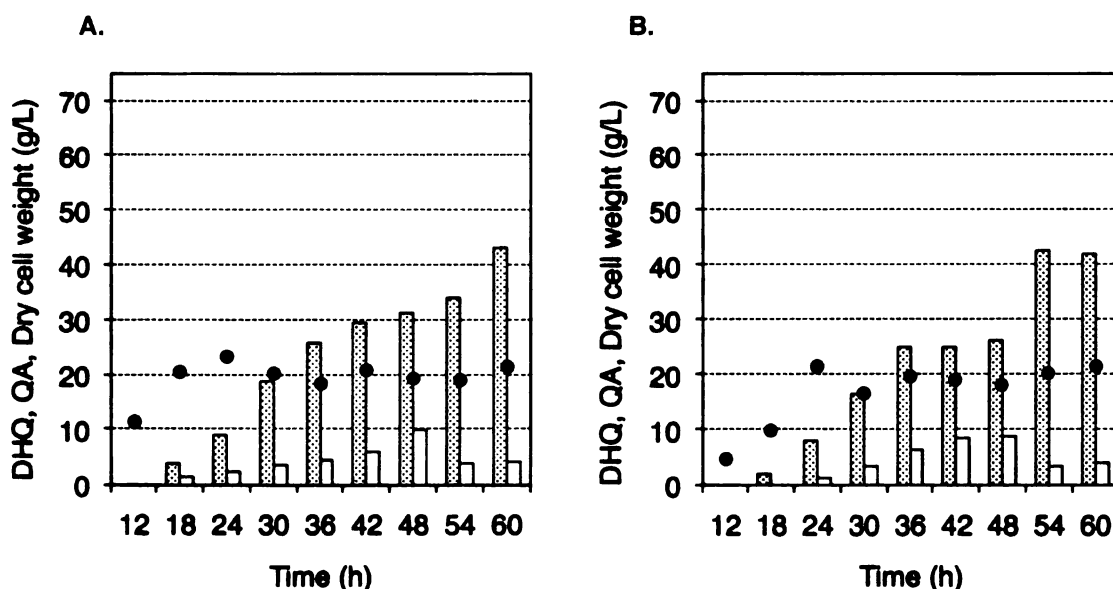
A. **B.**
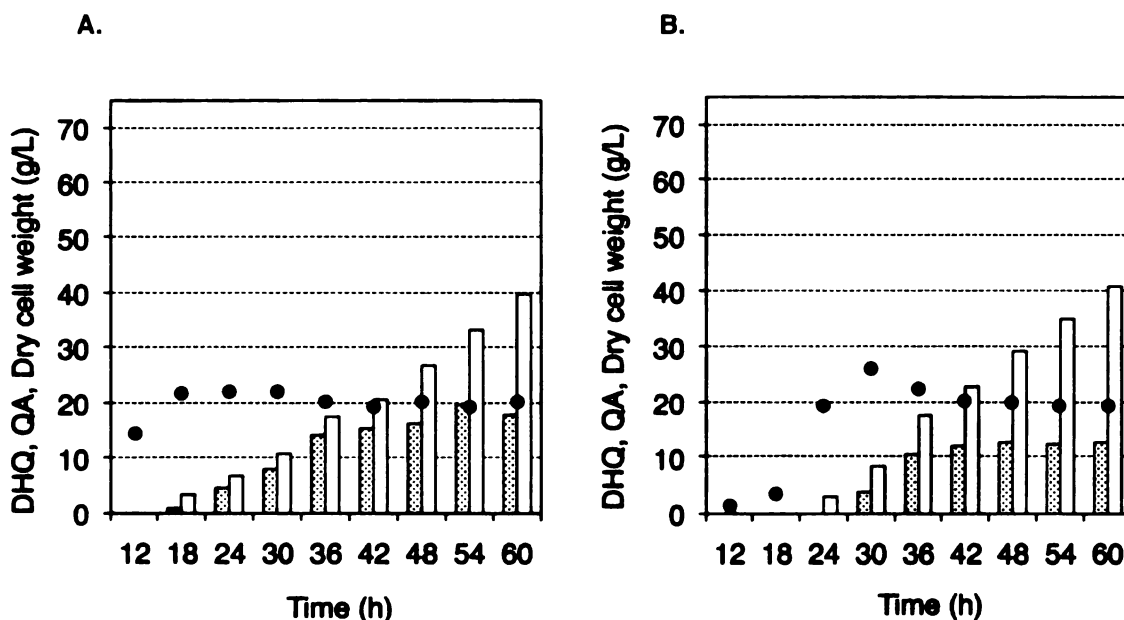
Figure 20. (A) *E. coli B serA::aroB ΔaroD*(new)::FRT–*cat*–FRT/pKD12.112 and (B) *E. coli B serA::aroB ΔaroD*(new)::FRT–*cat*–FRT/pKD12.138 cultured under glucose-limited conditions. Legend: (dotted bars) 3-dehydroquinic acid, (open bars) quinic acid, (black circles) dry cell weight.

However, this did not help to increase quinic acid concentration in the final culture supernatant. Microbial *E. coli B serA::aroB aroD*(new)::FRT-*cat*-FRT/pKD12.112 synthesis of quinic acid over an 84 h cultivation resulted in synthesized 37 g/L of quinic acid in 10% yield (Table 7, entry 5). *E. coli B serA::aroB aroD*(new)::FRT-*cat*-FRT/pKD12.138 synthesized 32 g/L of quinic acid in 10% yield (Table 7, entry 6) when cultivated under the same conditions. 3-Dehydroquinic acid accumulated at higher levels during *E. coli* B cultivation under fermentor-controlled conditions (Figure 20 and Figure 21) relative to *E. coli* K-12 (Figure 7A and Figure 25).
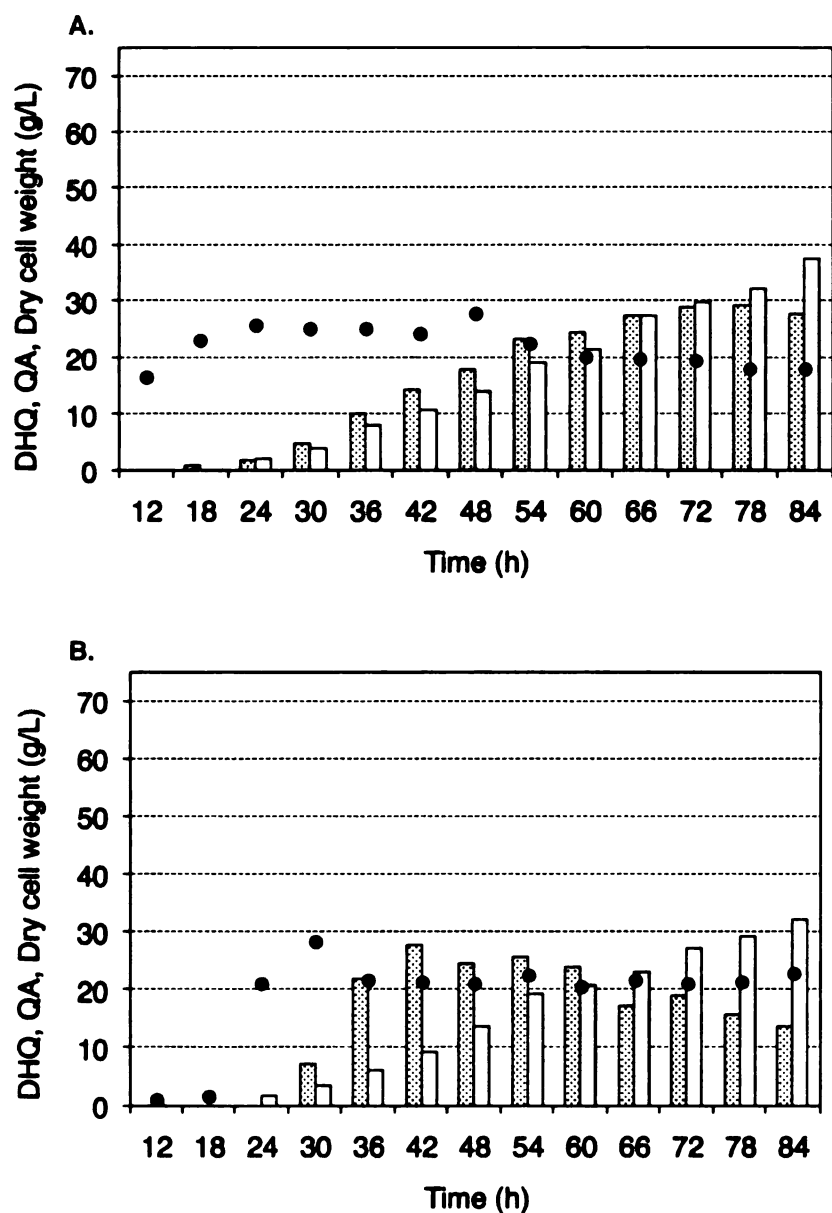
Figure 21. (A) *E. coli B serA::aroB ΔaroD*(new)::FRT–*cat*–FRT/pKD12.112 and (B) *E. coli B serA::aroB ΔaroD*(new)::FRT–*cat*–FRT/pKD12.138 cultured under glucose-limited conditions. Legend: (dotted bars) 3-dehydroquinic acid, (open bars) quinic acid, (black circles) dry cell weight.

The observed increase in 3-dehydroquinic acid concentration might be associated with the mechanism for 3-dehydroquinic acid export/import; from/ in to the cytoplasm.

If *E. coli* B has a slower transport system for importing 3-dehydroquinic acid from the culture medium back into the cytoplasm relative to *E. coli* K-12, then exported 3-dehydroquinic acid will not be recaptured and reduced to quinic acid by *E. coli* B at the same rate relative to *E. coli* K-12. Another reason for increased 3-dehydroquinic acid levels can be explained due to loss of glucose-limited condition control throughout the fermentor run. Glucose presence in the culture medium results in inhibition of the 3-dehydroquinic acid import system in *E. coli*, which will be discussed later in this chapter. Therefore, loss of glucose-limited control during *E. coli* B cultivation resulted in elevated levels of 3-dehydroquinic acid. This indicates that a better glucose-limited control conditions needs to be elaborated in order to reduce 3-dehydroquinic acid accumulation.

The mutants with successfully removed chloramphenicol resistance were evaluated under glucose-limited fermentor-controlled conditions. *E. coli* B *serA::aroB* *aroD*(new)::FRT/pKD12.112 synthesized 22 g/L of quinic acid in 10% yield over 84 h and the total hydroaromatics yield was 13% (Table 7, entry 7). The quinic acid and 3-dehydroquinic acid molar ratio was low again (3.1). These results are an average of two runs. Interestingly, transketolase overexpression had a profound effect this time, and *E. coli* B *serA::aroB* *aroD*(new)::FRT/pKD12.138 accumulated 42 g/L of quinic acid in 17% yield over 84 h with the total synthesized hydroaromatics yield of 21% (Table 7, entry 8). Further investigation is required in order to determine why after pFT-A treatment of *E. coli* B *serA::aroB* *aroD*(new)::FRT-*cat*-FRT, the *E. coli* B *serA::aroB* *aroD*(new)::FRT/pKD12.112 (Table 7, entry 7) synthesized less quinic acid relative to the *E. coli* B *serA::aroB* *aroD*(new)::FRT-*cat*-FRT/pKD12.112 (Table 7, entry 5) and the

E. coli B *serA::aroB aroD*(new)::FRT/pKD12.138 (Table 7, entry 8) when cultivated under the same conditions.
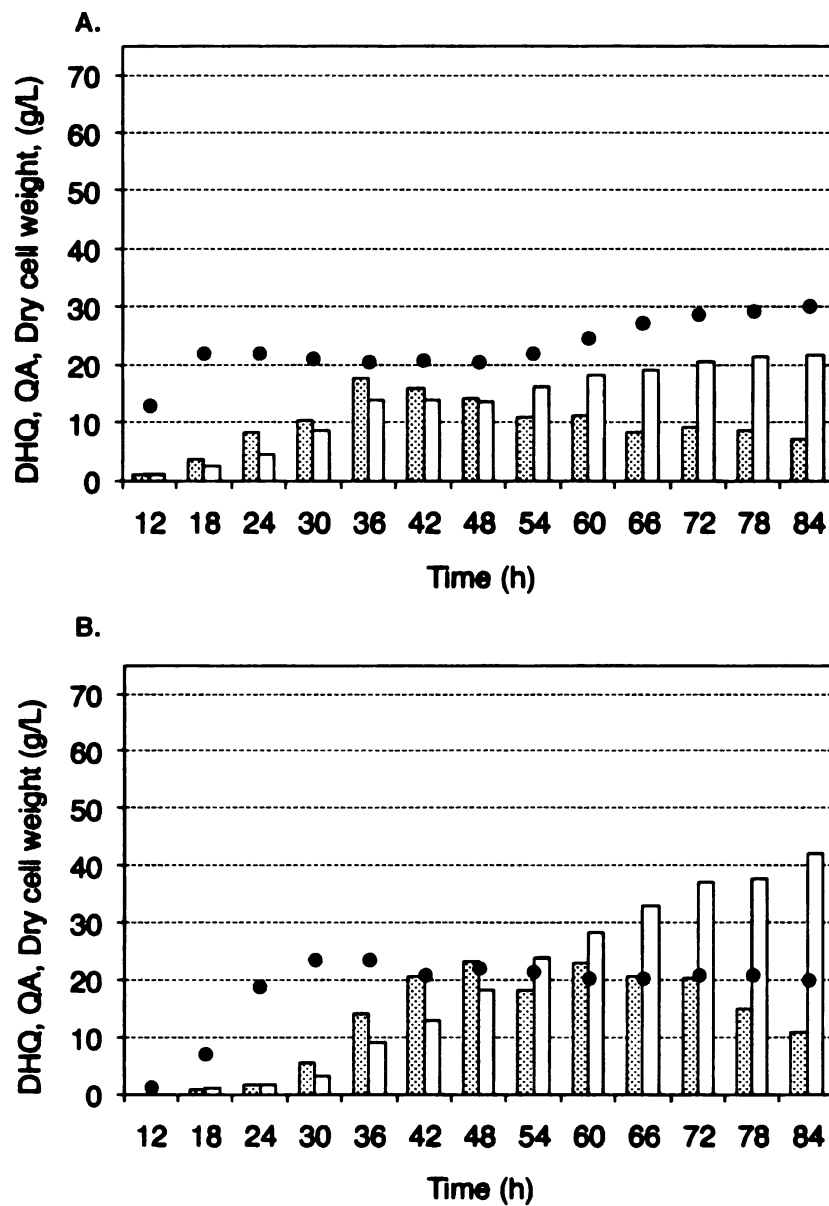
Figure 22. (A) *E. coli* B *serA::aroB* Δ*aroD*(new)::FRT/pKD12.112 and (B) *E. coli* B *serA::aroB* Δ*aroD*(new)::FRT/pKD12.138 cultured under glucose-limited conditions. Legend: (dotted bars) 3-dehydroquinic acid, (open bars) quinic acid, (black circles) dry cell weight.

Optimization of quinic acid production by *E. coli* QP1.1/pKD12.138

FERMENTATION LENGTH

Previously discussed quinic acid production by *E. coli* QP1.1/pKD12.138 (Table 4, entry 1; Figure 7A) was run for 48 h and it afforded 58 g/L of quinic acid in 21% yield from glucose. As Figure 7 indicates, quinic acid concentration keeps increasing until the end of the fermentor run. Therefore, maybe a longer culture time would lead to higher quinic acid concentrations. Quinic acid fermentations were run under glucose-limited conditions for 60 and 132 h. QP1.1/pKD12.138 produced 60 g/L of quinic acid in 21% yield in 60 h (Table 8, entry 2). This result is very similar to the 48 h fermentation (Table 4, entry 1). The concentration of 3-dehydroquinic acid remained the same at 5 g/L, and the total hydroaromatics yield was 22%. The standard fermentation inoculation conditions were also probed. Conventionally, inoculum for a fermentor is prepared by inoculating a single colony of interest into 5 mL glucose-minimal salts medium. This inoculum is incubated at 37 °C for 24 h. The next day, a 5 mL culture is transferred into 95 mL of fresh glucose-minimal salts medium and incubated at 37 °C for an additional 11 h.

Table 8. Concentrations and yields of products synthesized by quinic acid producing *E. coli* QP1.1/pKD12.138 during various length of fermentation.

Entry	Inoculation conditions	Time, h	[DHQ]^a g/L	[QA], g/L	QA^b yield, %	Total^c yield, %
1	Standard (24h 5mL, 11h 100 mL)	48	5	58	21	22
2*	Standard	60	5	60	21	22
3*	17 h 5 mL, 11 h 100 mL	60	3	55	19	20
4*	Standard	132	3	73	20	21
5	Standard	84	5	67	18	19

* Single run fermentation. ^{a}Abbreviations: DHQ – 3-dehydroquinic acid, QA – quinic acid. ^{b}(mol QA)/(mol glucose consumed). ^{c}(mol DHQ + mol QA)/(mol glucose consumed).
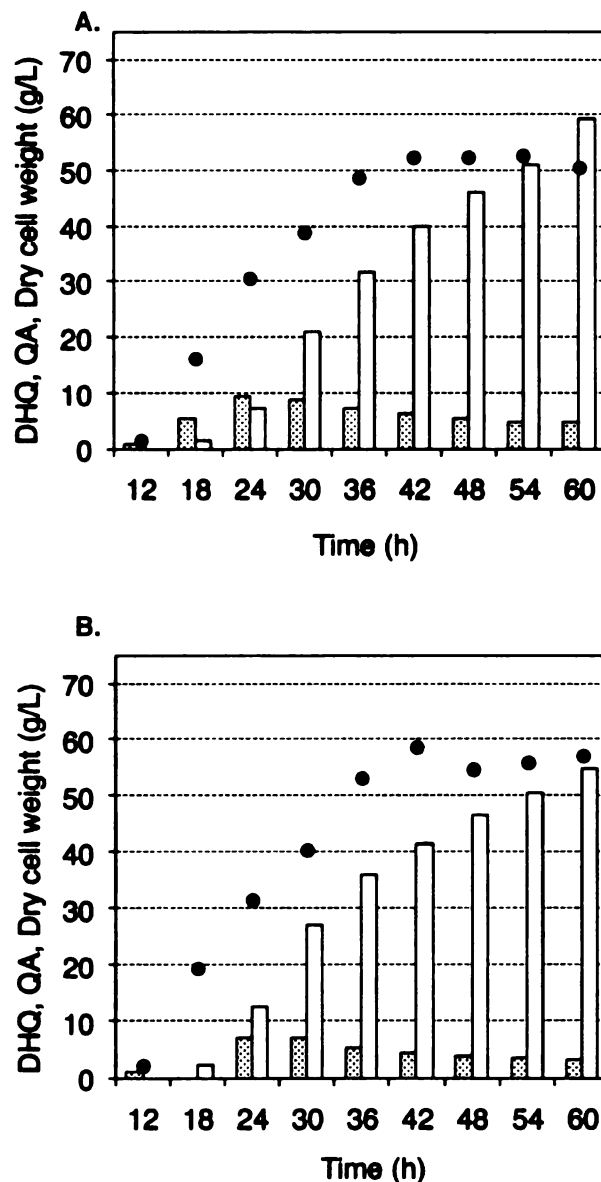
Figure 23. *E. coli* QP1.1/pKD12.138 cultured under glucose-limited conditions: (A) 60 h and standard inoculation; (B) 60 h and non standard inoculation. Legend: (dotted bars) 3-dehydroquinic acid, (open bars) quinic acid, (black circles) dry cell weight.

A new inoculation protocol was tested where a 5 mL culture was incubated for 17 h rather than 24 h, hoping that a fresher culture will lead to synthesis of a higher concentration of quinic acid. However, quinic acid accumulated at 55 g/L concentration in 19% yield after 60 h cultivation (Table 8, entry 3). Accumulation of 3-dehydroquinic acid remained very similar at 3 g/L and the total yield of synthesized hydroaromatics was

20%. Synthesis of hydroaromatics using the standard inoculation conditions and using the newly tested inoculation conditions can be compared in Figure 23A and Figure 23B. Interestingly, initiation of the fermentor run with a fresh inoculant produced more biomass throughout entire fermentation process as compared to the standard inoculation conditions. The highest level of biomass was 59 g/L of dry cell weight using the fresh inoculant (Figure 23B) compared to 51 g/L of dry cell weight using the standard inoculant (Figure 23A).

E. coli QP1.1/pKD12.138 cultivation time was prolonged to 132 h. This time 73 g/L of quinic acid was synthesized in 20% yield (Table 8, entry 4). While more quinic acid was synthesized, the yield remained almost the same. Accumulation of 3-dehydroquinic acid also remained the same. The highest quinic acid production was achieved at approximately 102 h, when the quinic acid concentration reached 76 g/L. The highest dry cell weight was observed at 36 and 42 h at 53 g/L. Cultivation of E. coli QP1.1/pKD12.138 for 84 h was also examined. It produced 67 g/L of quinic acid in 18% yield (Table 8, entry 5). Measured quinic acid concentrations varied between 60 and 84 h with and averag quinic acid concentration of 68 g/L.
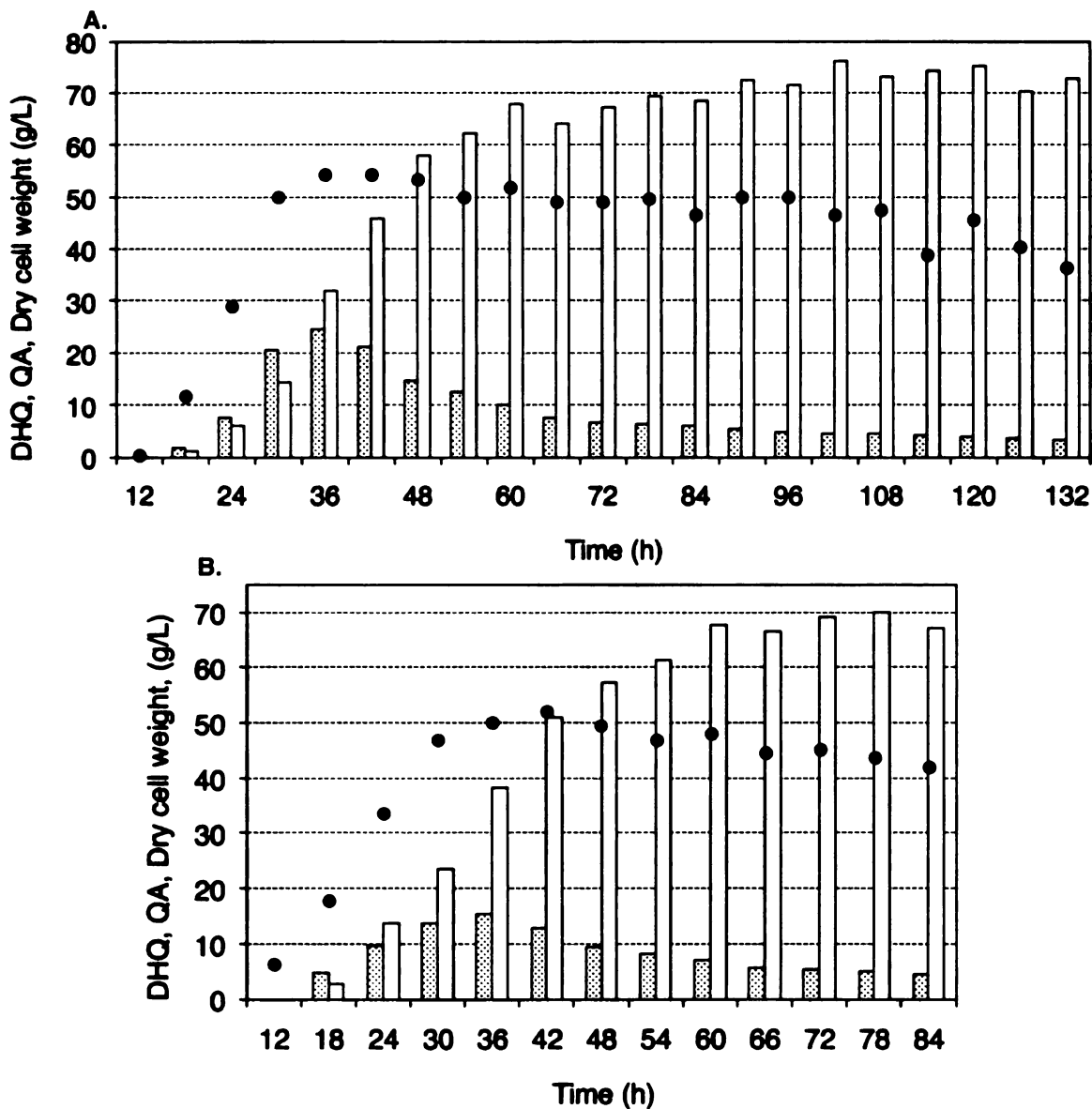
Figure 24. *E. coli* QP1.1/pKD12.138 cultured under glucose-limited conditions: (A)132 h; (B) 84h. Legend: (dotted bars) 3-dehydroquinic acid, (open bars) quinic acid, (black circles) dry cell weight.

EFFECT OF TRANSKETOLASE OVEREXPRESSION

Transketolase overexpression in quinate synthesizing *E. coli* K-12 constructs was also investigated. Fermentation time was extended beyond 60 in order to capture the highest concentrations of quinic acid synthesized by the constructs. *E. coli*

QP1.1/pKD12.112 did not have plasmid-localized *tktA* and it synthesized 52 g/L of quinic acid over 84 h (Table 9, entry 2; Figure 25). This result is an average of two runs. It clearly indicates that transketolase overexpression is required for *E. coli* K-12 strains, because QP1.1/pKD12.138 synthesized 67 g/L of quinic acid (Table 9, entry 1). Quinic acid yield also increased from 15%, without transketolase overexpression in QP1.1.pKD12.112 to 19% with transketolase overexpression in QP1.1/pKD12.138.

Table 9. **Concentrations and yields of products synthesized by quinic acid producing *E. coli* K-12 strain with and without transketolase overexpression.**

Entry	Inoculation conditions	Time, h	[DHQ]^a g/L	[QA], g/L	QA^b yield, %	Total yield,^{c} %
1	QP1.1/pKD12.138	84	5	67	18	19
2	QP1.1/pKD12.112	84	2	52	15	15

^{a}Abbreviations: DHQ – 3-dehydroquinic acid, QA – quinic acid. ^{b}(mol QA)/(mol glucose consumed). ^{c}(mol DHQ + mol QA)/(mol glucose consumed).
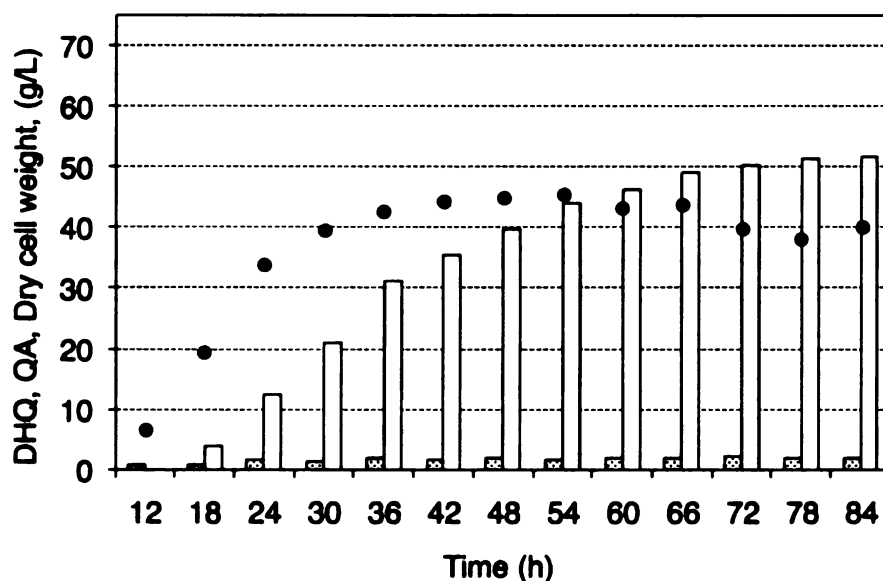
Figure 25. *E. coli* QP1.1/pKD12.112 cultured under glucose-limited conditions. Legend: (dotted bars) 3-dehydroquinic acid, (open bars) quinic acid, (black circles) dry cell weight.

Optimization of fermentation medium components

The detailed description of the composition of fermentation medium is described

in Chapter 4. The key ingredients are potassium phosphate, required to maintain buffer

conditions and also as a phosphorous source for the bacteria. Aromatic amino acids are

required as a supplement due to an inactivated shikimate pathway. Therefore, the

concentration of aromatic amino acids added in the medium can control the biomass and

ultimately influence quinic acid synthesis. Three precursors for aromatic vitamin

synthesis p-hydroxybenzoic acid, p-aminobenzoic acid, and 2,3-dihydroxybenzoic acid

are also required as supplements. Ammonium iron citrate is required as the iron source

and citric acid is used as metal ion chelator, because $E.$ $coli$ does not have catabolic

pathway for citric acid degradation.

Table 10. Concentrations and yields of products synthesized by quinic acid producing strain QP1.1/pKD12.138 with various phosphate concentration in the medium.

Entry	[K₂HPO₄]	Time, h	[DHQ] [a] g/L	[QA], g/L	QA [b] yield, %	Total yield, [c] %
1	43 mM (standard)	60	5	60	21	22
2*	35 mM	60	5	62	22	23
3*	20 mM	60	3	51	21	22

* Single run fermentation. [a] Abbreviations: DHQ – 3-dehydroquinic acid, QA – quinic acid. [b] (mol QA)/(mol glucose consumed). [c] (mol DHQ + mol QA)/(mol glucose consumed).

Separation of inorganic salts from quinic acid fermentation broth is an important

step in purification of quinic acid, which will be described in detail later in this chapter.

Reduction of unconsumed potassium phosphate could lead to an easier process for

isolation and purification of quinic acid. Various potassium phosphate concentrations

were investigated for cultivation of QP1.1/pKD12.138 under fermentor-controlled,

glucose-limited conditions.
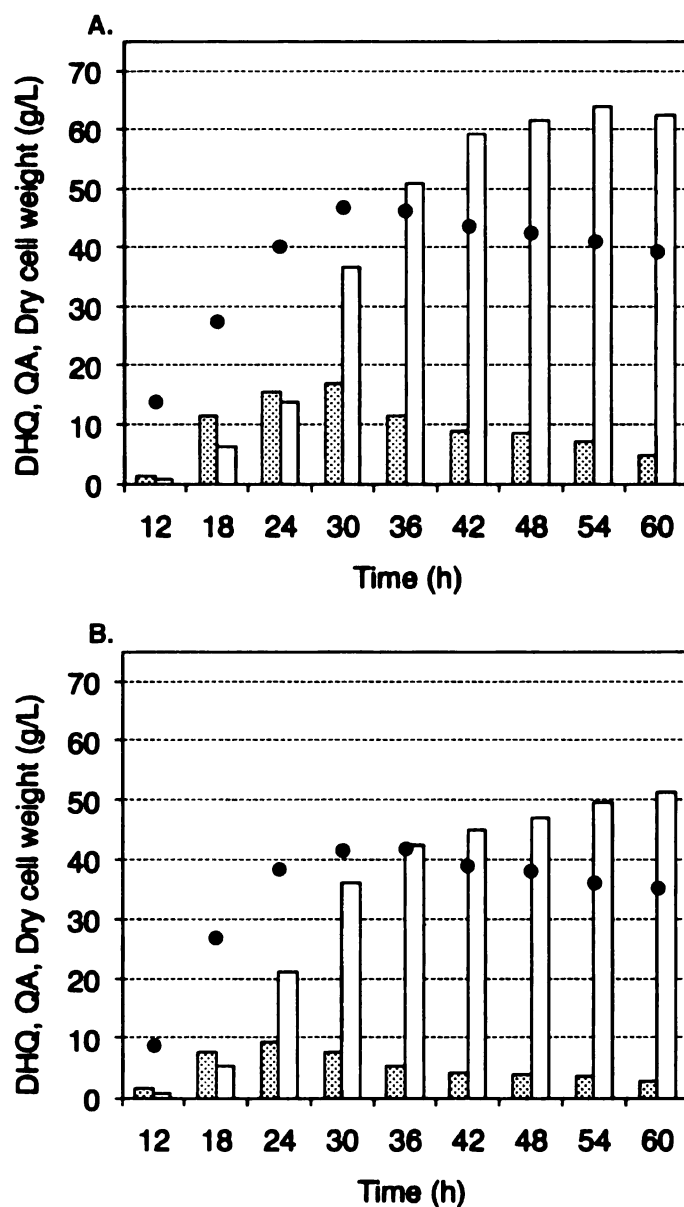
Figure 26. *E. coli* **QP1.1/pKD12.138 cultured under glucose-limited conditions in: (A) 35 mM K₂HPO₄; (B) 20 mM K₂HPO₄ medium.** Legend: (dotted bars) 3-dehydroquinic acid, (open bars) quinic acid, (black circles) dry cell weight.

A standard potassium phosphate concentration was 7.5 g/L (43 mM) of K_2HPO_4. Quinic acid was synthesized at 62 g/L concentration in 22% yield in 35 mM K_2HPO_4 medium (Table 10, entry 2) and was approximately the same relative to the standard cultivation conditions (Table 10, entry 1). Therefore, a 60 h quinic acid synthesis by *E. coli* QP1.1/pKD12.138 could be efficiently achieved in 35 mM phosphate medium. Quinic acid production declined from 60 g/L for the QP1.1/pKD12.138 cultivated in the standard

43 mM K_2HPO_4 medium (Table 10, entry 1) to 51 g/L cultivated in 20 mM K_2HPO_4 cultivation medium (Table 10, entry 3). Reduced phosphate concentrations in the medium resulted in reduced biomass (Figure 27 A). Interestingly, fermentations reached stationary phase at approximately the same time (30 h), but the cell growth rate during exponential phase (0 – 30 h) was higher under reduced phosphate concentrations than compared to the QP1.1/pKD12.138 cultivation under standard conditions (Figure 27).
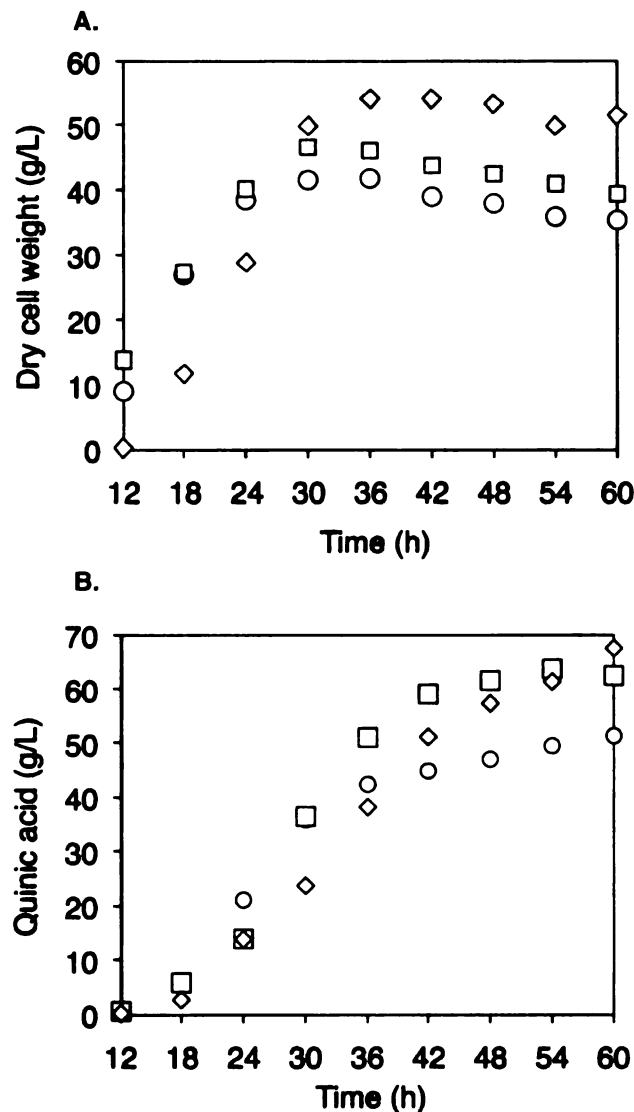
Figure 27. Comparison of the impact of phosphate concentration on *E. coli* QP1.1/pKD12.138: (A) dry cell weight; (B) quinic acid synthesis. Legend: (diamonds) 43 mM K_2HPO_4, (squares) 35 mM K_2HPO_4 and (circles) 20 mM K_2HPO_4.

71

Aromatic amino acid supplementation was another investigated culture medium component. The concentration of aromatic amino acids was reduced by 25%, 50% and 75% relative to the typically employed concentration. The results are summarized in Table 11 and shown as a single entry and not as an average value, because the synthesized metabolite concentrations were widely dispersed even for the same concentration of aromatic amino acids. The main reason for high result dispersion was difficulty in controlling glucose-limited conditions. Reduced concentration of aromatic amino acids translated into reduced biomass formation (Figure 28 A). Since at lower concentrations of aromatic amino acids there was less biomass, use of pO2 control to maintain glucose-limited conditions was more difficult. The max stir speed varies depending on fermentor set up in order to maintain the same oxygen transfer rate (OTR). Fermentors were previously calibrated for OTR and they revealed that under the same conditions (volume of culture and airflow) the stir rate has to be adjusted differently in order to obtain the same OTR. The small differences in fermentor vessel shape, relative location of sparger and impellers have major effect on OTR. Due to this reason, the maximum stir rate to maintain the same OTR for each experiment in Table 11 is different and listed in parentheses. Cultures were purged with 1 vvm (volume of airflow per volume of culture medium per minute) of airflow under standard cultivation conditions.

Table 11. Concentrations and yields of products synthesized by quinic acid producing strain QP1.1/pKD12.138 with various aromatic amino acid concentrations in the medium.

Entry	Aromatic amino acid conc.	Airflow, vvm	Stir (max stir), rpm	Time, h	[DHQ],[a] g/L	[QA], g/L	QA[b] yield, %	Total yield,[c] %
1	100%	1.0	1100 (1100)	84	5	67	18	19
2*	25% reduced	1.0	1000 (1000)	60	23	34	13	23
3*	25% reduced	1.0	940 (940)	84	13	50	14	17
4*	50% reduced	0.5	1000 (1000)	60	31	31	13	26
5*	50% reduced	1.0	740 (940)	84	5	58	17	18
6*	50% reduced	0.5	940 (940)	84	16	40	14	20
7*	75% reduced	0.5	750 (1100)	84	8	43	18	22
8*	100% increased	1.0	1100 (1100)	84	4	64	18	19
9*	15 g/L yeast extract	1.0	1100 (1100)	84	7	68	18	20

* Single run fermentation. [a]Abbreviations: DHQ − 3-dehydroquinic acid, QA − quinic acid. [b] (mol QA)/(mol glucose consumed). [c](mol DHQ + mol QA)/(mol glucose consumed). Note: aromatic amino acids 100% are: 0.7 g/L of L-tyrosine, 0.35 g/L of L-tryptophane, 0.7 g/L L-phenylalanine.
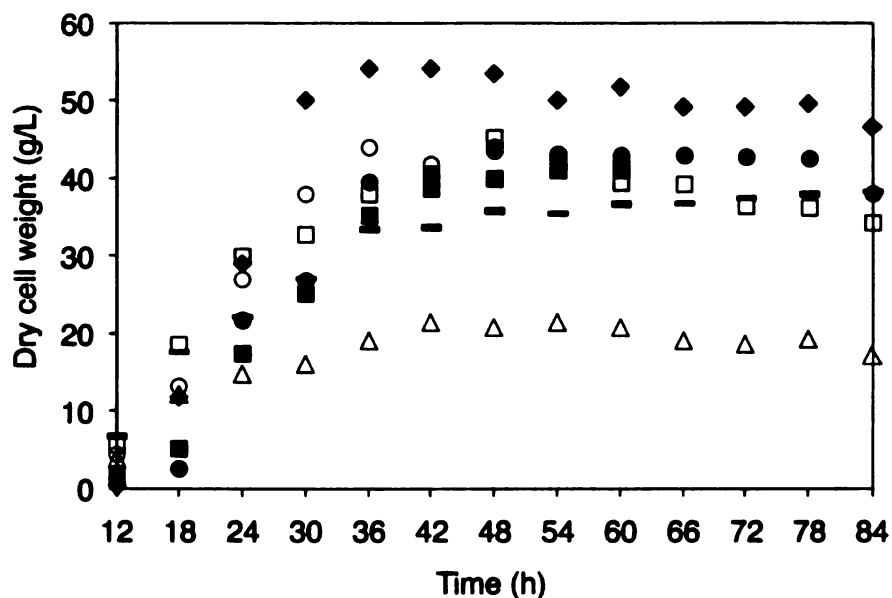
Figure 28. Comparison of the impact of aromatic amino acid concentrations on E. coli QP1.1/pKD12.138 dry cell weight. Legend: (diamonds) 100%, (open circle) 25% reduced, (solid circle) 25% reduced, (solid square) 50% reduced, (open square) 50% reduced, (dashes) 50% reduced, (triangular) 75% reduced.

E. coli QP1.1/pKD12.138 produced 34 g/L (Table 11, entry 2) in 60 h and 50 g/L (Table 11, entry 3) of quinic acid 84 h when aromatic amino acid concentration were reduced by 25% in culture medium. Accumulation of 3-dehydroquinic acid was observed at higher levels of 23 g/L (Table 11, entry 2) and 13 g/L (Table 11, entry 3). The relatively high 3-dehydroquinic acid concentration can be explained by imperfect maintenance of glucose-limited culture conditions, because glucose concentration rose to 4 g/L towards the end of the fermentation. By contrast, a typical glucose concentration for glucose-limited culture conditions is bellow 0.03 g/L. Both fermentations were run under standard conditions (1 vvm and OTR-optimized stir rate), but it was already obvious that pO_2 response is slower than during the standard fermentation conditions. Cultures with a 50% reduced in the concentration of aromatic amino acids had to be run with either 0.5 vvm airflow (Table 11, entry 4 and entry 6) or reduced stir rate (Table 11, entry 5) in order to maintain glucose-limited conditions. Due to better maintenance of glucose-limited culture conditions, QP1.1/pKD12.138 synthesized higher quinic acid concentration at 58 g/L (Table 11, entry 5) and 40 g/L (Table 11, entry 6) relative to 31 g/L (Table 11, entry 4). Accumulation of the major byproduct 3-dehydroquinic acid at 16 g/L (Table 11, entry 6) was related to the glucose concentration in the medium. At the same time, quinic acid was produced at lower concentration relative to the control experiment (Table 11, entry 1). Reduction by 25% of aromatic amino acid concentration, yielded even lower biomass accumulation. However, quinic acid concentrations remained approximately the same at 43 g/L (Table 11, entry 7). Reduced biomass ultimately resulted in reduced airflow and lower stir rates in order to maintain glucose-limited culture conditions. Interestingly, reduction in aromatic amino acids by 25% and

50% resulted in approximately the same biomass accumulation, while a 75% reduction in aromatic amino acids had a major impact on the biomass formation (Figure 28A). The final concentration of synthesized quinic acid with different levels of aromatic amino acid supplementation varied from 40-50 g/L. The general trend observed was that reduction in aromatic amino acid supplementation reduced biomass formation and cultures' oxygen requirement. Therefore, in order to establish reliable and reproducible fermentation conditions, more fermentor runs will be required to screen for optimal airflow and impeller speed.

The effect of a twofold increase in aromatic amino acid concentration in the culture medium was also examined. Initially standard fermentation conditions were used with the normal concentration of aromatic amino acids in the culture medium. Once cells reached the end of the exponential growth phase at approximately 18 h after the beginning of fermentation an additional 50% of the normal concentration of aromatic amino acids were added twice in 6 h intervals, which led to the final twofold increase in the concentration of aromatic amino acids in the culture medium. This incremental addition was done in order to avoid the feedback inhibition of plasmid-localized $aroF^{FBR}$ by L-tyrosine.[9] Quinic acid accumulated to 64 g/L in 18% yield over 84 h (Table 11, entry 8). The highest quinic acid concentration of 66 g/L was reached at 78 h (Figure 29 A). Accumulation of 3-dehydroquinic acid remained at a low level (4 g/L) and the total yield of synthesized hydroaromatics was the same at 19% (Table 11, entry 8) as for the control experiment (Table 11, entry 1). The increase in aromatic amino acids did not have any effect on total yield on synthesized hydroaromatics.

75
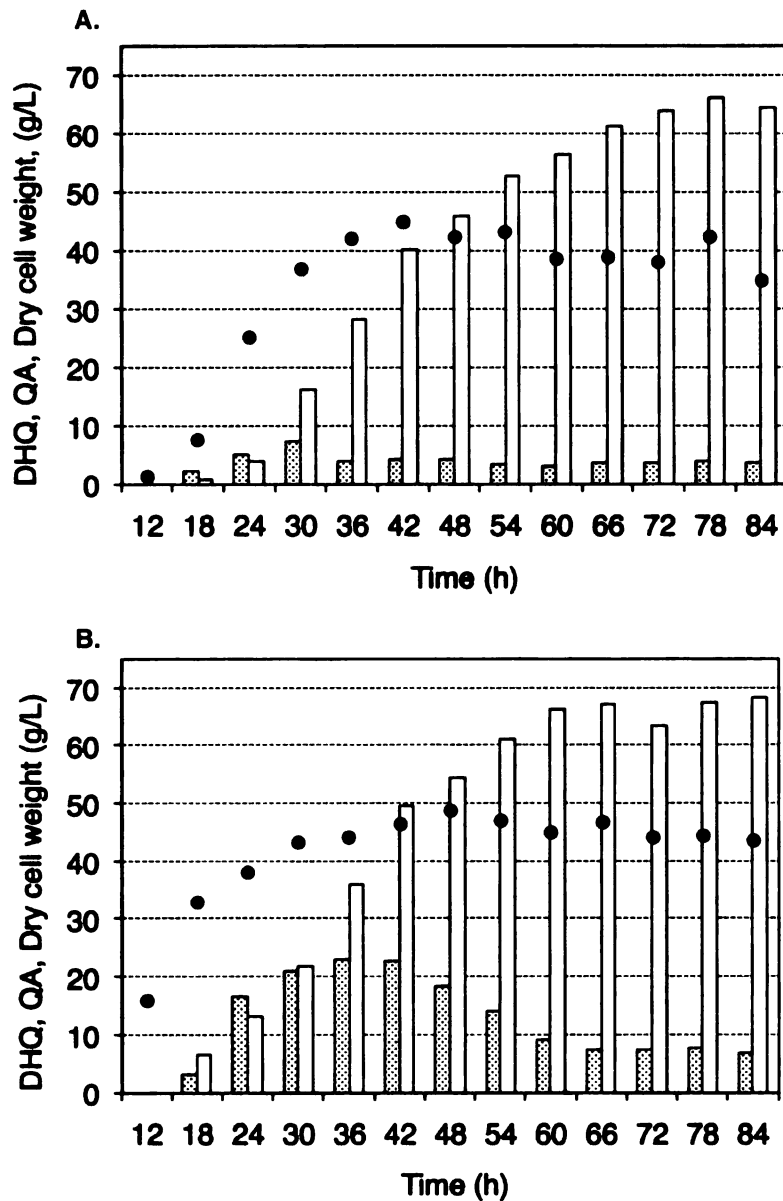
Figure 29. *E. coli* QP1.1/pKD12.138 cultured under glucose-limited conditions with: (A) twofold increased aromatic amino acid; (B) 15 g/L yeast extract supplementation. Legend: (dotted bars) 3-dehydroquinic acid, (open bars) quinic acid, (black circles) dry cell weight.

A positive effect of shikimic acid biosynthesis during glucose-rich, fermentor-controlled conditions with yeast extract supplementation was previously reported.[13] Chandran *et. al.*

reported that shikimic acid titter and yield increased from 62 g/L and 26% to 84 g/L and

33%.[13] Yeast extract supplementation was also investigated for quinic acid biosynthesis,

where 15 g/L of yeast extract was added in the beginning of the fermentation. The final

synthesized quinic acid concentration was 68 g/L in 84 h (Table 11, entry 9). It was

synthesized in 18% yield with 20% total yield of synthesized hydroaromatics.

Accumulation of 3-dehydroquinic acid was observed at 7 g/L at the end of the

fermentation. Although glucose concentration was not detectable during the fermentor

run, 3-dehydroquinic acid concentration kept increasing during the first half of the

fermentor run to 21 g/L (Figure 29 B). Apparently, yeast extract had the same effect as

glucose and caused 3-dehydroquinic acid accumulation.
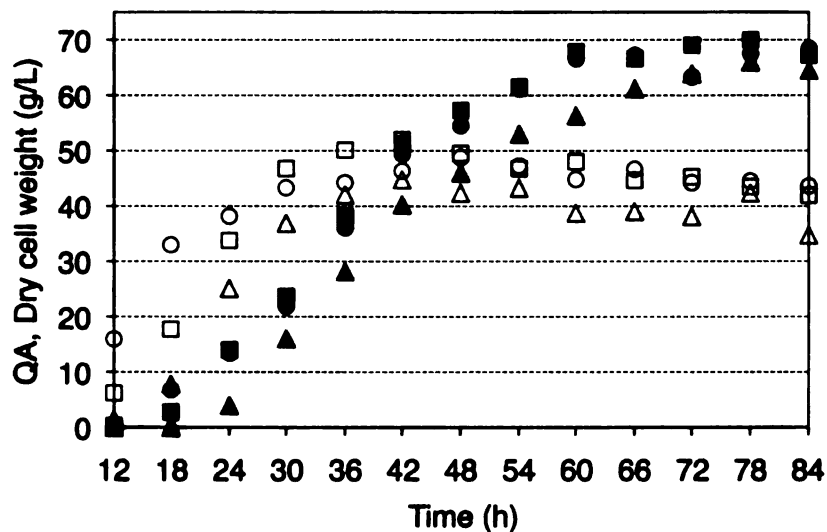
Figure 30. Comparison of the impact of twofold increased aromatic amino acid concentration and 15 g/L yeast extract supplementation in the culture medium on dry cell weight and quinic acid synthesis by *E. coli* QP1.1/pKD12.138 under glucose-limited culture conditions. Legend: (open squares) dry cell weight standard conditions, (open triangular) dry cell weight twofold increased aromatic amino acids, (open circles) dry cell weight 15 g/L yeast extract supplementation, (solid squares) quinic acid standard conditions, (solid triangular) quinic acid twofold increased aromatic amino acids, (solid circles) quinic acid 15 g/L yeast extract supplementation.

Interestingly, the quinic acid accumulation profile for the standard fermentor run (solid squares, Figure 30) was identical with the yeast extract supplemented fermentor run (solid circles, Figure 30). Twofold increase in aromatic amino acid supplementation (solid triangular, Figure 30) probably caused DAHP synthase inhibition early in the fermentor run. Therefore, quinic acid synthesis in the first 30 h was slower, but seemed to resume to a normal rate after 36 h. However, the total amount of synthesized quinic acid did not catch up with the standard fermentation. Yeast extract supplementation resulted in increased cell biomass (open circles, Figure 30) early in the fermentor run. However, after 48 h it reached the same level as the standard fermentation (open squares, Figure 30) and it remained the same throughout fermentor run. Counter intuitively, a lower biomass profile was observed for the twofold aromatic amino acid (open triangular, Figure 30) supplementation.

RECAPTURE OF 3-DEHYDROQUINIC ACID UNDER GLUCOSE-LIMITED CONDITIONS

Under glucose-limited, fermentor-controlled conditions, time-dependent the change in concentration of 3-dehydroquinic acid during microbial synthesis of quinic acid suggested that 3-dehydroquinic acid could be exported outside the cell prior to the reduction step and imported back into the cytoplasm (recaptured) with subsequent reduction to afford quinic acid (Figure 7, Figure 24A, Figure 24B, and Figure 26). To test this hypothesis, Ran constructed *E. coli* QP1.1/pNR4.276 incapable of *de novo* quinic acid synthesis from glucose.[11] The construct had inactivated plasmid-localized DAHP synthase *aroF*[FBR] together with other shared genomic elements for quinic acid production. Genomic expression of all three DAHP synthase isozymes (AroF, AroG and

78

AroH) was inhibited by adding aromatic amino acids to the culture medium. This ensured no carbon flow into the shikimate pathway (Figure 1). The construct was cultured under glucose-limited conditions and no formation of quinic acid or 3-dehydroquinic acid was observed in the culture medium. Addition of 5 g/L of 3-dehydroquinic acid resulted in formation of 2.5 g/L quinic acid with 2.1 g/L of 3-dehydroquinic acid remaining after 30 h under glucose-limited, fermentor-controlled conditions. Another way to test whether initially formed 3-dehydroquinic acid is recaptured over the course of microbial synthesis of quinic acid is to initially run the microbial synthesis under glucose-rich culture conditions and then switch to glucose-limited culture conditions. Metabolite recapture would be implicated if 3-dehydroquinic acid synthesized under glucose-rich culture conditions decreases in concentration and is replaced by quinic acid when the culture is switched to glucose-limited culture conditions. Interestingly, for the most times when 3-dehydroquinic acid formation was observed at higher concentrations, the total yield of synthesized hydroaraomtics increased for *E. coli* K-12 QP1.1/pKD12.138 (Table 11, entry 2 and entry 4) and for *E. coli* B *serA::aroB aroD*(new)*::* FRT-*cat*-FRT/pKD12.112 (Table 7, entry 3), *E. coli* B *serA::aroB aroD*(new)*::* FRT-*cat*-FRT/pKD12.138 (Table 7, entry 4) relative to the standard 19-22% yield obtained by QP1.1/pKD12.138 (Table 8, entry 5 and entry1). Therefore, maybe fermentor controlled culture conditions where 3-dehydroquinic acid is first formed under glucose-rich conditions with subsequent conversion to quinic acid under glucose-limited conditions will lead to higher quinic acid concentration and yields.

Table 12. Concentrations and yields of products synthesized by quinic acid producing strain QP1.1/pKD12.138 under various glucose fermentation conditions.

Entry	Fermentation type	Time, h	[DHQ],[a] g/L	[QA], g/L	QA[b] yield, %	Total yield,[c] %
1*	Glucose-limited	132	3	73	18	19
2*	Glucose-rich 66h**	132	8	48	13	15
3*	Glucose-rich 36h**	84	16	40	10	14

* Single run fermentation. ** Fermentor was run under glucose-rich culture conditions for 66 h or 36 h and then switched to glucose-limited culture conditions. [a]Abbreviations: DHQ – 3-dehydroquinic acid, QA – quinic acid. [b](mol QA)/(mol glucose consumed). [c](mol DHQ + mol QA)/(mol glucose consumed).

E. coli QP1.1/pKD12.138 was cultivated under standard glucose-rich culture conditions for 66 h and then switched to glucose-limited culture conditions. The total synthesized quinic acid concentration after 132 h was 48 g/L in 13% yield, while 3-dehydroquinic acid accumulated at 8 g/L (Table 12, entry 2). The total yield of synthesized hydroaromatics was 15%, which is lower than the 19% observed during the control experiment (Table 12, entry 1). The concentration of 3-dehydroquinic acid increased until 36 h and then started a gradual decline simultaneous with an increase in quinic acid concentrations (Figure 31A). Even though the culture medium had approximately 10 g/L of glucose, the rate of 3-dehydroquinic acid accumulation in the culture medium began to decrease after 36 h. Once the fermentor-controlled culture was switched to glucose-limited culture conditions (after 66 h) a steady decline in the concentration of 3-dehydroquinic acid was observed, but this did not correlate with a comparable rate in the increase in concentration of quinic acid. This experiment was revisited with another fermentor run where glucose-rich conditions were changed to glucose-limited conditions after 36 h. This time, 40 g/L of quinic acid was synthesized in 10% yield over 84 h (Table 12, entry 3). The total yield of synthesized hydroaromatics

was 14%. As with the previous experiment, where the concentration of 3-dehydroquinic

acid rose faster than that of quinic acid under glucose-rich conditions (until 42 h, Figure

31 B). After the culture was switched to glucose-limited conditions, the concentration of

3-dehydroquinic acid declined faster than the concentration of quinic acid increased.
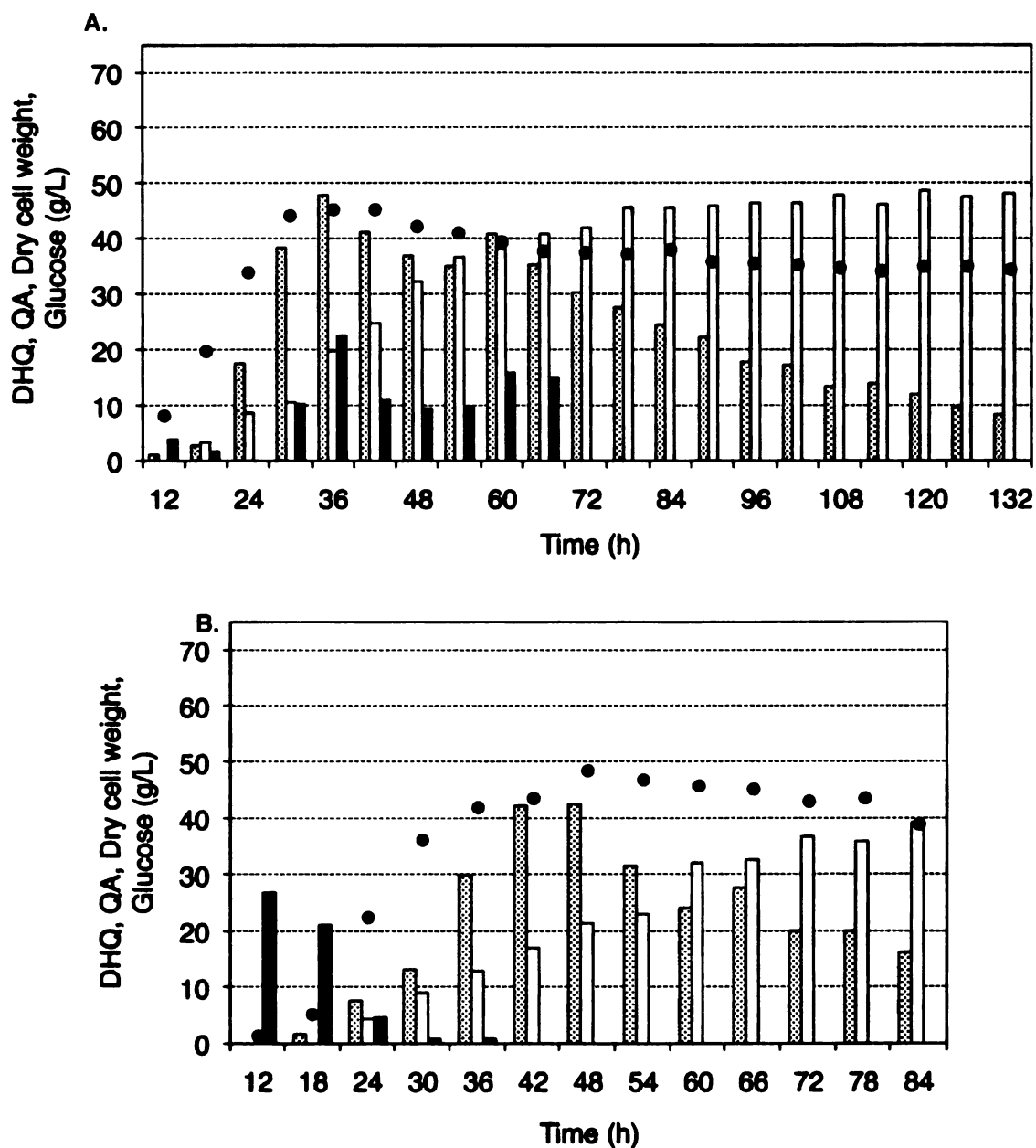
Figure 31. *E. coli* QP1.1/pKD12.138 cultured under glucose-rich conditions for (A) 66 h and (B)36 h and subsequently switched to glucose-limited culture conditions. Legend: (dotted bars) 3-dehydroquinic acid, (open bars) quinic acid, (black bars) glucose, (black circles) dry cell weight
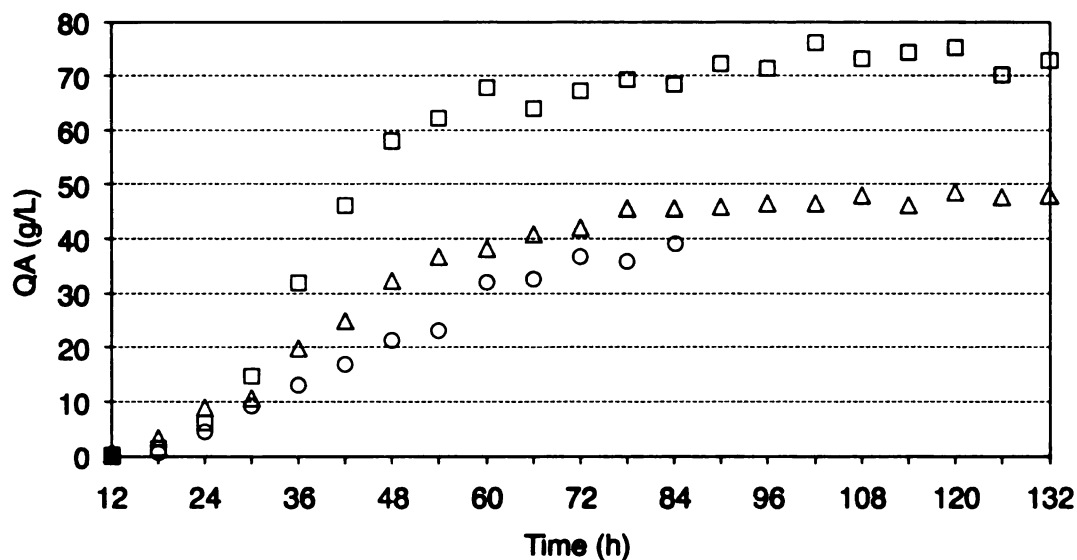
Figure 32. Quinic acid accumulation profiles obtained during cultivation of *E. coli* QP1.1/pKD12.138 under glucose-rich culture conditions and subsequently switched to glucose-limited culture conditions. Legend: (squares) glucose-limited culture conditions, (triangular) glucose-rich culture conditions until 66 h, (circles) glucose-rich culture conditions until 36 h.

These experiments indicate that it is very important to maintain strictly glucose-limited culture conditions during the first 60 h of microbial quinic acid synthesis, because the rate of quinic acid formation is the highest during glucose-limited conditions (squares, Figure 32) and the rate of quinic acid synthesis does not recover to the same rate after exposure to glucose-rich culture conditions (triangular and circle, Figure 32). A loss of glucose-limited culture condition control towards the end of the fermentation process does not have a drastic impact since the rate of quinic acid accumulation is restored to the normal rate once the residual glucose is consumed from the culture medium. Even though the total concentration and yield of microbe-synthesized quinic acid was lower than for the control experiment, it was demonstrated that *de novo* synthesized and exported 3-dehydroquinic acid can be later transported back into the cytoplasm and reduced to quinic acid. Even under glucose-rich culture conditions, quinic acid

concentration kept increasing (Figure 32), which indicates that a portion of 3-dehydroquinic acid gets reduced to quinic acid prior to export. However, recapture of 3-dehydroquinic acid under glucose-limited conditions is also important in quinic acid biosynthesis. The hydroaromatics transport system in *E. coli* was not yet been identified. An attempt to identify such a transport system will be described in Chapter 3. Hydroaromatics transport in *E. coli* may be an evolutionary remnant from which a progenitor microbe to *E. coli* exploited 3-dehydroquinic acid and quinic acid as a sole source of carbon for growth and metabolism. *Klebsiella pneumoniae*, which is evolutionary closely related to *E. coli*, is capable of exploiting quinic acid as sole carbon source for growth and metabolism.[4] The glucose concentration in the culture medium can control transport of hydroaromatics, since it would be expected that glucose would inhibit other carbon source uptake pathways. Therefore, under glucose-rich culture conditions, the recapture of 3-dehydroquinic acid is slows with the highest recapture rates apparently realized under glucose-limited culture conditions. For quinic acid-producing *E. coli*, a remnant hydroaromatic transport pathway is beneficiary, since it is the combination of 3-dehydroquinic acid reduction prior to export and after recapture that affords the highest concentrations and yields of microbe-synthesized quinic acid.

Quinic acid purification

Purification of quinic acid from fermentation broth faces a couple of challenges. First, there is the need to separate away inorganic salts. Secondly, there are biosynthetic byproducts that must be removed.

Cell-free culture medium was obtained by centrifugation of crude culture medium at 10,000 *g* for 15 min. Protein was removed by acidification of cell-free culture medium

to pH 3 with concentrated H_2SO_4 with stirring at low temperature (0 or 4 °C) for at least two hours. Precipitated proteins were filtered through Whatman No.1 filter paper. No filtering agent, such as Celite, was required, because proteins coagulated in large pieces. Alternatively, refluxing of the acidified cell-free culture medium was used to separate protein and aromatize 3-dehydroquinic acid simultaneously. All proteins precipitated after refluxing. However some adhered tightly to the sides of the flask. Refluxing neutral cell-free culture medium did not result in separation of protein from the cell-free culture medium.

Industrially, ultrafiltration of cell-free culture medium is likely a preferred route for protein removal. Accordingly, ultrafiltration of cell-free culture medium was primarily used elaboration of a purification scheme for microbe-synthesized quinic acid. Ultrafiltration employed Millipore 10 kDa membrane to separate proteins from the cell-free culture medium.

Previously by the Frost group it was demonstrated that protocatechuic acid could be obtained in a 100% conversion yield from 3-dehydroquinic acid by refluxing culture medium containing 3-dehydroquinic acid (Figure 33).[27] Therefore, refluxing of cell-free, protein-free culture medium was used to aromatize 3-dehydroquinic acid, which was the major byproduct in quinic acid microbial synthesis. Neutral or cell-free, protein-free culture medium acidified to pH 3 was refluxed for 1 h to aromatize 3-dehydroquinic acid. Aromatized byproduct was then removed by adsorption on activated carbon. Treatment with activated carbon was used to decolorize the dark brown cell-free, protein-free culture medium after aromatization of 3-dehydroquinic acid. Activated carbon was added to cell-free, protein-free culture medium at room temperature and the mixture was

stirred for 1.5 h. After filtration through a Celite pad, the resulting solution was pale yellow.
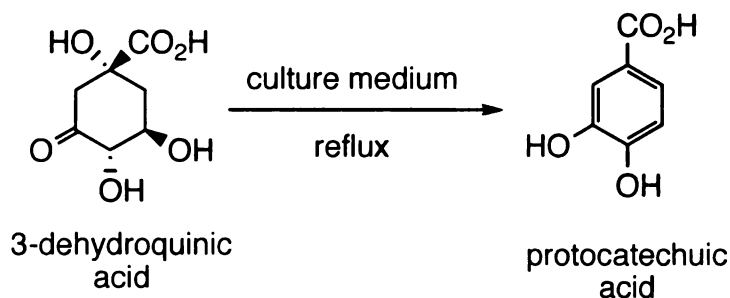
Figure 33. Conversion of 3-dehydroquinic acid to protocatechuic acid.

A pH effect was observed during treatment with activated carbon. Cell-free, protein free culture medium at pH 3 required 2% (w/v) of activated carbon (20 g of charcoal for 1 L of broth), while at pH 7 7-8% of activated carbon was required to obtain the same pale yellow cell-free, protein-free culture medium. After treatment with activated carbon at pH3 broth, a small portion of this solution was neutralized and the pale yellow color remained. Therefore, decolorization was not dependent on maintenace of an acidic pH. Grades of activated carbon employed included: activated carbon Norit® SA3 100 mesh and Darco® KB 100 mesh. Decolorization required 2% (w/v) of Norit charcoal, while 4% (w/v) of Darco charcoal was required to reach the same decolorization level. For elaboration of all subsequent steps in the purification of microbe-synthesized quinic acid, Norit® activated carbon was used.

Separation of quinic acid from inorganic salts in the culture medium was the most challenging step. Organic solvent extraction of quinic acid could not be used since quinic acid has very low solubility in organic solvents. A negative adsorption method was examined where a strong anion exchange resin (AG1-X8) and strong cation exchange

resin (Dowex 50 WX4) were used to remove inorganic salts from the cell-free, protein-free, decolorized culture medium. The resulting salt-free solution was evaporated to dryness and quinic acid was recrystalized from ethanol, yielding 18% final purification yield based on the quinic acid originally present in the culture medium. In order to remove inorganic salts from 1 L of cell-free, protein-free, decolorized culture medium, 1 L of cation exchange resin and 1 L of anion exchange resin were required. This was unlikely to be an industrially viable process.

Table 13. Quinic acid purification from microbial culture medium.

Step	Description	Volume (L)	[QA] (g/L)	QA (g)	Yield (%)
1	Ultrafiltration of cell-free broth through 10 kDa membrane	1.20	33	40	
2	Reflux 1 h, acidify cell-free, protein-free culture medium to pH 3, 4% (w/v) charcoal treatment	0.96	40	38	95
3	Concentrate fivefold, add three volumes of EtOH, remove inorganic salt precipitate	0.82	46	38	95
4	Concentrate to dryness, dissolve in boiling EtOH, filter insoluble precipitates	1.18	30	35	88
5	Collect QA that precipitated after 30 min at room temperature, (1st crop), chill at 4 °C overnight			22.1	55
6	Collect QA precipitate (2nd crop). Concentrate fourfold, chill at 4 °C overnight			6.4	16
7	Collect QA precipitates (3rd crop)			5.6	14
8	Total QA recovered			34.1	85

After screening of numerous methods, the final quinic acid purification was obtained (Table 13). After filtration of ethanol precipitated inorganic salts, the resulting filtrate was concentrated to dryness and the residue was redissolved in 1 L of boiling ethanol. Solids remaining in solution were removed by filtration. Partial concentration of quinate-containing filtrate led to formation of the first crop of quinic acid precipitate and was filtered. Two more rounds of concentration, chilling and precipitate collection were performed. Overall, 85% of quinic acid in the starting culture medium was isolated.

The quality of quinic acid was determined by elemental analysis (Table 14). The third crop of quinic acid precipitates was not submitted for elemental analysis, due to its pale yellow color.

Table 14. Quinic acid elemental analysis.

entry	sample	expt. (cald.) (%)	
		C	H
1	1st crop	43.79 (43.75)	6.35 (6.29)
2	2nd crop	43.50 (43.75)	6.53 (6.29)
3	Aldrich	43.41 (43.75)	6.61 (6.29)

First crop of purified quinic acid was also evaluated by ^{1}H and ^{13}C NMR analysis with D_2O as a solvent and TSP as an internal standard. Proton NMR (Figure 34) revealed correct quinic acid peaks as they were compared to literature reported values and standard NMR, which was obtained from quinic acid sample purchased from Aldrich. Proton NMR also revealed that purified quinic acid had some residual EtOH, which methionine triplet can be seen at 1.15 ppm and methilyne quadruplet can be seen at 3.61 ppm (Figure 34). Also, a triplet at 1.25 ppm and a quadruplet at 4.21 ppm corresponds to methionine and methilyne of ethyl group in quinic acid ethyl ester (Figure 34), which was obtained during purification of quinic acid in step 4 (Table 13). Carbon NMR (Figure 35) analysis revealed quinic acid peaks which were identical to literature reported values and to standard quinic acid NMR.
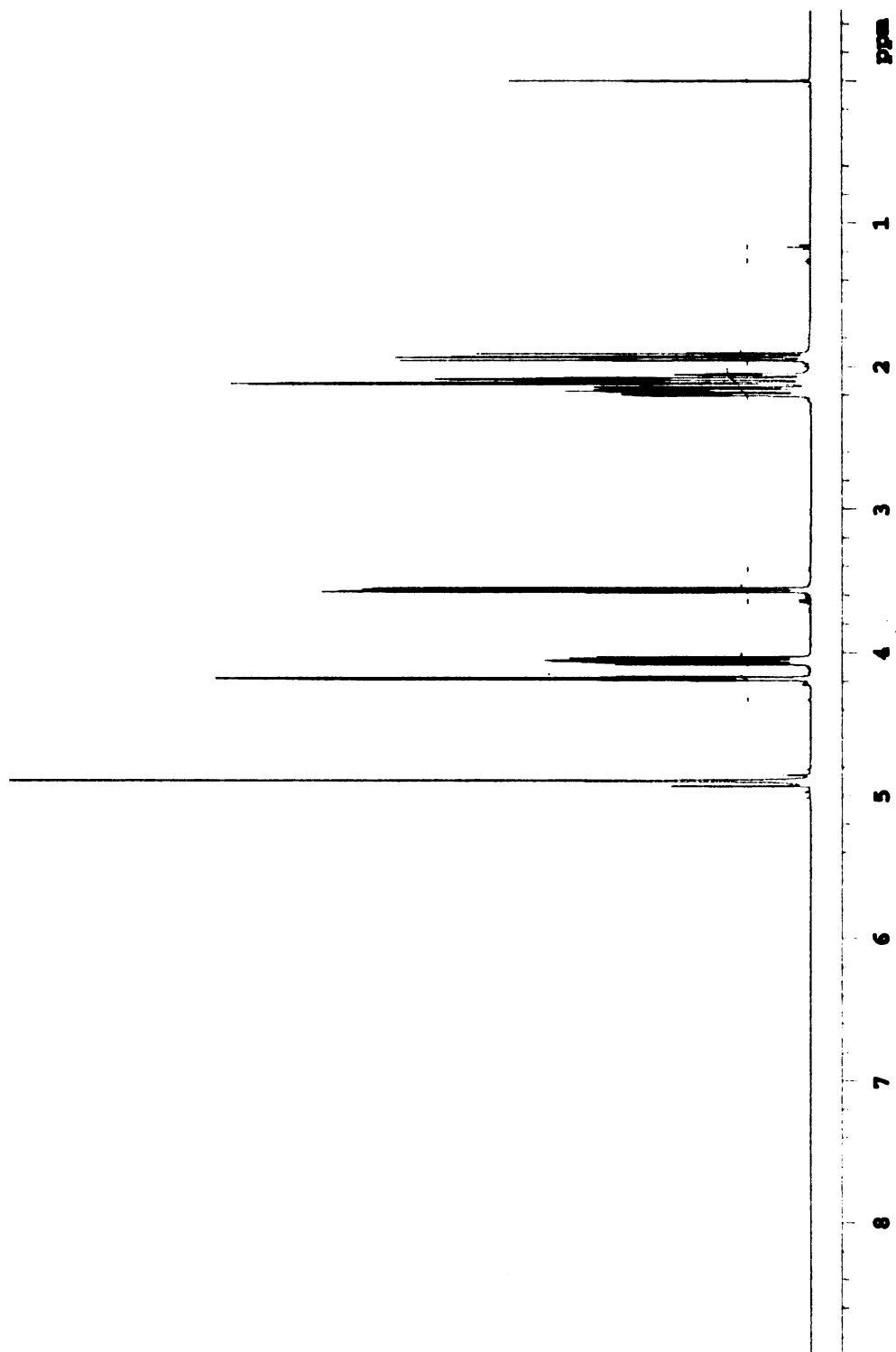
Figure 34. ^{1}H NMR of purified 1st crop of quinic acid.
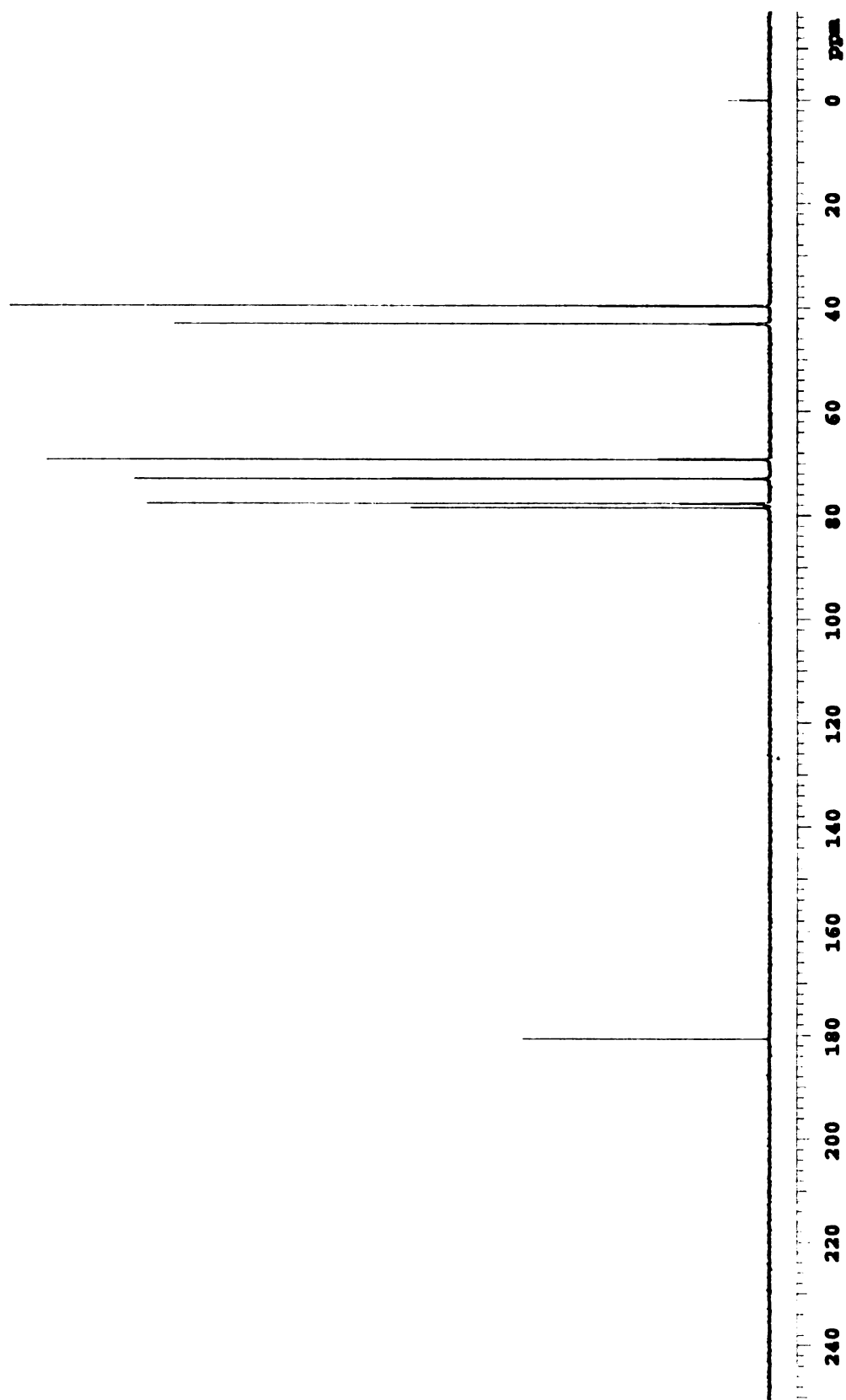
Figure 35. ^{13}C NMR of purified 1st crop of quinic acid.

Discussion

The first reported microbial synthesis of quinic acid relied on heterologous expression in *E. coli* of the *Klebsiella pneumoniae qad* gene, which encodes quinate dehydrogenase.[3] In a later variant a native *E. coli aroE*-encoded shikimate dehydrogenase in an *E. coli aroD* mutant lacking 3-dehydroquinate dehydratase enzyme activity, resulted in an *E. coli* construct, which synthesized quinic acid from glucose.[5] Homologous overexpression of all genetic elements avoids the differences between *K. pneumoniae* and *E. coli* in codon usage, promoter strength and protein folding. More recently, another *E. coli* shikimate/quinate dehydrogenase encoded by *ydiB* locus was discovered.[18] Disruption of the genomic *ydiB* sequence in *E. coli* construct that synthesized shikimic acid resulted in complete elimination of byproduct quinic acid formation during synthesis of shikimic acid. This clearly indicated that YdiB is involved in quinic acid biosynthesis. Therefore, overexpression of plasmid-encoded *ydiB* rather than *aroE* as a shikimate/quinate dehydrogenase was evaluated. However, *E. coli* QP1.1/pJJ5.069 and QP1.1/pJJ5.073 failed to produce quinic acid at the same concentration and yield as the control strain relaying on *aroE* overexpression (Table 4). The primary reason was low YdiB specific activity (Table 5).

Deletion of the entire ORF of the *aroD* gene was unsuccessful in *E. coli* B and only half of *aroD* was deleted in the final construct, which yielded *E. coli* B capable of synthesizing quinic acid. However, the *E. coli* B quinic acid producers (Table 7) did not synthesize quinic acid in as high a concentration and yield as quinic acid-synthesizing constructs based on *E. coli* K-12 (Table 4, entry 1). Plasmid-localized transketolase

overexpression had no effect on synthesized hydroaromatics concentrations by *E. coli B serA::aroB* Δ*aroD*(new)::FRT–*cat*–FRT/pKD12.112 (Figure 20A) relative to *E. coli B serA::aroB* Δ*aroD*(new)::FRT–*cat*–FRT/pKD12.138 (Figure 20B). On the other hand, transketolase overexpression had an impact on biomass accumulation in the beginning of cultivation, where from 0 – 24 h of cultivation of *E. coli B serA::aroB* Δ*aroD*(new)::FRT–*cat*–FRT/pKD12.138 cells grew slower with transketolase overexpression (Figure 20B) as compared to the *E. coli B serA::aroB* Δ*aroD*(new)::FRT–*cat*–FRT/pKD12.112 without transketolase overexpression (Figure 20A). Overexpression of transketolase did not have an impact on biomass production *E. coli* K-12 QP1.1/pKD12.138 (Figure 24B) relative to *E. coli* K-12 QP1.1/pKD12.112 (Figure 25) as they accumulated the same biomass throughout the cultivation. Interestingly, the total of synthesized the hydroaromatics, quinic acid and 3-dehydroquinic acid, by *E. coli B serA::aroB aroD*(new)::FRT-*cat*-FRT/pKD12.112 was 65 g/L in 18% yield(Table 7, entry 5), while *E. coli* K-12 QP1.1/pKD12.112 synthesized 54 g/L in 15% yield(Table 9, entry 2) and QP1.1/pKD12.138 synthesized 72 g/L in 19% yield (Table 9, entry 1). This indicates that *E. coli* B *serA::aroB aroD*(new)::FRT-*cat*-FRT/pKD12.112 is a better hydroaromatics (3-dehydroquinic acid + quinic acid)-synthesizing construct relative to *E. coli* K-12 QP1.1/pKD12.112 when transketolase is not overexpressed. However, with transketolase overexpression *E. coli* K-12 QP1.1/pKD12.138 is a better host strain for synthesizing hydroaromatics relative to than *E. coli* B *serA::aroB aroD*(new)::FRT-*cat*-FRT/pKD12.112 without transketolase overexpression or even *E. coli B serA::aroB aroD*(new)::FRT-*cat*-FRT/pKD12.138 with transketolase overexpression, which synthesized 46 g/L in 15% yield of total hydroaromatics (Table 7, entry 6).

Accumulation of higher levels than usual of 3-dehydroquinic acid by *E. coli* B *serA::aroB* *aroD*(new)::FRT-*cat*-FRT/pKD12.112 and *E. coli* B *serA::aroB* *aroD*(new)::FRT-*cat*-FRT/pKD12.138 may be explained by *E. coli* B recapture mechanism for 3-dehydroquinic acid transported into the culture medium is not as active/efficient as the recapture mechanism in *E. coli* K-12.

The optimal quinic acid production time for *E. coli* K-12 QP1.1/pKD12.138 was determined to be 78 h (Figure 24 B) with a standard inoculum preparation. When a fresher inoculum was used, quinic acid accumulation was slower (Figure 23 B) than for the experiment with the standard inoculum preparation (Figure 23 A), even though a fresher inoculm resulted in higher biomass accumulation. The transketolase overexpression in quinate-producing *E. coli* K-12 strain had a more profound effect and it increased quinic acid concentration in the medium from 52 g/L synthesized by QP1.1/pKD12.112 in 15% yield (Table 9, entry 2) to 67 g/L synthesized by QP1.1/pKD12.138 in 18% yield (Table 9, entry 1).

An interesting effect was observed for QP1.1/pKD12.138 cultivated with reduced potassium phosphate or aromatic amino acid concentrations. During both cultivation conditions, reduction in accumulated biomass was observed (Figure 27 A and Figure 28 A) although only in the presence of aromatic amino acids was a reduction in dissolved oxygen requirement observed. *E. coli* QP1.1/pKD12.138 did not display a reduced oxygen requirement even when the dry cell weight decreased from 55 g/L to 40 g/L upon lowering the concentration of potassium phosphate in the culture medium. However, when biomass decreased to 40 g/L with lowered concentration of aromatic amino acid, *E. coli* QP1.1/pKD12.138 required less dissolved oxygen in the medium and therefore

airflow and/or impeller rate had to be changed. Supplementation of fermentation medium with 15 g/L of yeast extract did not afford higher concentrations and yields of quinic acid (Table 11, entry 9). Another experiment could be done in the future where addition of yeast extract is done not in the beginning of a fermentor run, but towards the end, when E. coli might lack some essential nutrients. Further optimization of QP1.1/pKD12.138 culture conditions is required in order to determine the impact on quinic acid biosynthesis with reduced airflow. Large volume industrial fermenors can not support a 1 vvm airflow rate. Reduction of airflow will reduce dissolved oxygen concentration in the culture medium, which ultimately can translate to reduction in quinic acid concentrations and yield. Therefore, optimization of impeller speeds, impeller shape and size, and introduction of baffles inside the fermentor is required in order to detremine the best aeration conditions compatible with large-volume fermentor runs. To summarize, the best quinic acid microbial synthesis by E. coli QP1.1/pKD12.138 over 78 h was determined with standard inoculation and culture medium and afforded 70 g/L of quinic acid in 18% yield and a low 5 g/L level of byproduct 3-dehydroquinic acid.

Recapturing on 3-dehydroquinic acid was shown to be an important step for quinic acid producing E. coli K-12. It was also shown that maintaining glucose-limited conditions during the first 60 h of fermentation is very important since during this time quinic acid biosynthesis is at its highest rate. 3-Dehydroquinic acid recapturing was slow in E. coli QP1.1/pKD12.138 when fermentor-controlled culture conditions were switched from glucose-rich to glucose-limited conditions. Loss of glucose-limited control, which leads to glucose-rich conditions, towards the end of a fermentor run does not have a substantial impact on quinic acid synthesis.

A purification procedure was developed for microbe-synthesized quinic acid that allowed for isolation of 85% quinic acid originally in the culture medium in pure form. It involved aromatization of 3-dehydroquinic acid by refluxing cell-free, protein-free culture medium, treatment with activated carbon to remove aromatized 3-dehydroquinic acid product and decolorize culture medium, and the use of EtOH to selectively precipitate inorganic salts from quinic acid. EtOH was also used to purify quinic acid by crystallization.

A further optimization of quinic acid purification process required where spray drying could be used of cell-free, protein-free culture medium. This could reduce the number of unit operations in the purification process and would amiable to large volume fermentor runs. Quinic acid and inorganic salt powder mixture obtained after spray drying could be redissolved in hot ethanol and insoluble slats filtered from solution. After filtration and partial concentration, quinic acid could be isolated in pure form.

References

1   (a) Bestmann, H. J.; Heid, H. A. Stereospecific synthesis of optically pure quinic acid and shikimic acid from D-arabinose. *Angew. Chem., Int. Ed. Engl,.* **1971**, *10*, 336-337.   (b) Hiroya, K.; Ogasawara, K. A concise enantio- and diastereo-controlled synthesis of (-)-quinic acid and (-)-shikimic acid. *Chem. Commun.* **1998**, 2033-2034.

2   Haslam, E. In *Shikimic Acid: Metabolism and Metabolites*; Wiley & Sons: New York, **1993**, p. 56.

3   Draths, K. M.; Ward, T. L.; Frost, J. W.   Biocatalysis and nineteenth century organic chemistry: Conversion of D-glucose into quinoid organics. *J. Am. Chem. Soc.* **1992**, *114*, 9725-9726.

4   (a) Mitsuhashi, S.; Davis, B. D. Aromatic biosynthesis XIII. Conversion of quinic acid to 5-dehydroquinic acid by quinic dehydrogenase. *Biochim. Biophys. Acta* **1954**, *15*, 268-280. (b) Davis, B. D.; Gilvarg, C.; Mitsuhashi, S. Enzymes of aromatic biosynthesis: Quinic dehydrogenase from *Aerobacter aerogenes*. *Methods Enzymol.* **1955**, *2*, 307-311.

5   Draths, K. M.; Knop, D. R.; Frost, K. M. Shikimic acid and quinic acid: replacing isolation from plant sources with recombinant biocatalysis. *J. Am Chem. Soc.* **1999**, *121*, 1603-1604.

6   (a) Draths, K. M.; Pompliano, D. L.; Conley, D. L.; Frost, J. W.; Berry, A.; Disbrow, G. L.; Staversky, R. J.; Lievense, J. C. Biocatalytic Synthesis of Aromatics from D-Glucose: The Role of Transketolase. *J. Am. Chem. Soc.* **1992**, *114*, 3956-3962. (b) Gubler, M.; Jetten, M.; Lee, S. H.; Sinskey, A. J. Cloning of the Pyruvate-Kinase Gene (Pyk) of *Corynebacterium glutamicum* and Site-Specific Inactivation of Pyk in a Lysine- Producing *Corynebacterium lactofermentum* Strain. *Appl. Env. Microbiol.* **1994**, *60*, 2494-2500. (c) Miller, J. E.; Backman, K. C.; O'Conner, M. J.; Hatch, R. T. Production of Phenylalanine and Organic-Acids by Phosphoenolpyruvate Carboxylase-Deficient Mutants of *Escherichia coli. J. Ind. Microbiol.* **1987**, *2*, 143-149. (d) Patnaik, R.; Liao, J. C. Engineering of *Escherichia coli* Central Metabolism for Aromatic Metabolite Production with Near Theoretical Yield. *Appl. Environ. Microbiol.* **1994**, *60*, 3903-3908. (e) Patnaik, R.; Spitzer, R. G.; Liao, J. C. Pathway Engineering for Production of Aromatics in *Escherichia coli*: Confirmation of Stoichiometric Analysis by Independent Modulation of AroG, TktA, and PpsA Activities. *Biotechnol. Bioeng.* **1995**, *46*, 361-370. (f) Li, K.; Mikola, M. R.; Draths, K. M.; Worden, R. M.; Frost, J. W. Fed-Batch Fermentor Synthesis of 3-Dehydroshikimic Acid Using Recombinant *Escherichia coli. Biotechnol. Bioeng.* **1999**, *64*, 61-73.

7   (a) Flores, N.; Xiao, J.; Berry, A.; Bolivar, F.; Valle, F. Pathway Engineering for the Production of Aromatic Compounds in *Escherichia coli. Nat. Biotechnol.* **1996**, *14*, 620-623. (b) Chen, R.; Yap, W. M. G. J.; Postma, P. W.; Bailey, J. E. Comparative Studies of *Escherichia coli* Strains Using Different Glucose Uptake Systems: Metabolism and Energetics. *Biotechnol. Bioeng.* **1997**, *56*, 583-590. (c) Chen, R.; Hatzimanikatis, V.; Yap, W. M. G. J.; Postma, P. W.; Bailey, J. E. Metabolic Consequences of Phosphotransferase (PTS) Mutation in a Phenylalanine-Producing Recombinant *Escherichia coli. Biotechnol. Prog.* **1997**, *13*, 768-775. (d) Baez, J. L.; Bolivar, F.; Gosset, G. Determination of 3-Deoxy-D-*Arabino*-Heptulosonate 7-Phosphate Productivity and Yield from Glucose in *Escherichia coli* Devoid of the Glucose Phosphotransferase Transport System. *Biotechnol. Bioeng.* **2001**, *73*, 530-535. (e) Flores, S.; Gosset, G.; Flores, N.; De Graaf, A. A; Bolivar, F. Analysis of Carbon Metabolism in *Escherichia coli* Strains with an Inactive Phosphotransferase System by 13C Labeling and NMR Spectroscopy. *Metabol. Eng.* **2002**, *4*, 124-137.

8   Yi, J.; Li, K.; Draths, K. M.; Frost, J. W. Modulation of Phosphoenolpyruvate Synthase Expression Increases Shikimate Pathway Product Yields in *E. coli. Biotechnol. Prog.* **2002**, *18*, 1141-1148.

9   (a) Ogino, T.; Garner, C.; Markley, J. L.; Herrmann, K. M. Biosynthesis of Aromatic Compounds: 13C NMR Spectroscopy of Whole *Escherichia coli* Cells. *Proc. Natl. Acad. Sci. USA* **1982**, *79*, 5828-5832. (b) Weaver, L. M.; Herrmann, K. M. Cloning of an AroF Allele Encoding a Tyrosine-Insensitive 3-Deoxy-D-*Arabino*-Heptulosonate 7-Phosphate Synthase. *J. Bacteriol.* **1990**, *172*, 6581-6584.

10   Draths, K. M.; Pompliano, D. L.; Conley, D. L.; Frost, J. W.; Berry, A.; Disbrow, G. L.; Staversky, R. J.; Lievense, J. Biocatalytic Synthesis of Aromatics from D-Glucose: the Role of Transketolase. *J. Am. Chem. Soc.* **1992**, *114*, 3956-3962.

11   Ran, N. Synthesis of aromatics and hydroaromatics from D-glucose via a native and a variant of the shikimate pathway. Ph.D. dissertation. *Michigan State University*, **2004.**

12   Yi, J.; Draths, K. M.; Li, K.; Frost, J. W. Altered Glucose Transport and Shikimate Pathway Product Yields in *E. coli. Biotechnol. Prog.* **2003**, *19*, 1450-1459.

13   Chandran, S. C.; Yi, J.; Draths, K. M.; von Daeniken, R.; Weber, W.; Frost, J. W. Phosphoenolpyruvate availability and the biosynthesis of shikimic acid. *Biotechnol. Prog.* **2003**, *19*, 808-814.

14   Erickson, L. E.; Fung, D. Y-Ch. In: *Handbook of anaerobic fermentations*; Dekker: New York, **1988.**

15   Pittard, J.; Wallace, B. J. Distribution and function of genes concerned with aromatic biosynthesis in *Escherichia coli*. *J. Bacteriol*. **1966**, *91*, 1494-1508.

16   Snell, K. D.; Draths, K. M.; Frost, J. W. Synthetic modification of the *Escherichia coli* chromosome: enhancing the biocatalytic conversion of glucose into aromatic chemicals. *J. Am. Chem. Soc*. **1996**, *118*, 5605-5614.

17   Knop, D. R.; Draths, K. M.; Chandran, S. S.; Barker, J. L.; von Daeniken, R.; Weber, W.; Frost, J. W. Hydroaromatic equilibration during biosynthesis of shikimic acid. *J. Am. Chem. Soc*. **2001**, *123*, 10173-10182.

18   (a) Michel, G.; Roszak, A. W.; Sauve, V.; Maclean, J.; Matte, A.; Coggins, J. R.; Cygler, M.; Lapthorn, A. J. Structures of Shikimate Dehydrogenase AroE and Its Paralog YdiB. *J. Biol. Chem*. **2003**, *278*, 19463-19472. (b) Benach, J.; Lee, I.; Edstorm, W.; Kuzin, A. P.; Chiang, Y.; Acton, T. B.; Montelione, G. T.; Hunt, J. F. The 2.3-Å Crystal Structure of the Shikimate 5-Dehydrogenase Orthologue YdiB from *Escherichia coli* Suggests a Novel Catalytic Enviroment for an NAD-dependent Dehydrogenase. *J. Biol. Chem*. **2003**, *278*, 19176-19182.

19   Jancauskas, J. Strategies for improving synthesis of 3-dehydroshikimic acid and shikimic acid from D-glucose. M.S. thesis. *Michigan State University*, **2006**.

20   Brune, M.; Schumann, R.; Wittinghofer, F. Cloning and sequencing of the adenylate kinase gene (*adk*) of *Escherichia coli*. *Nuc. Acid Res*. **1985**, *13*, 7139-7151.

21   Chandran, S.S. Manipulation of genes and enzymes of the shikimate pathway. *Ph.D. Dissertation*, Michigan State University, **2000**.

22   (a) Studier, F. W.; Rosenberg, A. H.; Dunn, J.; Dubendorff, J. W. Use of T7 RNA polymerase to direct expression of cloned genes. *Methods Enzymol*. **1990**, *185*, 60-89 (b) Studier, F. W.; Moffatt, B. A. Use of bacteriophage T7 RNA polymerase to direct selective high-level expression of cloned genes *J. Mol. Biol*. **1986**, *189*, 113-130. (c) Grodberg, J.; Dunn, J. J. *ompT* encodes the Escherichia coli outer membrane protease that cleaves T7 RNA polymerase during purification. *J. Bacteriol*. **1988**, *170*, 1245-1253. (d) Phillips, T. A.; van Bogelen, R. A.; Neidhardt, F. C. *lon* gene product of *Escherichia coli* is a heat-shock protein. *J. Bacteriol*. **1984**, *159*, 283-287.

23   Datsenko, K.A.; Wanner, B.L. One-step inactivation of chromosomal genes in *Escherichia coli* K-12 using PCR products. *Proc. Natl. Acad. Sci. USA*. **2000**, *97*, 6640-6645.

24   Cherepanov, P. P.; Wackernagel, W. Gene disruption in Escherichia coli: TcR and KmR cassettes with the option of Flp-catalyzed excision of the antibiotic-resistance determinant. *Gene* **1995**, *158*, 9-14.

25   Miller, J. H. *A Short Course in Bacterial Genetics*; Cold Spring Harbor Laboratory: Plainview, NY, 1992.

26   (a) Posfai, G., Koob, M.D., Kirkpatrick, H.A., Blattner, F.R. Versatile insertion plasmids for targeted genome manipulations in bacteria: isolation, deletion, and rescue of the pathogenicity island LEE of the *Escherichia coli* O157:H7 genome. *J. Bacteriol.* **1997**, *179*, 4426-4428. (b) Martinez-Morales, F., Borges, S., Martinez, A., Shanmugam, K.T., Ingram, L.O. Chromosomal integration of heterologous DNA in *Escherichia coli* with precise removal of markers and replicons used during construction *J. Bacteriol.* **1999**, *181*, 7143-7148.

27   Li, W.; Xie, D.; Frost, J. W.. Benzene-free synthesis of catechol: interfacing microbial and chemical catalysis. *J. Am. Chem. Soc.* **2005**, *127*, 2874-2882.

CHAPTER THREE

A search for a better shikimic acid producer

Introduction

Previously reported construction of a shikimic acid producing *E. coli* host strain

SP1.1. began with the homologous recombination of the *aroB* gene into the *serA* locus of

E. coli RB791 resulting in RB791 *serA::aroB*.[4] An additional copy of *aroB* in the final

shikimic acid producing strain, increased the specific activity of 3-dehydroquinate

synthase to a level where the 3-dehydroquinic acid synthesis rate from 3-deoxy-D-

arabino-heptulosonic acid 7-phosphate (DAHP) (Figure 1) was no longer an impediment

to carbon flow through the shikimate pathway.[1] Disruption of *serA* locus in RB791

serA::aroB led to inactive 3-phosphoglycerate dehydrogenase, which is an enzyme

required for L-serine biosynthesis in wild type *E. coli*. Therefore, a copy of the *serA* gene

was inserted in plasmids and that provided the basis for plasmid maintenance when

cultures were cultivated under minimal salt conditions. In order to accumulate shikimic

acid in fermentation media, shikimate kinases isozymes AroK and AroL had to be

inactivated (Figure 1). This was done by two successive P1 phage-mediated

transductions to transfer *aroL478*::Tn*10* and *aroK*::Cm[R] loci from ALO807[2] into RB791

serA::aroB, which afforded the final shikimic acid producing *E. coli* host SP1.1.

Increases in the intracellular concentration of phosphoenolpyruvate resulted in the

direction of more carbon flow into the shikimate pathway when feedback resistant DAHP

synthase and transketolase were expressed.[3] The benchmark strain for shikimic acid

production, SP1.1/pKD12.138, had overexpressed *aroE*-encoded shikimate dehydrogenase, *tktA*-encoded transketolase and *aroF*^{FBR}-encoded DAHP synthase and synthesized 52 g/L of shikimic acid from glucose in 18% yield with a 24% total combined yield of shikimic acid, 3-dehydroshikimic acid and quinic acid.[4] Overexperession of transketolase ensured higher E4P availability inside the cell and therefore the direction of increased carbon flow into the shikimate pathway was observed (Figure 1). *E. coli* SP1.1/pKD12.112, which lacked plasmid-localized transketolase overexpression produced 38 g/L of shikimic acid from glucose in 12% yield and a 15% total of shikimic acid, 3-dehydroshikimic acid and quinic acid yield under glucose-rich conditions.[4] With increased E4P availability, PEP availability became a limiting factor for shikimic acid biosynthesis. Two strategies were employed to increase PEP availability. *E. coli* SP1.1/pKD15.071B with expression of plasmid-localized *ppsA*-encoded phosphoenolpyruvate synthase in addition to AroF^{FBR}, TktA and AroE, synthesized 66 g/L of shikimic acid in 23% yield and a combined 29% yield of shikimic acid and hydroaromatic byproducts.[3a] This strategy relied on the fact that pyruvate, which is generated from PEP during PTS glucose transport, was recycled back to PEP by phosphoenolpyruvate synthase. The second strategy employed Glf-mediated glucose transport by facilitated diffusion in a PTS-inactive *E. coli* strain SP1.1*pts*/pSC6.090B. Shikimic acid was synthesized at 71 g/L in 27% yield with combined of shikimic acid and hydroaromatic byproducts 34% yield.

The strategies examined so far for improving shikimic acid biosynthesis were based on increasing carbon flow into the shikimate pathway. As described earlier, they

employed increasing specific activities of DAHP synthase and transketolase, and increasing intracellular phosphoenolpyruvate levels. With increased carbon flow into the shikimate pathway, synthesized shikimic acid yield was increased from 12% (Table 15, entry 1) to 23% (Table 15, entry 4) and total hydroaromatic yield was increased from 15% (Table 15, entry 1) to 29% (Table 15, entry 4).[3a, 4] However, the ratio between shikimic acid and 3-dehydroshikimic acid declined from 5.9 to 4.1 (Table 15). Previous work determined that accumulation of 3-dehydroshikimic acid and quinic acid is caused by hydroaromatic equilibration where shikimic acid is transported back inside the cell and converted to quinic acid through intermediacy of 3-dehydroshikimic acid and 3-dehydroquinic acid.[4] It was also shown that quinic acid accumulation during shikimic acid biosynthesis was successfully reduced from 19 g/L, under glucose-limited culture conditions to 4 g/L, under glucose-rich culture conditions.[4] Glucose-rich culture conditions also yielded a higher concentration and yield of shikimic acid. Previous work has also determined that shikimate dehydrogenase AroE exhibits linear mixed-type inhibition with 3-dehydroshikimic acid and an inhibition constant (K_i) of 0.16 mM associated with shikimic acid.[5] Therefore, accumulation of 3-dehydroshikimic acid (decrease in SA/DHS) during hydroaromatic equilibration can be caused by feedback inhibition of aroE-encoded shikimate dehydrogenase by shikimic acid.

Table 15. **Shikimic acid and 3-dehydroshikimic acid molar ratios, shikimic acid yield and total hydroaromatic yield produced by recombinant *E. coli* under fermentor-controlled, glucose-rich conditions.**

Entry	Strain	Relevant characteristics	Ratio^a	SA Yield^b	Total Yield^c
1	SP1.1/pKD12.112	*serA, aroF*^{FBR}, P$_{tac}$*aroE*	5.9	12%	15%
2	SP1.1/pKD12.138	*serA, aroF*^{FBR}, P$_{tac}$*aroE, tktA*	3.2	18%	24%
3	SP1.1*pts*/pSC6.090A	*pts⁻/serA, aroF*^{FBR}, P$_{tac}$*aroE, tktA,* P$_{tac}$*glt glk*	4.7	27%	34%
4	SP1.1/pKD15.071B	*serA, aroF*^{FBR}, P$_{tac}$*aroE, tktA, ppsA*	4.1	23%	29%

^{a}(mol produced shikimic acid)/(mol produced 3-dehydroshikimic acid). ^{b}(mol shikimic acid)/(mol glucose consumed). ^{c}(mol shikimic acid + mol 3-dehydroshikimic acid + mol quinic acid)/(mol glucose consumed).

Removing feedback inhibition from shikimate dehydrogenase by shikimic acid might decrease 3-dehydroshikimic acid accumulation and therefore increase synthesized shikimic acid concentration and yield. Two strategies were developed to obtain a feedback insensitive shikimate dehydrogenase. One strategy called for identification of a non-*E. coli* shikimate dehydrogenase that was insensitive to shikimic acid inhibition followed by heterologous expression of the enzyme in an *E. coli* shikimate-producing strain. Quinate dehydrogenase Qad from *Klebsiella pneumoniae* and shikimate dehydrogenase AroD from *Bacillus subtilis* were investigated as alternatives to *E. coli* shikimate dehydrogenase AroE.[6] However, *B. subtilis* shikimate dehydrogenase was more sensitive to shikimic acid inhibition relative to *E. coli* AroE and was not evaluated under fermentor-controlled conditions.[6] Overexpression of plasmid-localized *qad* afforded very low shikimate dehydrogenase activity and Qad was not evaluated under fermentor-controlled conditions.[6]

The second strategy for obtaining a feedback insensitive shikimate dehydrogenase was directed evolution of *E. coli* wild-type shikimate dehydrogenase.[6] It was previously shown that use of feedback resistant DAHP synthase led to increased carbon flow into the shikimate pathway.[7] A high-throughput screening of mutant shikimate dehydrogenase library was performed. However, no improvement was obtained and mutant AroE was inhibited by shikimic acid at the same level as wild-type AroE.

Fermentation conditions

The impact of *E. coli* genetic modifications on the yields and concentrations of synthesized shikimic acid and shikimate pathway byproducts was evaluated under fed-batch controlled conditions. Fermentations were run under glucose-rich and glucose-limited conditions in a 2.0 L working volume fermentor. A concentration range of 55-170 mM glucose in the fermentation medium was maintained by manually adjusting the rate of glucose addition under glucose-rich conditions while a steady state concentration of approximately 0.2 mM glucose was maintained under glucose-limited conditions. During cultivation under glucose-limited conditions, glucose addition was controlled automatically through PID control loop by maintaining a steady concentration of dissolved oxygen. Glucose-rich conditions can lead to excessive generation of acetic acid, which is toxic to *E. coli* and many other microbes.[8] Glucose-limited conditions minimize generation of acetic acid but can lead to excessive CO_2 generation resulting in lower product yields.[8] However, it was previously discovered that shikimic acid producing *E. coli* had to be cultivated under glucose-rich conditions in order to obtain higher concentration and yield and more important to minimize quinic acid

accumulation.[4] Quinic acid accumulation in the shikimic acid broth at 10% or higher

concentration relative to the concentration of shikimic acid complicates shikimic acid

purification by crystallization.[9] Thus, mostly glucose-rich conditions were used to

evaluate synthesis of shikimic acid and shikimate pathway byproducts. A temperature of

36 °C and pH 7.0 were maintained. Dissolved oxygen concentration was maintained at

20% of air saturation under both glucose-rich and glucose-limited conditions. All

fermentations were run in duplicate and reported results represent the average of two runs

unless otherwise stated. Metabolite concentrations were determined using ^{1}H NMR.

Fermentations were terminated once metabolite concentrations stopped increasing.

Inactivation of *ydiB*

E. coli native second shikimate/quinate dehydrogenase YdiB was previously

discovered and was shown to have shikimate dehydrogenase activity *in vitro*[10] and *in*

vivo by restoring E. coli AB2834 growth on glucose-minimal plates.[6] Chapter 2

revealed, that overexpression of plasmid-localized *ydiB* in quinic acid producing strain

resulted in quinic acid accumulation in the fermentation broth. However, YdiB was not

as efficient in quinic acid production (Chapter 2) or shikimic acid production[6] as

compared to AroE. The overexpression of plasmid-localized *ydiB* in shikimic acid

producer SP1.1/pJJ4.171A led to equilibration of shikimic, 3-dehydroshikimic and quinic

acids to almost 1:1:1 molar ratio under glucose-rich culture conditions.[6] This supported a

hypothesis, that YdiB may be responsible for quinic acid accumulation during microbial

synthesis of shikimic acid. To evaluate this hypothesis, a shikimic acid producing E. coli

host with deleted genomic *ydiB* sequence was constructed. As mentioned earlier, production of shikimic acid is performed under glucose-rich conditions in order to minimize quinic acid accumulation. Chapter 2 revealed that recapturing of 3-dehydroquinic acid from culture medium is reduced or totally inhibited under glucose-rich culture conditions. Therefore, both glucose-rich and glucose-limited conditions were evaluated for shikimic acid synthesis using *E. coli ydiB* mutant host.

The construction of *ydiB* mutant began with deletion of the entire *ydiB* ORF in *E. coli* BW25113 using the Wanner methodology[11] described in Chapter 2 and afforded BW25113 Δ*ydiB*::FRT-*kan*-FRT. *E. coli* BW25113 was chosen due to high transformation efficiency and it was previously used by the Wanner group to generate various gene knock-outs.[11] A succesiful P1 phage-mediated transduction of the *ydiB*::FRT-*kan*-FRT mutation from BW25113 *ydiB*::FRT-*kan*-FRT to *E. coli* SP1.1 resulted in SP1.1 Δ*ydiB*::FRT-*kan*-FRT, which was designated as *E. coli* JJ2*kan*. The mutation was confirmed by PCR analysis. Additionally, *E. coli* JJ2*kan* showed no sensitivity to kanamycin due to the FRT-*kan*-FRT insertion in genomic DNA and it was insensitive to chloramphenicol and tetracycline due to mutations in *aroK* and *aroL*, respectively. *E. coli* JJ2*kan* was treated with pCP20 plasmid-encoded FLP, which led to *E. coli* JJ2 (SP1.1 Δ*ydiB*::FRT). Deletion of the *ydiB* gene in JJ2 was confirmed by PCR analysis and growth characteristics on selective plates. *E. coli* JJ2 showed sensitivity towards kanamycin, which indicated loss of the FRT-*kan*-FRT fragment, sensitivity to ampicillin, which indicated loss of the pCP20 plasmid, and resistance to chloramphenicol and tetracycline, like the parent *E. coli* host SP1.1.

Table 16. **Concentrations and yields of products synthesized by shikimic acid producing _E. coli_ with _ydiB_ mutation.**

Entry	Strain	[SA]^c, g/L	SA yield^d, %	[DHS], g/L	[DHQ], g/L	[QA], g/L	Total yield^e, %
1^a	SP1.1/pKD12.138	30	13	9	0	12	21
2^b	SP1.1/pKD12.138	60	26	11	0	7	33
3^a	JJ2/pKD12.138	23	10	13	27	0	26
4^b	JJ2/pKD12.138	17	8	8	41	0	34
5^a*	JJ2/pKD12.112	18	9	7	12	0	19
6^a*	JJ2/pKD12.152A	31	15	7	0	0	18
7^a	JJ2.2/pKD12.138	49	20	13	4	0	27
8^b	JJ2.2/pKD12.138	51	20	12	3	0	26

^{a}Glucose-limited conditions. ^{b}Glucose-rich conditions. *Single run fermentation. ^{c}Abbreviations: shikimic acid (SA), 3-dehydroshikimic acid (DHS), quinic acid (QA). ^{d}(mol SA)/(mol glucose consumed). ^{e}(mol SA + mol DHS + mol QA)/(mol glucose consumed).

E. coli SP1.1/pKD12.138 was used as a control strain and it synthesized 30 g/L of shikimic acid in 13% yield for glucose over 60 h under glucose-limited culture conditions (Table 16, Entry 1). Quinic acid accumulated at 12 g/L and 3-dehydroshikimic acid at 9 g/L with the total hydroaromatics yield of 21%. Cultivation of SP1.1/pKD12.138 under glucose-rich culture conditions resulted in a twofold increase in shikimic acid concentration (60 g/L) and twofold increase in yield (Table 16, entry 2) relative to culturing under glucose-limited culture conditions (Table 16, entry 1). Formation of quinic acid was reduced to 7 g/L, when _E. coli_ QP1.1/pKD12.138 was cultivated under glucose-rich culture conditions (Table 16, entry 2) relative to 12 g/L obtained under glucose-limited culture conditions. However 3-dehydroshikimic acid accumulated to concentrations in excess 11 g/L (Table 16, entry 2). The total yield of synthesized hydroaromatics increased to 33% (Table 16, entry 2) when _E. coli_ SP1.1 was cultivated

under glucose-rich culture conditions relative to totally yield of 21% obtained under glucose-limited culture conditions. Metabolite accumulation reveals that quinic acid started to accumulate in the early stage of the fermentor-controlled cultivation and kept increasing until the end of the cultivation under glucose-limited conditions (Figure 36A). Under glucose-rich culture conditions quinic acid started to accumulate during the second half of the cultivation (Figure 36B).
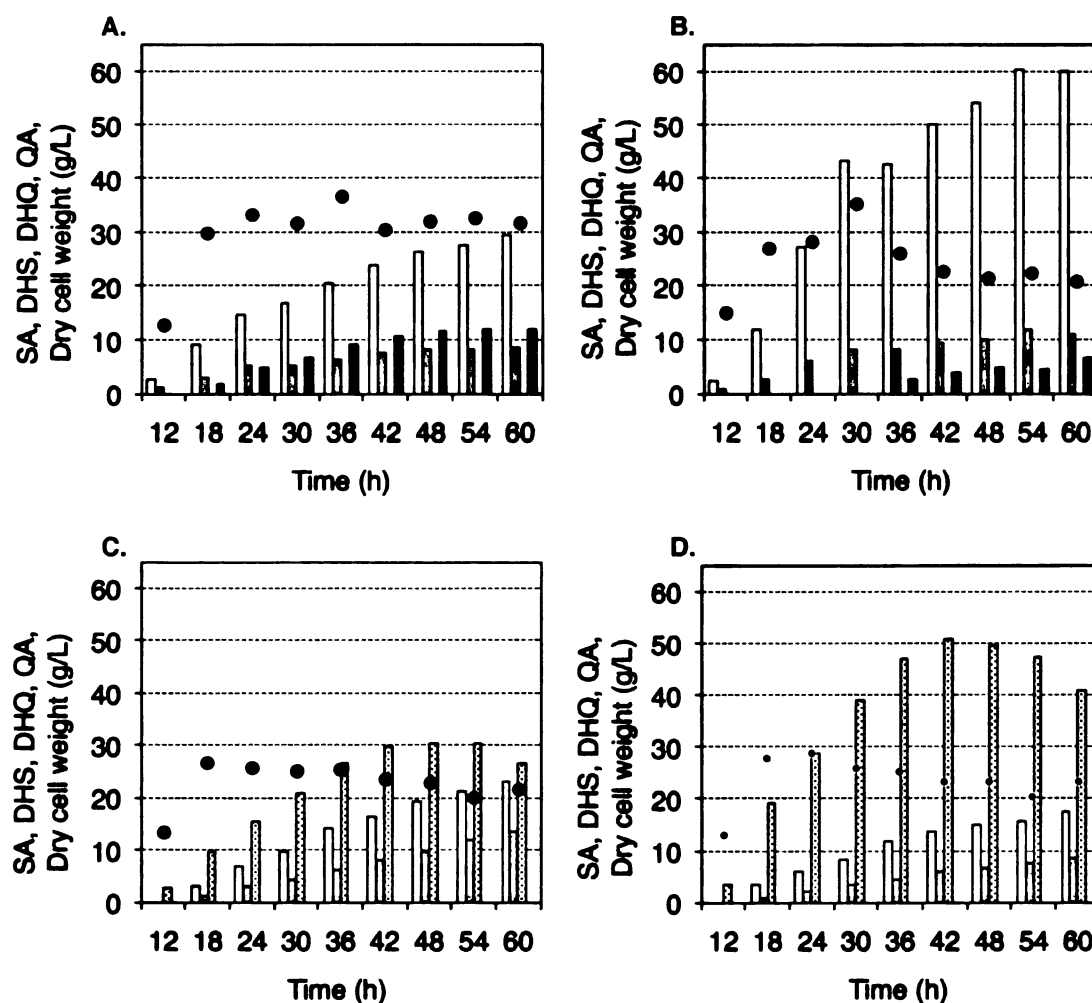
Figure 36. (A) SP1.1/pKD12.138 and (C) JJ2/pKD12.138 cultured under glucose-limited conditions, and (B) SP1.1/pKD12.138 and (D) JJ2/pKD12.138 cultured under glucose-rich conditions. Legend: shikimic acid (open bars), 3-dehydroshikimic acid (grey bars), 3-dehydroquinic acid (dotted bars), quinic acid (black bars), dry cell weight (circles).

E. coli JJ2/pKD12.138 synthesized 23 g/L of shikimic acid under glucose-limited

conditions in 10% yield together with 27 g/L 3-dehydroquinic acid and 13 g/L 3-

dehydroshikimic acid (Table 16, entry 3). The total yield of synthesized hydroaromatics

was 26%, which was higher than 21% compared to *E. coli* SP1.1/pKD12.138 cultured

under the same conditions (Table 16, entry 1). The major product synthesized by *E. coli*

JJ2/pKD12.138 was 3-dehydroquinic acid rather than shikimic acid and the highest

concentration of 3-dehydroquinic acid was 30 g/L, which was reached at 42 h (Figure 36

C). The concentration of 3-dehydroquinic acid synthesized by *E. coli* JJ2/pKD12.138

actually matched the concentration of shikimic acid (30 g/L) synthesized by

SP1.1/pKD12.138 at 60 h when cultured under identical conditions (Figure 36 A; Table

16, entry 1). Cultivation of *E. coli* JJ2/pKD12.138 under glucose-rich conditions

afforded only 17 g/L of shikimic acid in 8% yield over 60 h fermentor run (Table 16,

entry 4). The major metabolite synthesized by *E. coli* JJ2/pKD12.138 was 3-

dehydroquinic acid and it accumulated at 40 g/L concentration by the end of the

fermentor run with the highest concentration of 50 g/L obtained at 42 h (Figure 36 D).

This time, the total yield of synthesized hydroaromatics was 34% (Table 16, entry 4),

which is almost the same as 33% synthesized by *E. coli* SP1.1/pKD12.138 when cultured

under the same conditions. Dry cell weight for *E. coli* JJ2/pKD12.138 dropped

approximately 10 g/L as compared to *E. coli* SP1.1/pKD12.138 under the same

conditions (Figure 36). Interestingly, no quinic acid was detected in JJ2/pKD12.138

fermentations. This indicated that YdiB was essential for quinic acid accumulation in

SP1.1/pKD12.138 when cultured under glucose-limited and glucose-rich culture

conditions. Accumulation of 3-dehydroquinic acid as a major metabolite indicated that

3-dehydroquinic acid dehydratase AroD was not as active as it was in SP1.1/pKD12.138.

To further probe this possibility, synthesis of shikimic acid using *E. coli* JJ2 as a host

strain was probed where plasmid-encoded *aroD* was used in order to reconstitute the lost

of genomic AroD activity. Plasmid pKD12.152A was constructed by introducing an

aroDi insert to pKD12.112. *E. coli* JJ2/pKD12.112 synthesized 18 g/L of shikimic acid

in 9% yield together with 12 g/L of 3-dehydroquinic acid and 7 g/L of 3-dehydroshikimic

acid over 60 h glucose-limited cultivation (Table 16, entry 5). No quinic acid

accumulation was observed at any time during the fermentor run. *E. coli*

JJ2/pKD12.152A synthesized 31 g/L of shikimic acid in 15% yield along with 7 g/L of 3-

dehydroshikimic acid under glucose-limited conditions (Table 16, entry 6). Most

importantly, *E. coli* JJ2/pKD12.152A did not accumulate 3-dehydroquinic acid or quinic

acid. Total yield of synthesized hydroaromatics for JJ2/pKD12.152 was 18% (Table 16,

entry 6), which was comparable to the 19% total yield of hydroaromatics synthesized by

E. coli JJ2/pKD12.112 (Table 16, entry 5). The lower yields and concentrations were

obtained by *E. coli* JJ2/pKD12.112 (Table 16, entry 5) and JJ2/pKD12.152 (Table 16,

entry 6) relative to *E. coli* JJ2/pKD12.138 (Table 16, entry 3) because plasmid

pKD12.112 and pKD12.152 did not cary transketolase *tktA* insert as did plasmid

pKD12.138. However it was clearly shown, that plasmid overexpression of *aroD*

removed 3-dehydroquinic acid accumulation in the culture. This indicated that deletion

of the entire *ydiB* gene from the *E. coli* SP1.1 genomic DNA resulted in reduced AroD

activity *in vivo*. A closer examination of the *aroD* locus revealed that the distance

between *ydiB* and *aroD* gene is only 30 bp (*ATGC* in Figure 37).

Additionally Coggins and co-workers predicted that *aroD* has its own promoter, which is part of the *ydiB* sequence shown as boxed letters in Figure 37.[12] Therefore, a new strategy was developed where deletion of *ydiB* gene was carried in such a way that the predicted promoter sequence was left intact.

A.

B.

```
   1 atggatgtta ccgcaaaata cgaattgatt gggttgatgg cctatcctat
  51 ccgccacagt ttatcgcccg aaatgcagaa taaagcctta gaaaaagcgg
 101 gattgccatt tacctatatg gccttcgaag tggataacga tagctttcct
 151 ggagcaattg aaggattaaa agccctcaaa atgcgcggaa ctggtgtatc
 201 gatgccgaac aaacaactgg cgtgtgaata tgttgatgaa ttaacaccag
 251 ctgccaaact ggtgggggcc atcaacacca tcgttaatga tgatggctat
 301 ctgcgtggct ataacaccga cggcacgggc catattcgcg ccattaaaga
 351 gagcggtttt gatatcaaag gcaaaacgat ggtgctgtta ggggccggtg
 401 gtgcctcaac ggcaattggc gcgcaggggg caattgaagg tttaaaagaa
 451 attaaactct ttaaccgtcg ggatgagttc ttcgataaag ccctcgcctt
 501 cgcgcagcgg gttaatgaaa acaccgattg tgtcgtcacg gtcaccgatc
 551 tcgccgatca gcaagccttt gctgaagccc tggcttccgc cgacatttta
 601 accaatggca caaagtggg tatgaaaccc cttgagaatg aatcattggt
 651 taatgatatc agtctgttac atccgggact tctggtcact gaatgcgtgt
 701 ataacccgca tatgacgaag ttattgcagc aggcgcaaca agctggttgc
 751 aaaacgattg atggatacgg catgttgttg tggcaagggg ctgaacagtt
 801 cacattatgg actggcaaag atttccctct ggaatatgtt aaacaggtca
 851 tggggttcgg tgcctgaCAG GCTGACCGCG TGCAGAAAGG GTAAAAAATG
 901 AAAACCGTAA CTGTAAAAGA TCTCGTCATT GGTACGGGCG CACCTAAAAT
 951 CATCGTCTCG CTGATGGCGA AAGATATCGC CAGCGTGAAA TCCGAAGCTC
1001 TCGCCTATCG TGAAGCGGAC TTTGATATTC TGGAATGGCG TGTGGACCAC
1051 TATGCCGACC TCTCCAATGT GGAGTCTGTC ATGGCGGCAG CAAAAATTCT
1101 CCGTGAGACC ATGCCAGAAA AACCGCTGCT GTTTACCTTC CGCAGTGCCA
1151 AAGAAGGCGG CGAGCAGGCG ATTTCCACCG AGGCTTATAT TGCACTCAAT
1201 CGTGCAGCCA TCGACAGCGG CCTGGTTGAT ATGATCGATC TGGAGTTATT
1251 TACCGGTGAT GATCAGGTTA AAGAAACCGT CGCCTACGCC CACGCGCATG
1301 ATGTGAAAGT AGTCATGTCC AACCATGACT TCCATAAAAC GCCGGAAGCC
1351 GAAGAAATCA TTGCCCGTCT GCGCAAAATG CAATCCTTCG ACGCCGATAT
1401 TCCTAAGATT GCGCTGATGC CGCAAAGTAC CAGCGATGTG CTGACGTTGC
1451 TTGCCGCGAC CCTGGAGATG CAGGAGCAGT ATGCCGATCG TCCAATTATC
1501 ACGATGTCGA TGGCAAAAAC TGGCGTAATT TCTCGTCTGG CTGGTGAAGT
1551 ATTTGGCTCG GCGGCAACTT TTGGTGCGGT AAAAAAAGCG TCTGCGCCAG
1601 GGCAAATCTC GGTAAATGAT TTGCGCACGG TATTAACTAT TTTACACCAG
```

Figure 37. *E. coli* K-12 *ydiB* and *aroD* genomic DNA locus: (A) graphic representation; (B) DNA sequence. Legend: (atgc) *ydiB* sequence, (ATGC) *aroD* sequence, (boxed atgc) predicted *aroD* promoter sequence, (atgc) primer sequences for generating JJ2.2 mutant.

Construction of the new shikimic acid producer started from construction of *E. coli* BW25113 Δ*ydiB*(H1, H2.2)::FRT-*kan*-FRT using Wanner gene disruption methodology, where H1 (single underlined) and H2.2 (double underlined) sequences are shown in Figure 37. A successful P1 phage-mediumted transduction of a new *ydiB* mutation into SP1.1 afforded SP1.1 Δ*ydiB*(H1, H2.2)::FRT-*kan*-FRT, which was named as JJ2.2*kan*. This mutant was treated with pCP20 plasmid-encoded FLP and resulting *E. coli* SP1.1 Δ*ydiB*(H1, H2.2)::FRT was named JJ2.2. Mutants were successfully verified by PCR analysis. *E. coli* JJ2.2*kan* was insensitive to kanamycin, tetracycline and chloramphenicol, while JJ2.2 and SP1.1 showed sensitivity only to kanamycin. The growth pattern on glucose-minimal salt plates was identical with JJ2.2*kan*, JJ2.2 and SP1.1 requiring L-serine, aromatic amino acid and aromatic vitamin supplementation.

E. coli JJ2.2/pKD12.138 was evaluated under glucose-limited conditions and it synthesized 49 g/L of shikimic acid in 20% yield together with 4 g/L of 3-dehydroquinic acid and 12 g/L of 3-dehydroshikimic acid (Table 16, entry 7). Accumulation of 3-dehydroquinic acid was reduced as compared to the 27 g/L synthesized by JJ2/pKD12.138 (Table 16, entry 3) under the same conditions, however it was not totally eliminated. For comparison, the control strain SP1.1/pKD12.138 did not produce any 3-dehydroquinic acid. No accumulation of quinic acid was observed at any point during the cultivation of JJ2.2/pKD12.138 under fermentor-controlled glucose-limited culture conditions (Figure 38A). A continuous increase in shikimic acid concentration was observed (Figure 38A). The total synthesized shikimic acid concentration of 49 g/L (Table 16, entry 7) for JJ2.2/pKD12.138 was approximately the same as the total shikimic acid (23 g/L) plus 3-dehydroquinic acid (27 g/L) for JJ2/pKD12.138 (Table 16,

entry 3) and higher that the total shikimic acid (30 g/L) plus quinic acid (12 g/L) synthesized by SP1.1/pKD12.138 (Table 16, entry 1). This indicates that YdiB is essential for quinic acid equilibration with shikimic acid when shikimate-synthesizing *E. coli* constructs are cultivated under glucose-limited culture conditions. Cultivation of JJ2.2/pKD12.138 under glucose-rich culture conditions yielded 51 g/L of shikimic acid (Table 16, entry 8), which was lower as compared to the 60 g/L of shikimic acid produced by SP1.1/pKD12.138 under the same glucose-rich culture conditions. However, JJ2.2/pKD12.138 did not produce quinic acid at any point during the fermenor run (Figure 38B) although of 3 g/L of 3-dehydroquinic acid was synthesized (Figure 38 B). The total yield of hydroaromatics synthesized by *E. coli* JJ2.2/pKD12.138 was 26 – 27% (Table 16, entry 7 and Table 16, entry 8), which is higher than the 21% total yield of hydroaromatics synthesized by SP1.1/pKD12.138 under glucose-limited culture conditions (Table 16, entry 1), but lower than the 33% total yield of hydroaromatics synthesized by SP1.1/pKD12.138 under glucose-rich culture conditions (Table 16, entry2).

Figure 38. (A)JJ2.2/pKD12.138 cultured under glucose-limited conditions and (B) JJ2.2/pKD12.138 cultured under glucose-rich conditions. Legend: shikimic acid (open bars), 3-dehydroshikimic acid (grey bars), 3-dehydroquinic acid (dotted bars), quinic acid (black bars), dry cell weight (circles).

112

A new SP1.1 variant

As mentioned earlier, shikimic acid producing host *E. coli* SP1.1 was constructed by introducing shikimate kinase *aroL478*::Tn*10* and *aroK*::Cm^R mutations from ALO807[2] into RB791 *serA::aroB*, which resulted in SP1.1 resistance to tetracycline and chloramphenicol. Resistance genes can introduce a polar effect on the downstream genes. In order to eliminate the posibility of the polar effects a new shikimic acid producing host was constructed using Wanner gene deletion methodology. It was also suggested in the literature that *E. coli* shikimate kinase encoded by the *aroL* gene is a principal shikimate kinase responsible for the majority of shikimic acid phosphorylation inside the cell.[13] Therefore, it was postulated that an *E. coli* mutant with only *aroL* mutation might be able to grow on glucose-minimal salts conditions without aromatic amino acid and aromatic vitamin supplementation. The remaining minor shikimate kinase activity encoded by *aroK* might channel enough shikimic acid down the shikimate pathway to ensure *de novo* biosynthesis of adequate level of aromatic amino acid and aromatic vitamins to sustain growth. Deletion of the principal shikimate kinase encoded by *aroK* also needed to be evaluated for whether accumulation of shikimic acid in the culture medium would still take place. To answer these questions, *E. coli* JJ5 (RB791 *serA::aroB* Δ*aroK*::FRT Δ*aroL*::FRT) was constructed, which carried a double shikimate kinase knock-out and JJ4 (RB791 *serA::aroB* Δ*aroL*::FRT) was constructed, which carried only *aroL* knock-out. Construction of both mutant strains was performed using Wanner gene disruptions methodology and both strains were cured of antibiotic

resistance. Gene deletions were performed directly in *E. coli* RB791 *serA::aroB* rather

than BW25113, as during JJ2 and JJ2.2 construction.

Table 17. Concentrations and yields of products synthesized by shikimic acid producing *E. coli* with *ydiB* mutation.

entry	Strain	Mutation	[SA]^c, g/L	SA yield^d %	[DHS], g/L	[DHQ], g/L	[QA], g/L	Total yield^e, %
1^a	SP1.1/pKD12.138	aroK-, aroL-	30	13	9	0	12	21
2^b	SP1.1/pKD12.138	aroK-, aroL-	60	26	11	0	7	33
3^{b}*	JJ4/pKD12.138	aroK+, ΔaroL-	18	3	16	0	23	10
4^{a}*	JJ5/pKD12.138	ΔaroK-, ΔaroL-	29	12	12	0	28	27

^{a}Glucose-limited conditions. ^{b}Glucose-rich conditions. *Single run fermentation. ^{c}Abbreviations: shikimic acid (SA), 3-dehydroshikimic acid (DHS), quinic acid (QA). ^{d}(mol SA)/(mol glucose consumed). ^{e}(mol SA + mol DHS + mol QA)/(mol glucose consumed)

E. coli JJ4/pKD12.138 was evaluated under glucose-rich, fermentor-controlled

culture conditions. Culture medium was not supplemented with aromatic amino acids

and aromatic vitamins. *E. coli* JJ4/pKD12.138 grew faster that SP1.1/pKD12.138 and

accumulated of 70 g/L of biomass by 36 h (Figure 39 B), which is double that of 35 g/L

of biomass produced by SP1.1/pKD12.138 under the same conditions (Figure 36 B) by

30 h. This clearly indicated that there was enough shikimate kinase AroK activity to

channel shikimic acid downstream into shikimate pathway to biosynthesize adequate

concentrations of aromatic amino acids and aromatic vitamins needed for growth.

However, JJ4/pKD12.138 produced only 18 g/L of shikimic acid in 3% yield over 60 h

(Table 17, entry 3). Synthesis by JJ4/pKD12.138 of 3-dehydroshikimic acid and quinic

acid was of 16 g/L and 23 g/L, respectively (Table 17, entry 3), consisted higher

concentration of these hydroaromatic byproducts relative to SP1.1/pKD12.138 (Table 17,

entry 2). Presumably, the remaining AroK activity in JJ4/pKD12.138 channeled more

carbon flow down the shikimate pathway than had been initially anticipated. Accumulation of higher biomass led to reduced product yields and the total yield of synthesized hydroaromatics was 10% (Table 17, entry 3), which was threefold lower than the 33% total yield of hydroaromatics synthesized by SP1.1/pKD12.138 under glucose-rich culture conditions.

A double shikimate kinase *aroK* and *aroL* knockout was evaluated under glucose-limited conditions. *E. coli* JJ5/pKD12.138 produced 29 g/L of shikimic acid in 12% yield over 60 h fermentor run (Table 17, entry 4) and it was close in performance to the 30 g/L of shikimic acid synthesized in 13% yield by SP1.1/pKD12.138 under glucose-limited conditions (Table 17, entry 1). However, it also accumulated higher levels of 3-dehydroshikimic acid (12 g/L) and quinic acid (28 g/L, Table 17, entry 4). The total yield of synthesized hydroaromatics was 27%, which is significantly higher relative to 21% total yield of synthesized hydroaromatics synthesized by SP1.1/pKD12.138 (Table 17, entry 1).
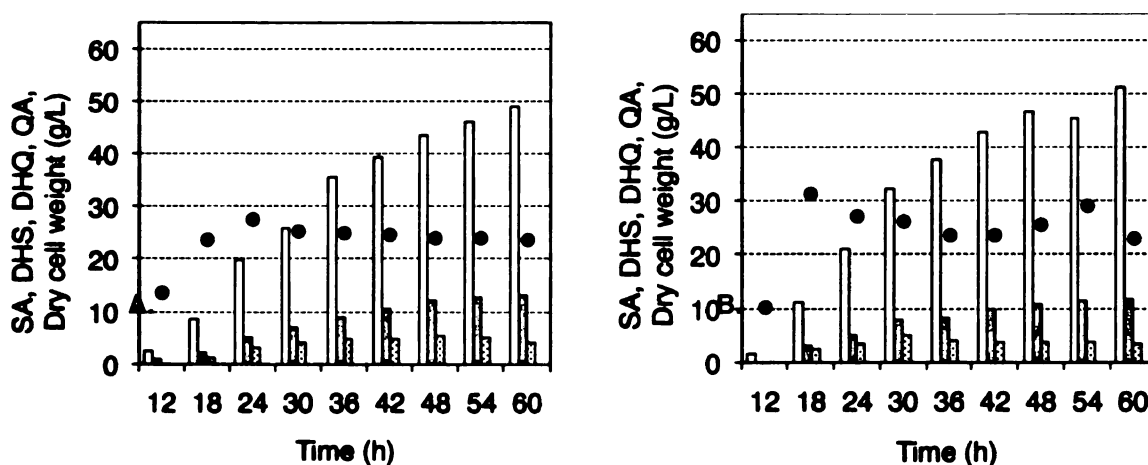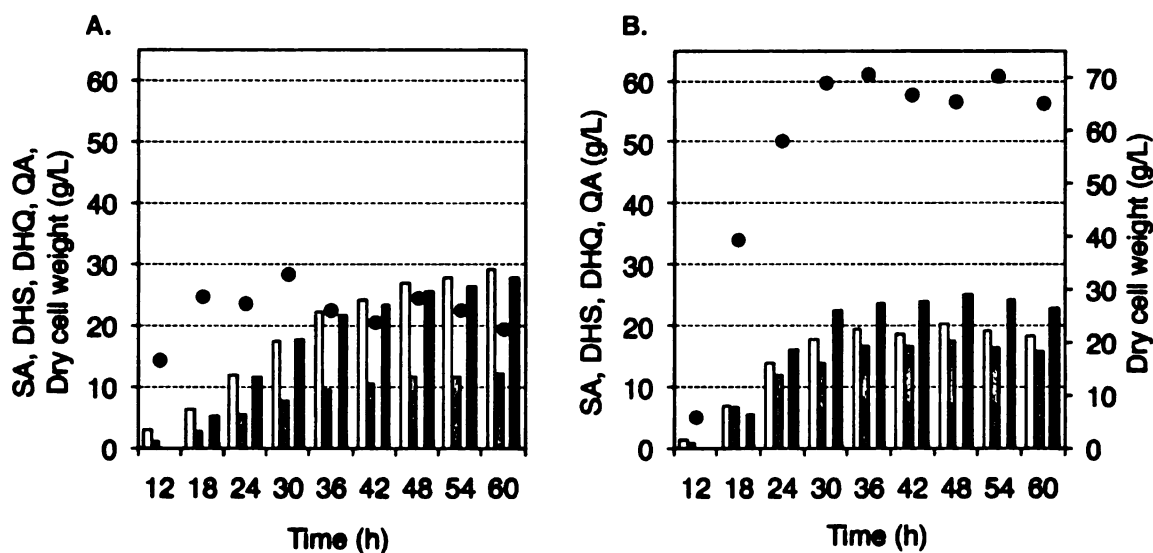

Figure 39. (A) JJ5/pKD12.138 cultured under glucose-limited conditions and (B) JJ4/pKD12.138 cultured under glucose-rich conditions. Legend: shikimic acid (open bars), 3-dehydroshikimic acid (grey bars), 3-dehydroquinic acid (dotted bars), quinic acid (black bars), dry cell weight (circles).

115

Shikimate dehydrogenase from *Gluconobacter oxydans*

As mentioned earlier, several attempts to identify a better shikimate dehydrogenase than *E. coli* AroE were made including overexpression of quinate dehydrogenase Qad from *Klebsiella pneumoniae* and shikimate dehydrogenase AroD from *Bacillus subtilis*.[6] A new shikimate dehydrogenase was reported from *Gluconobacter oxydans* IFO 3244 and it showed *in vitro* specific activity with shikimic acid and 3-dehydroshikimic acid as substartes.[14] Additionally this shikimate dehydrogenase showed no *in vitro* activity with quinic acid, 3-dehydroquinic acid and protocatechuic acid. More interestingly, *G. oxydans* IFO 3244 shikimate dehydrogenase has almost eightfold higher K_m value for shikimic acid as compared to *E. coli* shikimate dehydrogenase AroE (Table 18). During shikimic acid synthesis, 3-dehydroshikimic acid accumulation accounted for 14% of the total hydroaromatic and was by far the major byproduct (Table 16, entry 2). It was previously postulated that accumulation of 3-dehydroshikimic acid and quinic acid during shikimic acid biosynthesis is due to hydroaromatic equilibration, where shikimic acid is recaptured by the cells and converted back to 3-dehydroshikimic acid, 3-dehydroquinic acid and quinic acid in the reverse direction of the shikimate pathway (Figure 1).[4] The conversion of shikimic acid to 3-dehydroshikimic acid and of 3-dehydroquinic acid to quinic acid is performed by the same *E. coli* shikimate dehydrogenase AroE.[4] Therefore, overexpression of shikimate dehydrogenase from *G. oxydans* IFO 3244 with higher K_m value for shikimic acid should slow down shikimic acid/3-dehydroshikimic acid equilibration. Additionally, if quinic

acid is not a substrate for *G. oxydans* IFO 3244 shikimate dehydrogenase, then 3-dehydroquinic acid also might not be a substrate thereby precluding the reduction of 3-dehydroquinic acid to unwanted quinic acid. Successful heterologous overexpression of *Gluconobacter* genes in *E. coli* has been demonstrated by several groups.[15] Therefore, an attempt to overexpress shikimate dehydrogenase from *G. oxydans* IFO 3244 in *E. coli* shikimic acid producer was made.

Table 18. Shikimate dehydrogenase K_m values.

Organism	K_m, mM	
	shikimic acid	3-dehydroshikimic acid
G. oxydans IFO 3244	0.5 (ref. [14])	0.2 (ref. [14])
E. coli K-12	0.065 (ref. [10a])	0.1 (ref. [6])

The gene sequence for *G. oxydans* IFO 3244 shikimate dehydrogenase was not available. However, the entire genome sequence for *G. oxydans* H621 was available from the NCBI[16] and the ERGO[17] database. Interestingly, the NCBI and ERGO gene sequences for shikimate dehydrogenase from *G. oxydans* H621 did not match. ERGO annotated only one shikimate dehydrogenase, which uses PQQ (pyrroloquinoline quinone) as a cofactor, rather than NAD(P). Although, many bacteria can biosynthesize the cofactor PQQ required for several dehydrogenases, wild-type *E. coli* can not produce PQQ.[18] Therefore, use of this enzyme in an *E. coli* shikimic acid producer was not pursued. The shikimate dehydrogenase gene from the NCBI database had 19% identity with *E. coli* shikimate dehydrogenase AroE at the protein level. No data was available as to whether this dehydrogenase was PQQ or NAD(P) depended. The putative shikimate dehydrogenase gene sequence in ERGO was annotated as fructose 5-dehydrogenase.

The assumption was made that there was no important sequence difference between *G. oxydans* IFO 3244 and *G. oxydans* H621. PCR primers for shikimate dehydrogenase ORF from *G. oxydans* H621 were designed based on the NCBI sequence. *G. oxydans* IFO 3244 was ordered from the National Institute of Technology and Evaluation in Japan and genomic DNA was purified using a Qiagen genomic DNA isolation kit. Purified genomic DNA from *G. oxydans* IFO 3244 was used as a template for PCR. The 0.8 kb PCR product of was isolated using agarose gel and cloned under a P_{tac} promoter between the *Eco*RI and *Sma*I sites of pKK223-3 vector. The resulting plasmid was transformed into *E. coli* AB2834 host and the transformation mixture was plated on glucose-minimal salts plates. *E. coli* AB2834[19] has inactive shikimate dehydrogenase AroE, ad as consequence, this mutant is not able to grow on minimal salt medium without shikimic acid or aromatic amino acid and aromatic vitamins supplementation. If AB2834 is transformed with a plasmid encoding active shikimate dehydrogenase, transformants will able to grow on glucose-minimal salts medium.[6]

However, no growth after 7 days was observed in this case, which indicated that either the shikimate dehydrogenase gene sequence from *G. oxydans* H621 was PQQ depended or this sequence was annotated incorrectly by NCBI.

Genomic plasmid library approach was then taken to isolate shikimate dehydrogenase from *G. oxydans* IFO 3244. Purified genomic DNA was partially digested with *Bam*HI restriction endonuclease followed by ligation of 1-10 kb genomic DNA pieces into the *Bam*HI site of pBluescript SK (-) vector. The resulting plasmid library was electroporated into *E. coli* AB2834 and the transformants plated on glucose-minimal salts medium. After 48 h of incubation at 37 °C, two colonies were identified

and plasmids from these colonies were isolated. Multiple enzyme digestion of these plasmids yielded identical restriction enzyme digestion patterns, which indicated that genomic DNA pieces were identical or very similar. Overexpression of *G. oxydans* IFO 3244 shikimate dehydrogenase in AB2834 was investigated. Cell lysates were assayed in the forward direction using 3-dehydroshikimic acid as a substrate and NADP[14] as cofactor and in the reverse direction using shikimic acid and NADPH. Overexpression levels were only twofold higher (Table 19, entry 2 and entry 3) relative to the AB2834 background specific activity (Table 19, entry 1). As a consequence, further efforts directed towards heterologous expression of shikimate dehydrogenase from *G. oxydans* IFO 3244 were abbandoned.

Table 19. Shikimate dehydrogenase activity.

entry	Source	Specific activity[a], U/mg	
		3-dehydroshikimic acid	shikimic acid
1	AB2834	0.0005	0.0002
2	AB2834/pBlue IFO3244 #1	0.001	0.001
3	AB2834/pBlue IFO3244 #2	0.001	0.001

[a] One unit (U) of shikimate dehydrogenase corresponds to the formation of 1 μmole of NADP in the presence of 3-dehydroshikimic or consumption of 1 μmole of NADPH in the presence of shikimic acid per min at 25 °C.

An attempt to identify hydroaromatics transport system in *E. coli*

To identify the hydroaromatics transport system in *E. coli* is a crucial step in optimizing the production of shikimic acid and quinic acid. Increasing the rate of such transport system or rate might result in increased production of hydroaromatics. Several active efflux pumps have been identified in *E. coli* in response to treatment with chemicals or antiobiotics. Increased expression of the efflux pumps leads to decreased intracellular concentration of the externally added compounds, resulting in *E. coli* with a

higher tolerance to these compounds. The efflux systems range from broad to very narrow substrate specificity. For example, *E. coli* efflux system AcrAB-TolC is upregulated in response to exogenous compounds such as salicylic acid[20], methylviologen[21] or bile salts[22] and a wide range of compounds are the substrates for this pump.[23] On the other hand CusCFBA complex exports only copper and silver ions from *E. coli* cells.[24] Another specific efflux pump was identified for export of *p*-hydroxybenzoic acid in *E. coli*.[25] It was shown that this pump is triggered by internal and external *p*-hydroxybenzoic acid, a native metabolite of *E. coli*. Interestingly, only a few aromatic carboxylic acids were identified as a substrate for this pump. Pittard and co-workers have characterized a system encoded by the *shi*A locus, which is apparently responsible for shikimic acid transport in *E. coli*.[26] Later, Frost and co-workers showed that *shi*A knockout *E. coli* was still transporting the shikimic acid. Therefore, there must be another system involved in shikimic acid or hydroaromatics efflux.[2] The *E. coli ydiN* gene was found in the same operon as 3-dehydroquinate dehydratase encoded by *aroD* and the second shikimate/quinate dehydrogenase *ydiB* (Figure 37A). The function of YdiN is unknown, however it was annotated as an amino acid/amine MFS transporter[27] or multidrug resistance gene.[17] Additionally, upregulation of *ydiN* was observed at the transcriptome level during shikimic acid biosynthesis.[28] Might YdiN be involved in hydroaromatics transport across the cellular membrane? To gain insights into the possible function of YdiN, SP1.1 Δ*ydiN*::FRT mutant was constructed. If *E. coli* YdiN is involved in hydroaromatics transport alone or together in complex with some other

120

proteins, deletion of this gene will result in an inactive hydroaromatics efflux pump and therefore synthesized shikimic acid concentration should decrease.

Construction of SP1.1 Δ*ydiN*::FRT started from generating *E. coli* BW25113 Δ*ydiN*::FRT-*kan*-FRT mutant using previously described gene inactivation methodology. Multiple trials were performed to generate the desired BW25113 Δ*ydiN*::FRT-*kan*-FRT mutant, but only one colony was obtained. Once again P1 phage-mediumte transduction was used to transfer *ydiN* mutation to an *E. coli* SP1.1 host. However, all trials were unsuccessful and SP1.1 Δ*ydiN*::FRT-*kan*-FRT could not be obtained. If YdiN is responsible for multidrug resistance, as it was annotated, deletion of this gene probably resulted in hypersensitivity to antibiotics and therefore no colonies were observed on selective LB/kan plates. A new selection method was designed. Instead of inserting antibiotic resistance gene in a desired locus of genomic DNA, a *serA* insertion will be used. Therefore, a host lacking 3-phosphoglycerate dehydrogenase SerA activity has to be used for this method and mutant selection will be based on growth on glucose-minimal medium in the absense of any added antibiotics. This method should overcome issues related to antibiotic hypersensitivity.

(a)   *rpiA* P₁ P₂   *serA*   *ygfA*   BW25113
         0.7 kB   1.2 kB   0.5 kB

(b)   *rpiA* P₁ FRT *ygfA*   BW25113 Δ*serA2*::FRT
         0.7 kB   0.5 kB

(c)   FRT   *P2 serA* (ORF) 1.4 kB   FRT   pNR9.280
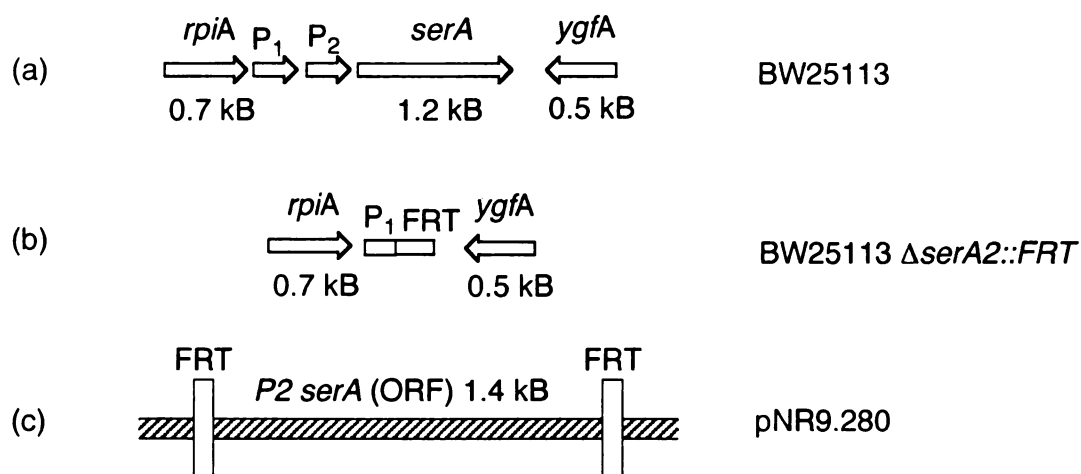
Figure 40. Modification of gene disruption method.

121

Since all hosts for microbial production in the Frost research group are *serA* (-), these hosts can be used for gene deletion using this method and the *serA* insertion can be eliminated using flippase in the final target host. *E. coli serA* transcription is controlled by two promoter sequences P1 and P2, where P2 is the principal promoter (Figure 40 A).[29] A new host was constructed where entire P2 and a part of P1 promoter sequence together with ORF of *serA* were deleted using standard gene deletion method described earlier and resulted in BW25113 Δ*serA*::FRT-*kan*-FRT. This host had 169 bp deletion upstream from *serA* ORF and a 100 bp downstream of *serA*. Kanamycin resistance gene was eliminated using pCP20 plasmid-encoded flippase and resulted in the *E. coli* BW25113 Δ*serA*::FRT ready to be used in the newly designed deletion method (Figure 40 B). The Frost group member constructed plamsid pNR9.280 where chloramphenicol resistance gene in pKD3 was replaced with the P2 *serA* sequence, flanked between two FRT sites (Figure 40C).

The newly constructed system (Figure 40) was used to knock-out the *ydiN* gene in *E. coli* SP1.1. Plasmid pNR9.280 was used as template for the initial PCR step where H1 and H2 40 bp primers where designed to be homologous to the 5' and 3' ends of the *ydiN* gene. Successful PCR yielded 1.4 kbp DNA size band on agarose gel. The PCR product was electroporated in BW25113 Δ*serA*::FRT/pKD46 expressing λ Red recombinase and mutants were selected on glucose-minimal plates. Approximately 200 colonies appeared on the selective plates, but after second round of replication on glucose-minimal plates only 5 of them continued to grow, indicating that the majority of the colonies were false positives. Genomic DNA was isolated from all 5 candidates for the PCR verification test. Verification primers were designed to have homology outside the *ydiN* region and PCR

reaction with 5 candidate genomic DNA resulted in a 1.2 kbp sized DNA band rather than 1.4 kbp sized as had been anticipated. Control PCR with *E. coli* K-12 genomic DNA also resulted in 1.2 kbp sized DNA, which indicated that none of the 5 candidates had a *ydiN* deletion. A second PCR test was performed with primers designed just outside *serA* and it resulted in approximately 300 – 400 bp sized DNA, which indicated that *serA* deletion was still present in the host. Construction of *ydiN* mutant was unsecsesful and was stopped.

Instead of deleting *ydiN* gene and expecting a lower concentration of synthesized shikimic acid, overexpression of the *ydiN* gene in a shikimic acid or quinic acid producer might lead to increased hydroaromatics accumulation in the medium, if *ydiN* is alone responsible for hydroaromatics transport. Construction of a *ydiN* overexpressing plasmid began with PCR amplification of a 1.2 kb *ydiN* ORF fragment from *E. coli* W3110 genomic DNA. Isolated PCR fragment was inserted into *Eco*RI and *Pst*I cloning site of the pKK223-3 vector under the P_{tac} promoter and yielded plasmid pJJ5.151 (Figure 41).

Plasmid pJJ5.151 served as a template for PCR of the 1.4 kbp size $P_{tac}ydiN$ fragment, which was eventually treated with Kelnow. Plasmid pKD12.112 was linerized with *Sal*I restriction endonuclease and treated with Klenow, subsequent ligation with $P_{tac}ydiN$ insert fragment afforded pJJ5.164 (Figure 42). Transketolase encoded by the 2.2 kbp *tktA* insert was excised from pNR8.146 with *Bam*HI restriction endonuclease and was treated with Klenow. Plasmid pJJ5.164 was linerized with *Xba*I restriction nuclease and treated with Klenow. DNA insert *tktA* was ligated to linerized pJJ5.164 and afforded the target plasmid pJJ5.165 (Figure 43). Newly constructed plasmid, pJJ5.165 was evaluated for

shikimic acid production under glucose-rich culture conditions and for quinic acid production under glucose-limited culture condition.
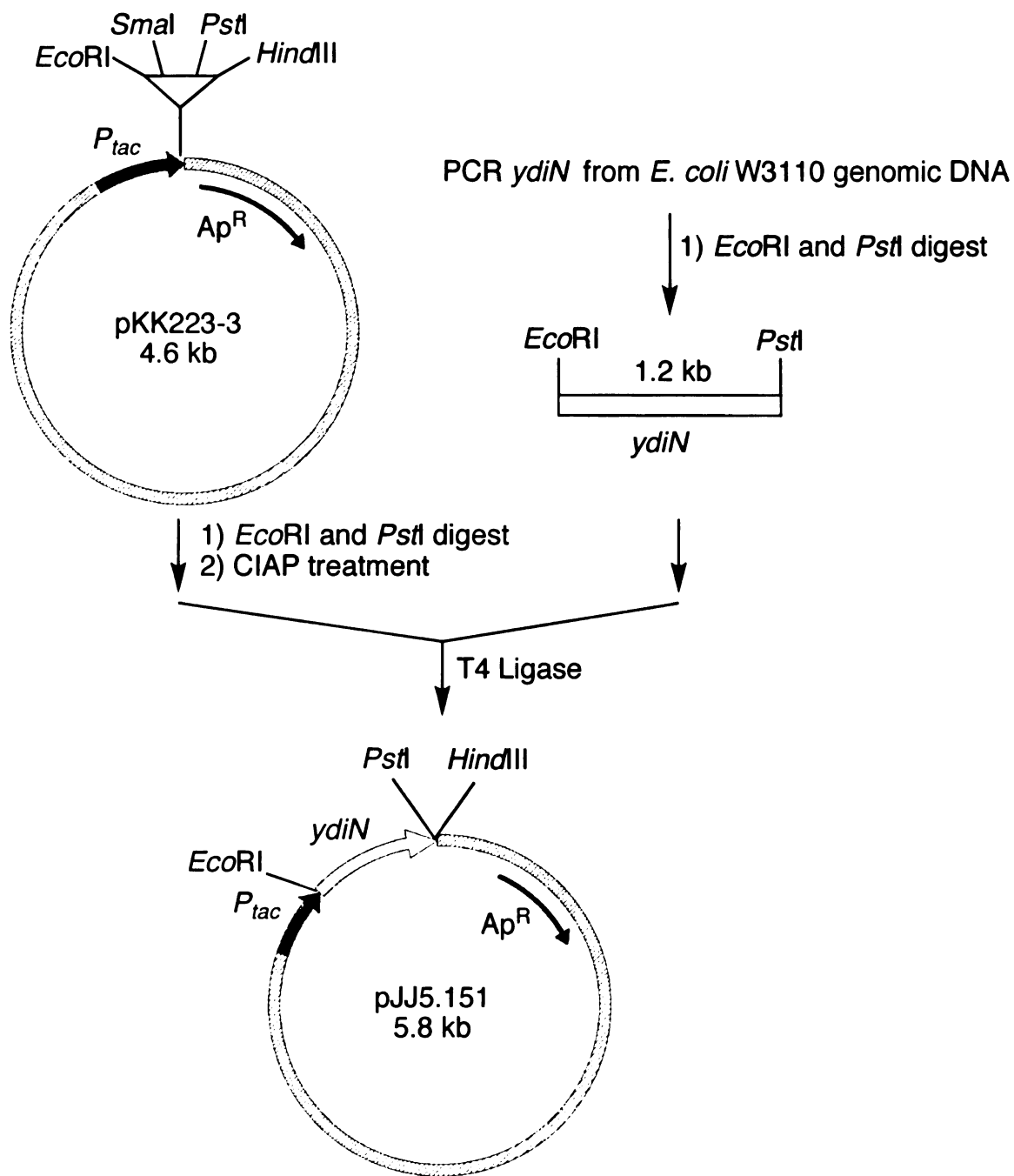
Figure 41. Construction of pJJ5.151.
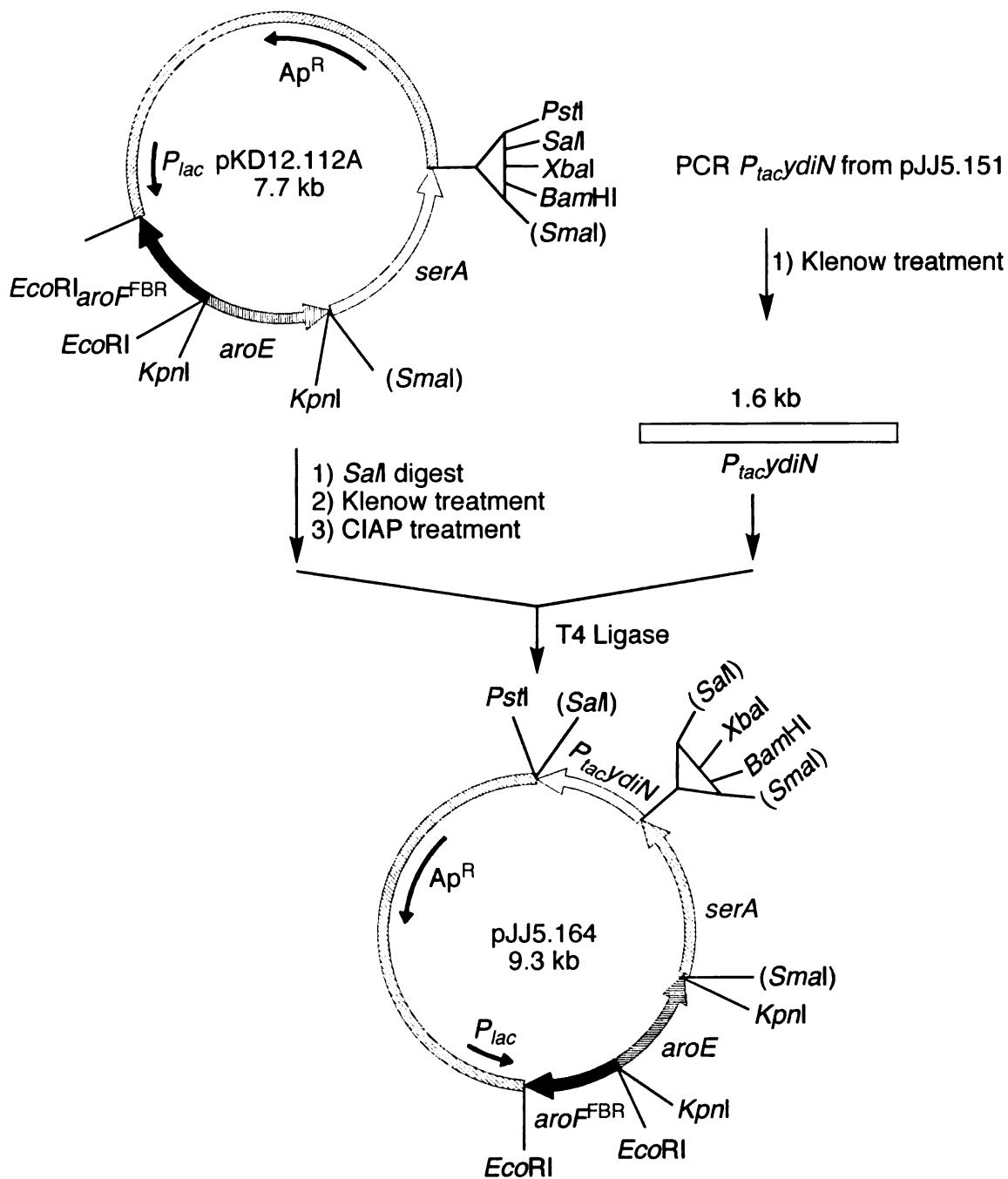
Figure 42. Construction of pJJ5.164.
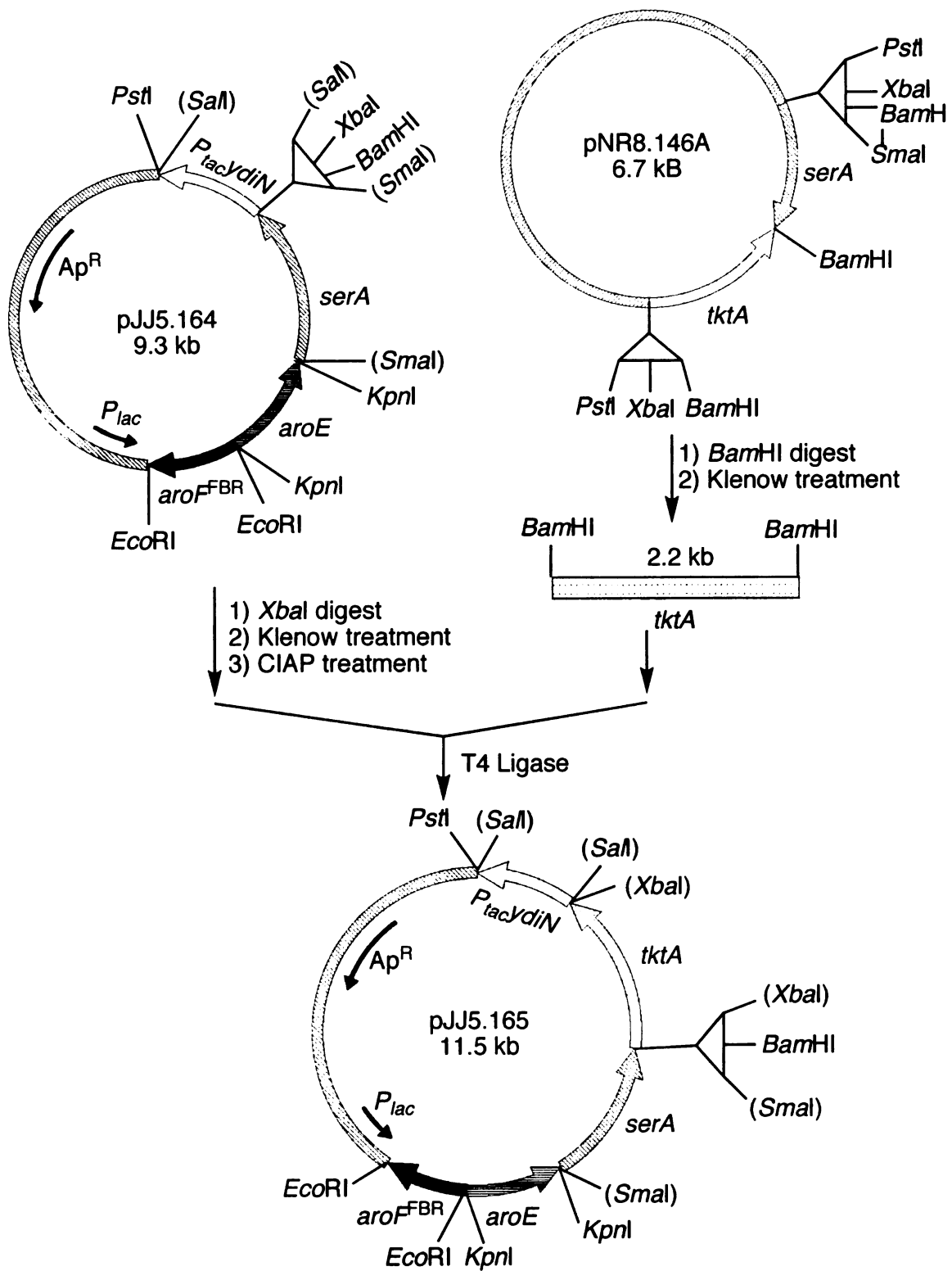
Figure 43. Construction of pJJ5.165.

Table 20. Concentrations and yields of products synthesized by shikimic acid and quinic acid producing *E. coli* with *ydiN* overexpression.

Entry	Construct	[SA][c], g/L	SA yield[d], %	[DHS], g/L	[DHQ], g/L	[QA], g/L	QA yield[e], %	Total yield[f], %
1[b]	SP1.1/pKD12.138	60	26	11	0	7	-	33
2[b]	SP1.1/pJJ5.165	51	20	10	0	5	-	26
3[a]	QP1.1/pKD12.138	-	-	-	5	58	21	21
4[a]*	QP1.1/JJ5.165	-	-	-	6	44	14	16

[a]Glucose-limited conditions. [b]Glucose-rich conditions. *Single run fermentation. [c]Abbreviations: shikimic acid (SA), 3-dehydroshikimic acid (DHS), quinic acid (QA). [d](mol SA)/(mol glucose consumed). [e](mol QA)/(mol glucose consumed). [f](mol SA + mol DHS + mol QA)/(mol glucose consumed).
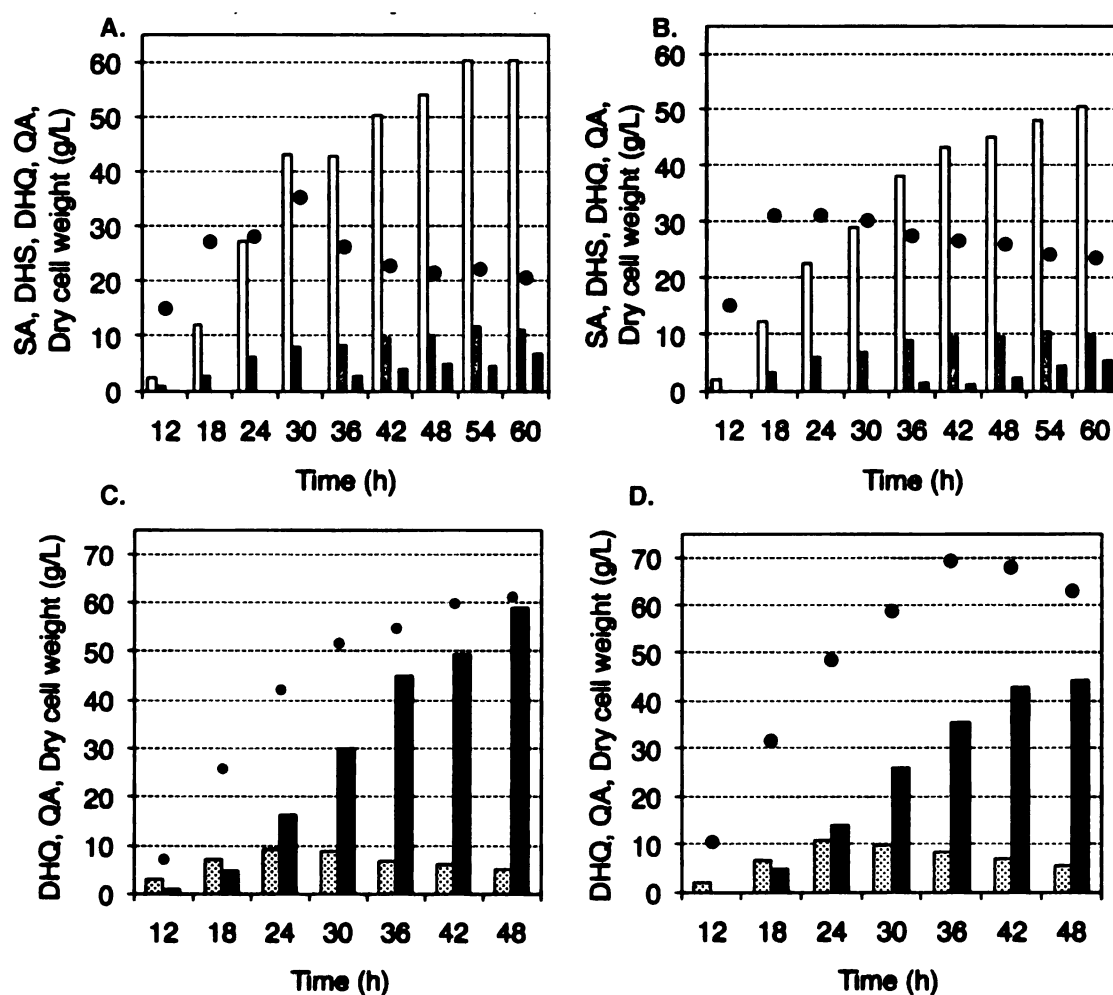
Figure 44. (A) SP1.1/pKD12.138 and (B) SP1.1/JJ5.165 cultured under glucose-rich conditions, and (C) QP1.1/pKD12.138 and (D) QP1.1/pJJ5.165 cultured under glucose-limited conditions. Legend: shikimic acid (open bars), 3-dehydroshikimic acid (grey bars), 3-dehydroquinic acid (dotted bars), quinic acid (black bars), dry cell weight.

SP1.1/pJJ5.165 synthesized 51 g/L of shikimic acid in 20% yield over 60 h fermentations (Table 20, entry 2), which was lower than the control strain SP1.1/pKD12.138 production of 60 g/L of shikimic acid in 26% yield (Table 20, entry 1). Accumulation of byproducts, 3-dehydroshikimic acid and quinic acid was observed (Table 6, entry 2) at approximately the same concentration of 10 g/L and 5 g/L, respectively. The total yield of hydroaromatics synthesized by SP1.1/pJJ5.165 was 26%. Dry cell weight and byproduct accumulation profile for the control strain SP1.1/pKD12.138 and the new construct SP1.1/pJJ5.165 looked very similar throughout the respective fermentation runs (Figure 44 A and B).

An larger decrease in synthesized products was observed for quinic acid production under glucose-limited conditions. *E. coli* QP1.1/pJJ5.165 synthesized 44 g/L of quinic acid in 14% yield over 48 h fermentation (Table 20, entry 4) while QP1.1/pKD12.138 produced 58 g/L of quinic acid in 21% yield under the same conditions (Table 20, entry 3). Accumulation of 3-dehydroquinic acid was about the same level at 6 g/L and the total yield of hydroaromatics declined to 16% (Table 6, entry 4). The highest observed biomass level was 69 g/L at 36 h, while the control strain accumulated 61 g/L of biomass at 60 h (Figure 44C and Figure 44D). These experiments clearly indicated that overexpression of *ydiN* did not have a positive effect on shikimic acid or quinic acid biosynthesis. Either YdiN is not responsible for hydroaromatics transport or it is working in the complex with other proteins.

Discussion

Inactivation of YdiB activity in a shikimic acid producer led to elimination of quinic acid accumulation in the fermentation broth under glucose-limited and glucose-rich conditions. However, the shikimic acid concentration under glucose-limited conditions was reduced from 60 g/L synthesized by SP1.1/pKD12.138 to 51 g/L synthesized by JJ2.2/pKD12.138. Interestingly, 3-dehydroquinic acid accumulation was still observed for JJ2.2/pKD12.138, while SP1.1/pKD12.138 showed no 3-dehydroquinic acid accumulation in the medium. This suggests that *E. coli* JJ2.2 had lower 3-dehydroquinate dehydratese AroD activity as compared to SP1.1. Since it was predicted that the promoter sequence for *aroD* is within the *ydiB* ORF[12], *E. coli* JJ2.2 was constructed by deleting only a part of *ydiB*, which left the predicted promoter sequence for *aroD* intact. This helped to reduce the concentration of 3-dehydroquinic acid synthesized by JJ2.2/pKD12.138 as compared to JJ2/pKD12.138. However, synthesis of 3-dehydroquinic acid was not completely eliminated (Table 16). It was demonstrated for the first time that YdiB is involved in the synthesis of quinic acid as a byproduct during the synthesis of shikimic acid under both glucose-rich and glucose-limited conditions. However, the full role of YidB in *E. coli* is not fully understood. The total concentration of hydroaromatics synthesized by SP1.1/pKD12.138 was 78 g/L, while JJ2/pKD12.138 and JJ2.2/pKD12.138 synthesized 66 g/L (Table 16, entry 2, entry 4 and entry 8). Successful deletion of *ydiB* channeled more carbon flow towards the shikimic acid and hydroaromatic byproducts under glucose-limited conditions. *E. coli* SP1.1/pKD12.138 produced 51 g/L of total hydroaromatics under glucose-limited conditions, while JJ2/pKD12.138 synthesized 63 g/L and JJ2.2/pKD12.138 synthesized 66 g/L (Table 16,

entry 1, entry 3 and entry 7). There was no observed quinic acid accumulation as well. Interestingly, total synthesized hydroaromatics by JJ2.2/pKD12.138 under glucose-limited and glucose-rich conditions was the same at 66 g/L. Elimination of quinic acid accumulation in shikimic acid production should simplify the purification of product shikimic acid. This eliminates problems encountered with in co-crystallization of quinic acid with shikimic acid during purification of the desired shikimic acid.[9]

The new shikimic acid construct JJ5/pKD12.138, which possessed deleted aroK and aroL, did not show any improvements in shikimic acid production over SP1.1/pKD12.138. Shikimic acid production using a single shikimate kinase *aroL* knockout *E. coli* JJ4/pKD12.138 did not produce as much shikimic acid as the double shikimate kinase knockout SP1.1/pKD12.138 (Table 17, entry 3 and 2). However, JJ4/pKD12.138 was able to grow in culture medium lacking supplementation with aromatic amino acids and aromatic vitamins channeled more carbon downstream the shikimate pathway. The downside of this accomplishment was an overly abundant supply of aromatics that translated into two-fold increase in the biomass (Figure 39 and Figure 36 B) and seven-fold decline in the synthesized hydroaromatics. This is consistant with the need to control biomass formation in order to achieve high concentration and yields of hydroaromatics.

Identification of a shikimate dehydrogenase that is highly selective for reduction of 3-dehydroshikimic acid over 3-dehydroquinic acid along with reduced sensitivity to feedback inhibition by shikimic acid remains an attractive goal. Along these lines, the selectivity reported for *G. oxydans* shikimate dehydrogenase calls further investigation.

However, a new strategy for isolating NADPH-dependent shikimate dehydrogenase from *G. oxydans* will be needed.

In route to delineate the system exploited by *E. coli* to export hydroaromatics, *E. coli* lacking YdiN activity could not be constructed using two different selection methods. With the alternative strategy of YdiN overexpression with plasmid-localized *ydiN*, shikimic and quinic acid production declined as compared to the control strains (Table 20). Alternative candidates of gene encoding functions essential to hydroaromatic export will need to be explored in the future.

References

1   Snell, K. D.; Draths, K. M.; Frost, J. W. Synthetic modification of the *Escherichia coli* chromosome: enhancing the biocatalytic conversion of glucose into aromatic chemicals. *J. Am. Chem. Soc.* **1996**, *118*, 5605-5614.

2   LØbner-Olesen, A.; Marinus, M. G. Identification of the gene (*aroK*) encoding shikimic acid kinase-I of *Escherichia coli*. *J. Bacteriol.* **1992**, *174*, 525-529.

3   (a) Chandran, S. S.; Yi, J.; Draths, K. M.; von Daeniken, R.; Weber, W.; Frost, J. W. Phosphoenolpyruvate availability and the biosynthesis of shikimic acid. *Biotechnol. Prog.* **2003**, *19*, 808-814. (b) Yi, J.; Li, K.; Draths, K. M.; Frost, J. W. Modulation of Phosphoenolpyruvate Synthase Expression Increases Shikimate Pathway Product Yields in *E. coli*. *Biotechnol. Prog.* **2002**, *18*, 1141-1148.

4   Knop, D. R.; Draths, K. M.; Chandran, S. S.; Barker, J. L.; von Daeniken, R.; Weber, W.; Frost, J.W. Hydroaromatic equilibration during biosynthesis of shikimic acid. *J. Am. Chem. Soc.* **2001**, *123*, 10173-10182.

5   Dell, K. A.; Frost, J. W. Identification and removal of impediments to biocatalytic synthesis of aromatics from D-glucose: Rate-limiting enzymes in the common pathway of aromatic amino acid biosynthesis. *J. Am. Chem. Soc.* **1993**, *115*, 11581-11589.

6   Jancauskas, J. Strategies for improving synthesis of 3-dehydroshikimic acid and shikimic acid from D-glucose. M.S. thesis. *Michigan State University*, **2006**.

7   (a) Weaver, L. M.; Herrmann, K. M. Cloning of an *aroF* allele encoding a tyrosine-insensitive 3-deoxy-D-*arabino*-heptulosonate 7-phosphate synthase. *J. Bacteriol.***1990**, *172*, 6581-6584. (b) Li, K.; Mikola, M. R.; Draths, K. M.; Worden, R. M.; Frost, J. W. Fed-batch fermentor synthesis of 3-dehydroshikimic acid using recombinant *Escherichia coli*. *Biotechnol. Bioeng.* **1999**, *64*, 61-73.

8   (a) Konstantinov, K. B.; Nishio, N.; Yoshida, T. Glucose Feeding Strategy Accounting for the Decreasing Oxidative Capacity of Recombinant *Escherichia coli* in Fed-Batch Cultivation for Phenylalanine Production. *J. Ferment. Bioeng.* **1990**, *70*, 253-260. (b) Konstantinov, K. B.; Nishio, N.; Seki, T.; Yoshida, T. Physiologically Motivated Strategies for Control of the Fed-Batch Cultivation of Recombinant *Escherichia coli* for Phenylalanine Production. *J. Ferment. Bioeng.* **1991**, *71*, 350-355. (c) Kleman, G. L.; Strohl, W. R. Acetate Metabolism by *Escherichia coli* in High-Cell-Density Fermentation. *Appl. Environ. Microbiol.* **1994**, *60*, 3952-3958.

9   Draths, K. M.; Knop, D. R.; Frost, J.W. Shikimic acid and quinic acid: replacing isolation from plant sources with recombinant biocatalysis. *J. Am Chem. Soc.* **1999**, *121*, 1603-1604.

10   (a) Michel, G.; Roszak, A. W.; Sauve, V.; Maclean, J.; Matte, A.; Coggins, J. R.; Cygler, M.; Lapthorn, A. J. Structures of shikimate dehydrogenase AroE and its paralog YdiB. *J. Biol. Chem.* **2003**, *278*, 19463-19472. (b) Benach, J.; Lee, I.; Edstorm, W.; Kuzin, A. P.; Chiang, Y.; Acton, T. B.; Montelione, G. T.; Hunt, J. F. The 2.3-Å crystal structure of the shikimate 5-dehydrogenase orthologue YdiB from *Escherichia coli* suggests a novel catalytic enviroment for an NAD-dependent dehydrogenase. *J. Biol. Chem.* **2003**, *278*, 19176-19182.

11   Datsenko, K.A.; Wanner, B.L. One-step inactivation of chromosomal genes in *Escherichia coli* K-12 using PCR products. *Proc. Natl. Acad. Sci. USA.* **2000**, *97*, 6640-6645.

12   Duncun, K.; Chaudhuri, S.; Campbell, M. S.; Coggins, J. R. The overexpression and complete amino acid sequence of *Escherichia coli* 3-dehydroquinase. *Biochem J.* **1986**, *238*, 475.

13   (a) DeFeyter, R. C., J. Pittard. Genetic and molecular analysis of *aroL*, the gene for shikimate kinase II in *Escherichia coli* K-12. *J. Bacteriol.* **1986**, *165*, 226-232. (b) DeFeyter, R. C., J. Pittard. Purification and properties of shikimate kinase II from *Escherichia coli* K-12. *J. Bacteriol.* **1986**, *165*, 331-333.

14   Adachi, O.; Ano, Y.; Toyama, H.; Matsushita, K. Purification and properties of NADP-dependent shikimate dehydrogenase from *Gluconobacter oxydans* IFO 3244 and its application to enzymatic shikimate production. *Biosci. Biotechnol. Biochem.* **2006**, *70*, 2786-2789.

15   (a) Park, Y.-C.; Kim, S.-J.; Choi, J.-H.; Lee, W.-H.; Park, K.-M.; Kawamukai, M.; Ryu, Y.-W.; Seo, J.-H. Batch and fed-batch production of coenzyme Q10 in recombinant *Escherichia coli* containing the decaprenyl diphosphate synthase gene from *Gluconobacter suboxydans*. *Appl. Microbiol. Biotechnol.* **2005**, *67*, 192-196. (b) Cheng, H.; Jiang, N.; Shen, A.; Feng, Y. Molecular cloning and functional expression of D-arabitol dehydrogenase gene from *Gluconobacter oxydans* in *Escherichia coli*. *FEMS Microbiol. Lett.* **2005**, *252*, 35-42.

16   http://www.ncbi.nlm.nih.gov/sites/entrez?db=genome

17   http://ergo.integratedgenomics.com/ERGO/

18   Matsushita, K.; Arents, J. C.; Bader, R.; Yamada, M.; Adachi, O.; Postma, P. W. *Escherichia coli* is unable to produce pyrroloquinoline quinone (PQQ). *Microbiol.* **1997**, *143*, 3149-3156.

19   Pittard, J.; Wallace, B. J.   Distribution and function of genes concerned with aromatic biosynthesis in *Escherichia coli*. *J. Bacteriol*. **1966**, *91*, 1494-1508.

20   Martin, R. G.; Rosner, J. L.   Binding of purified multiple antibioticresistance repressor protein (MarR) to *mar* operator sequences. *Proc. Natl. Acad. Sci. USA* **1995**, *92*, 5456–5460.

21   Rosner, J. L.; Storz, G.   Regulation of bacterial responses to oxidative stress. *Curr. Top. Cell. Regul.* **1997**, *35*, 163–177.

22   Saier, M. J.; Paulsen, I.; Sliwinski, M.; Pao, S.; Skurray, R.; Nikaido, H. Evolutionary origins of multidrug and drug-specific efflux pumps in bacteria. *FASEB J.* **1998**, *12*, 265–274.

23   Nikaido, H.; Zgurskaya, H. I.   AcrAB and related multidrug efflux pumps of *Escherichia coli*. *J. Mol. Microbiol. Biotechnol.* **2001**, *3*, 215–218.

24   Franke, S.; Grass, G.; Rensing, C.; Nies, D. H.   Molecular analysis of the copper-transporting efflux system CusCFBA of *Escherichia coli*. *J. Bacteriol.* **2003**, *185*, 3804–3812.

25   Van Dyk, T. K.; Templeton, L. J.; Cantera, K. A.; Sharpe, P. L.; Sariaslani, F. S. Characterization of the *Escherichia coli* AaeAB Efflux Pump: A metabolic relief valve? *J. Bacteriol.* **2004**, *186*, 7196-7204.

26   (a) Pittard, J.; Wallace, B. J.   Gene controlling the uptake of shikimic acid by *Escherichia coli*. *J. Bacteriol*. **1966**, *92*, 1070-1075. (b) Brown, K. D.; Doy, C. H.   Transport and utilization of biosynthetic intermediate shikimic acid in *Escherichia coli*. *Biochim. Biophys. Acta* **1976**, *428*, 550-562. (c) Whipp, M. J.; Camakaris, H.; Pittard, A. J.   Cloning and analysis of the *shiA* gene, which encodes the shikimate transport system of *Escherichia coli* K-12 *Gene* **1998**, *209*, 185-192.

27   http://BioCyc.org/ECOLI/substring-search?type=NIL&object=ydiN

28   Johansson, L.   Metabolic analysis of shikimic acid producing *Escherichia coli*. Ph. D. Disertation, *Lund University, Sweeden*, **2006**.

29   Yang, L.; Lin, R.T.; Newman, E.B.   Structure of the Lrp-regulated *serA* promoter of *Escherichia coli* K-12. *Mol. Microbiol.* **2002**, *43*, 323-333.

CHAPTER FOUR

Experimental

General methods

Spectroscopic measurements

^{1}H NMR spectra were recorded on a Varian 300 MHz VX-300 FT-NMR spectrometer. Chemical shifts were reported in parts per million (ppm) downfield from internal sodium 3-(trimethylsilyl)propionate-$2,2,3,3$-d_4 (TSP, δ = 0.00) with D_2O as solvent. TSP was purchased from Lancaster. UV and visible measurements were recorded on a Hewlett-Packard 8452A Diode Array Spectrophotometer equipped with HP 89532A UV-Visible Operating Software or on a Agilent 8453 UV/Vis equipped with Agilent ChemStation A.10.0 [81] or on a Beckman DU 530 UV/Vis spectrophotometer.

Chromatography

Gas chromatography was performed on an Agilent 6890N equipped with an HP-5 capillary column (30 m × 0.25 mm × 0.25 micron). Temperature programming began with an initial temperature of 120 °C for 3 min. The temperature was increased to 210 °C at a rate of 15 °C/min, and held at the final temperature for 1 min. The split injector was maintained at a temperature of 300 °C and the FID detector was kept at 350 °C. Samples analyzed by gas chromatography were derivatized using bis(trimethylsilyl)trifluoro-acetamide and quantified relative to an internal standard of dodecane against a calibration curve.

135

Dowex 50W×8-200 (H⁺) and Dowex 1×8-400 (Cl⁻) were purchased from Sigma- Aldrich. Previously used Dowex 50 (H⁺) was cleaned by treatment with bromine. An aqueous suspension of resin was adjusted to pH 14 by addition of solid KOH. Bromine was added to the solution until the suspension turned a golden yellow color. Additional bromine was added (1-2 mL) to obtain a saturated solution. The mixture stood at room temperature overnight, and the Dowex 50 resin was collected by filtration and washed exhaustively with water followed by 6 N HCl. Dowex 50 (H⁺) was stored at 4 °C. AG-1X8 (acetate form and chloride form) and hydroxyapatite Bio-Gel HTP gel were purchased from Bio-Rad.

Bacteria strains and plasmids

All the strains and plasmids used are shown in Table 21. *E. coli* K-12 strain RB791 was obtained from the American Type Culture Collection (ATCC strain 53622). *E. coli* AB2834,[1] AB2848[1] were obtained from the *E. coli* Genetic Stock Center at Yale University. *E. coli* KL3,[2] QP1.1,[3] SP1.1,[4] were constructed in the lab previously. Plasmid constructions were carried out in *E. coli* DH5α, which is available from Invitrogen. Plasmid pKK223-3[5] is available from GE Healthcare. Plasmid pSU18[6] were obtained previously by this lab. Plasmids pKD12.112,[4] pKD12.138,[4] pNR8.146,[7] were constructed in the lab previously.

136

Table 21. Bacterial strains and plasmids.

Strain/Plasmid	Relevant Characteristics	Source
	Strain	
DH5α	F^- $\phi80lacZ\Delta M15$ $\Delta(lacZYA\text{-}argF)$ $U169$ $recA1$ $endA1$ $hsdR17(r_{k-}, m_{k+})$ $phoA$ λ^- $supE44$ $thi\text{-}1$ $gyrA96$ $relA1$	Invitrogen
E. coli W3110	wild-type K-12	ATCC
E. coli BW25113	$lacI^q$ $rrnB_{T14}$ $\Delta lacZ_{WJ16}$ $hsdR514$ $\Delta araBAD_{AH33}$ $\Delta rhaBAD_{LD78}$	CGCS
Gluconobacter oxydans IFO3244	wild-type	NBRC
RB791	W3110 $lacL8I^q$	ATCC
RB791serA::aroB	RB791 serA::aroB	Lab[4]
AB2834	tsx-352 glnV42 λ aroE353 malT352	CGSC
AB2848	tsx-356 glnV42 aroD352 LAM-	CGSC
ALO807	F^- leuB6 thi-1 lacY1 ton A21 ΔlacIZ hsdR supE44 rfrbDl aroK::Cm^R aroL478::Tn10	Lab[8]
KL3	AB2834 serA::aroB	Lab[2]
JY1	KL3 ΔptsHptsIcrr::Kan^R	Lab[9]
SP1.1	RB791 serA::aroB aroL478::Tn10 aroK17::Cm^R	Lab[4]
SP1.1pts	SP1.1 ΔptsHptsIcrr::Kan^R	Lab[10]
QP1.1	AB2848 serA::aroB	Lab[3]
QP1.1pst	QP1.1 ΔptsHptsIcrr::Kan^R	Lab[7]
	E. coli B serA::aroB	Lab[11]
	E. coli W3110 ΔaroD(new)::FRT-cat-FRT	Chapter 2
	E. coli B serA::aroB ΔaroD(new)::FRT-cat-FRT	Chapter 2
	E. coli B serA::aroB ΔaroD(new)::FRT	Chapter 2
	BW25113 ΔserA::FRT-kan-FRT	Chapter 3
	BW2511 ΔserA::FRT	Chapter 3
	BW25113 ΔydiB::FRT-kan-FRT	Chapter 3
	BW25113 ΔydiB(H1, H2.2)::FRT-kan-FRT	Chapter 3
JJ2kan	SP1.1 ΔydiB::FRT-kan-FRT	Chapter 3
JJ2	SP1.1 ΔydiB::FRT	Chapter 3
JJ2.2kan	SP1.1 ΔydiB::FRT-kan-FRT	Chapter 3
JJ2.2	SP1.1 ΔydiB(H1, H2.2)::FRT	Chapter 3
JJ3cat	RB791 serA::aroB ΔaroK::FRT-cat-FRT	Chapter 3
JJ3	RB791 serA::aroB ΔaroK::FRT	Chapter 3
JJ4cat	RB791 serA::aroB ΔaroL::FRT-cat-FRT	Chapter 3
JJ4	RB791 serA::aroB ΔaroL::FRT	Chapter 3
JJ5cat	RB791 serA::aroB ΔaroK::FRT ΔaroL::FRT-cat-FRT	Chapter 3
JJ5	RB791 serA::aroB ΔaroK::FRT ΔaroL::FRT	Chapter 3

Table 21 (continued).

Strain/Plasmid	Relevant Characteristics	Source
	Plasmid	
pKK223-3	Ap^R, P_{tac}	GE Healthcare
pBluescrip SK (−)	Ap^R, lacZ	Stratagene
pKD3	Ap^R, FRT-flanked Cm^R	CGSC[12]
pKD4	Ap^R, FRT-flanked Km^R	CGSC[12]
pKD46	Ap^R, araC, $P_{araB}\gamma$, β, exo, ts-pA101 replicon	CGSC[12]
pCP20	Ap^R, Cm^R, Flp^+, λ cI857$^+$	CGSC[13]
pFT-A	Ap^R, Tc^R, Flp^+	Lab[14]
pKL5.17A	Cm^R, tktA in pKD11.291A	Lab[2]
pSC6.090	P_{tac}glf glk, aroF^{FBR}, tktA, P_{tac}aroE, serA	Lab[11]
pJY1.216A	Ap^R, serA, aroF^{FBR}, P_{aroF}, tktA, P_{tac}ppsA	Lab[17]
pJY2.183	Cm^R, serA, aroF^{FBR}, P_{aroF}, P_{tac}glf glk, tktA	Lab[9]
pNR4.230	Ap^R, aroF^{FBR}, P_{tac}aroE, serA, tktA	Lab[7]
pNR4.276	Ap^R, ppsA, P_{tac}aroE, serA, tktA	Lab[7]
pNR8.146	serA, tktA in p34e	Lab[7]
pNR9.280	Ap^R, FRT-flanked serA	Lab
pKD12.112	Ap^R, aroF^{FBR}, P_{tac}aroE, serA in pSU18	Lab[4]
pKD12.138	Ap^R, aroF^{FBR}, tktA, P_{tac}aroE, serA in pKD12.112	Lab[4]
pKD12.152	Ap^R, aroF^{FBR}, P_{tac}aroE, serA, aroD in pSU18	Lab
pKD15.071	ppsA, aroF^{FBR}, tktA, P_{tac}aroE, serA	Lab[10]
pBlue IFO 3244 #1	genomic DNA fragment from G. oxydans IFO3244	Chapter 3
pBlue IFO 3244 #2	genomic DNA fragment from G. oxydans IFO3244	Chapter 3
pJJ4.171A	Ap^R, aroF^{FBR}, P_{tac}ydiB (ORF), tktA, serA in pSU18	Lab[15]
pJJ5.067	Ap^R, P_{tac}ydiB in pKK223-3	Chapter 2
pJJ5.068	Ap^R, aroF^{FBR}, P_{tac}ydiB in pSU18	Chapter 2
pJJ5.069	Ap^R, tktA, serA in pJJ5.068	Chapter 2
pJJ5.072	Ap^R, aroF^{FBR} in pJJ5.067	Chapter 2
pJJ5.073	Ap^R, tktA, serA in pJJ5.072	Chapter 2
pJJ5.151	Ap^R, P_{tac}ydiN (ORF) in pKK223-3	Chapter 3
pJJ5.164	Ap^R, P_{tac}ydiN (ORF) in pKD12.112	Chapter 3
pJJ5.165	Ap^R, tktA in pJJ5.165	Chapter 3

Storage of bacterial strains and plasmids

All bacterial strains were stored at -78 °C in glycerol. Plasmids were transformed into DH5α for long-term storage. Glycerol samples were prepared by adding 0.75 mL of an overnight culture to a sterile vial containing 0.25 mL of 80% (v/v) glycerol. The solution was mixed, left at room temperature for 2 h and then stored at -78 °C.

Culture medium

All solutions were prepared in distilled, deionized water. LB medium[16] (1 L) contained Bacto tryptone (10 g), Bacto yeast extract (5 g), and NaCl (10 g). L-Broth[16] (1 L) contained Bacto tryptone (10 g), Bacto yeast extract (5 g), NaCl (5 g), glucose (1 g) and $CaCl_2$ (2.5 mM). Soft agar[16] (100 mL) contained Bacto tryptone (1 g), Difco agar (0.55 g), and NaCl (0.5 g). M9 salts[16] (1 L) contained Na_2HPO_4 (6 g), KH_2PO_4 (3 g), NH_4Cl (1 g), and NaCl (0.5 g). M9 medium contained carbon sources (D-glucose, D-xylose, D-maltose or D-mannitol, 10 g), $MgSO_4$ (0.12 g), and thiamine (0.001 g) in 1 L of M9 salts. Solutions of inorganic salts, magnesium salts, and carbon sources were autoclaved separately and then mixed. Antibiotics were added where appropriate to the following final concentrations unless noted otherwise: chloramphenicol, 20 μg/mL; ampicillin, 50 μg/mL; tetracycline, 12.5 μg/mL. Stock solution of antibiotics were prepared in water with the exception of chloramphenicol which was prepared in 95% ethanol and tetracycline which was prepared in 50% aqueous ethanol. L-Phenylalanine, L-tyrosine, L-tryptophan, and L-serine were added to M9 medium where indicated to a final concentration of 0.04 g/L. Antibiotics, isopropyl β-D-thioglucopyranoside (IPTG),

thiamine, and amino acid supplementations were sterilized through 0.22-μm membranes prior to addition to M9 medium. Solid medium was prepared by addition of 1.5% (w/v) Difco agar to the medium. Fermentation medium (1 L) contained K_2HPO_4 (7.5 g), ammonium iron (III) citrate (0.3 g), citric acid monohydrate (2.1 g), L-phenylalanine (0.7 g), L-tyrosine (0.7 g), and L-tryptophan (0.35 g), and concentrated H_2SO_4 (1.2 mL). The culture medium was adjusted to pH 7.0 by addition of concentrated NH_4OH before autoclaving. The following supplementations were added immediately prior to initiation of the fermentation: glucose (19-24 g under glucose-limited conditions or 30 g under glucose-rich conditions), $MgSO_4$ (0.24 g), aromatic vitamins p-aminobenzoic acid (0.01 g), 2,3-dihydroxybenzoic acid (0.01 g), and p-hydroxybenzoic acid (0.01 g), and trace minerals $(NH_4)_6(Mo_7O_{24})\cdot4H_2O$ (0.0037 g), $ZnSO_4\cdot7H_2O$ (0.0029 g), H_3BO_3 (0.0247 g), $CuSO_4\cdot5H_2O$ (0.0025 g), and $MnCl_2\cdot4H_2O$ (0.0158 g). D-Glucose and $MgSO_4$ were autoclaved separately while aromatic vitamins and trace minerals were sterilized through 0.22-μm membranes prior to addition to the medium.

Fed-batch fermentation (general)

Fermentations[17] employed a 2.0 L working capacity B. Braun M2 culture vessel fitted with a stainless steel baffle cage consisting of four 1/2" x 5" baffles. Utilities were supplied by a B. Braun Biostat MD controlled by a DCU-1 or DCU-3. Data acquisition utilized a Dell Optiplex Gs+ 5166M personal computer (PC) equipped with B. Braun MFCS/Win software (v2.0). Temperature, pH, and dissolved oxygen (D.O.) were controlled with PID control loops. Temperature was maintained at 36 °C, and pH was maintained at 7.0 by addition of concentrated NH_4OH or 2 N H_2SO_4. Dissolved oxygen

was measured using a Mettler-Toledo 12 mm sterilizable O_2 sensor fitted with an Ingold A-type O_2 permeable membrane. D.O. was maintained at 20% air saturation. Exhaust CO_2 was measured using gas analyzer purchased from Sartorius/BBI. Antifoam (Sigma 204) was added as needed.

Inoculants were prepared by introduction of a single colony into 5 mL of M9 medium. The culture was grown at 37 °C with agitation at 250 rpm until they were turbid (~18-30 h) and subsequently transferred to 100 mL of M9 medium. Cultures were grown at 37 °C for an additional 12 h. The inoculant (OD_{600} = 1.0-2.0) was then transferred into the fermentor vessel and the batch fermentation was initiated (t = 0 h).

Glucose-rich fermentor conditions

The initial glucose concentration in the fermentation medium was 30 g/L. Three staged methods were used to maintain D.O. levels at 20% air saturation during the course of the fermentations. With the airflow at an initial setting of 0.06 L/L/min, D.O. concentration was maintained by increasing the impeller speed from its initial set point of 50 rpm to a preset maximum of 750 rpm. With the impeller rate constant at 750 rpm, the mass flow controller then maintained D.O. levels by increasing the airflow rate from 0.06 L/L/min to a preset maximum of 1.0 L/L/min. After the preset maxima of 750 rpm and 1.0 L/L/min were reached, the third stage of the fermentation was initiated in which glucose (65% w/v) was added to the vessel at a rate sufficient to maintain a glucose concentration in the range of 5 to 30 g/L for the remainder of the run. Airflow was maintained at 1.0 L/L/min, and the impeller was allowed to vary in order to maintain the D.O. concentration at 20% air saturation. The impeller speed typically varied from 750 rpm to 1400 rpm during the remainder of the run. A solution of IPTG (100 mM; 0, 0.25,

0.50, 0.75, 1.0, and 2.0 mL) was added at timed intervals after initiation of the run to achieve reported IPTG concentrations of 0, 6.0, 12, 18, 24, and 48 mg/L, respectively in the fermentation medium.

Glucose-limited fermentor conditions

The initial glucose concentration in the fermentation medium was 19-24 g/L, depending on the strain being examined. Three staged methods were used to maintain D.O. levels at 20% air saturation, with the first two stages identical to those described for the glucose-rich conditions. After the preset maxima of 750 rpm and 1.0 L/L/min of airflow were reached, the third stage of the fermentation was initiated in which the D.O. concentration was maintained at 20% air saturation for the remainder of the run by oxygen sensor-controlled glucose feeding. At the beginning of this stage, the D.O. concentration initially fell below 20% air saturation due to residual glucose in the medium. This lasted for up to 30 min before glucose (65% w/v) feeding commenced. The glucose feed PID control parameters were set to 0.0 s (off) for the derivative control (τ_D) and 999.9 s (minimum control action) for the integral control (τ_I). X_P was set to 950% to achieve a K_c of 0.1. A solution of IPTG (100 mM; 0, 0.25, 0.50, 0.75, 1.0, and 2.0 mL) was added at timed intervals after initiation of the run to achieve reported IPTG concentrations of 0, 6.0, 12, 18, 24, and 48 mg/L, respectively in the fermentation medium.

Analysis of fermentation broths

Samples (5 mL) of fermentation broth were taken at the indicated timed intervals. Cell densities were determined by dilution of fermentation broth with water (1:100)

142

followed by measurement of absorption at 600 nm (OD_{600}). Dry cell weight (g/L) was calculated using a conversion coefficient of 0.43 $g/L/OD_{600}$. The remaining fermentation broth was centrifuged to obtain cell-free broth.

Glucose concentrations in cell-free broth were measured using the Glucose Diagnostic Kit purchased from Sigma. Solute concentrations in the cell-free broth were quantified by ^1H NMR. Solutions were concentrated to dryness under reduced pressure, concentrated to dryness one additional time from D_2O, and then redissolved in D_2O containing a known concentration of the sodium salt of 3-(trimethylsilyl)propionic-2,2,3,3-d_4 acid (TSP). ^1H NMR spectra were recorded and concentrations were determined by comparison of integrals corresponding to each compound with the integral corresponding to TSP (δ = 0.00 ppm). A standard concentration curve was determined for each metabolite using solutions of authentic, purified metabolites. The following resonances were used to quantify each compound: shikimic acid (δ 4.45, d, J = 3.7 Hz, 1 H); 3-dehydroshikimic acid (δ 4.28, d, J = 11.5 Hz, 1 H); 3-dehydroquinic acid (δ 4.38, d, J = 9.3 Hz, 1 H); quinic acid (δ 4.16, m, 1 H); 3-deoxy-D-arabino-heptulosonic acid (δ 1.81, dd, J = 12.4, 12.4 Hz, 1 H); and gallic acid (δ 7.02, s, 2 H). The following response factor was used for each molecule: shikimic acid, 0.70; 3-dehydroshikimic acid, 0.95; 3-dehydroquinic acid, 0.89; quinic acid 0.75; 3-deoxy-D-arabino-heptulosonic acid, 1.22; gallic acid, 1.36.

The concentration of quinic acid in cell-free broth was quantified by GC analysis as well. A portion of the fermentation broth (0.1 mL) was concentrated to dryness under reduced pressure, and the residue was redissolved in pyridine (0.99 mL). To this pyridine solution, dodecane (0.01 mL) and bis(trimethylsilyl)trifluoroacetamide (BSTFA, 1 mL,

143

7.53 mmol) were sequentially added. Silyation of quinic acid were carried out at room temperature with stirring for 10 h. Samples were then analyzed using gas chromatography. Concentration was determined based on calibration curve obtained with authentic samples.

Genetic manipulations

General

Recombinant DNA manipulations generally followed methods described by Sambrook.[18] Restriction enzymes were purchased from Invitrogen or New England Biolabs. Fast-Link[TM] DNA Ligation Kit was obtained from Epicentre. Zymoclean Gel DNA Recovery Kit and DNA Clean & Concentrator Kit was obtained from Zymo Research Company. Maxi, Midi and Mini Plasmid Purification Kits were obtained from Qiagen. Calf intestinal alkaline phosphatase was obtained from New England Biolabs. Agarose (electrophoresis grade) was obtained from Invitrogen. Phenol was prepared by addition of 0.1% (w/v) 8-hydroxyquinoline to distilled, liquefied phenol. Extraction with an equal volume of 1 M Tris-HCl (pH 8.0) two times was followed by extraction with 0.1 M Tris-HCl (pH 8.0) until the pH of the aqueous layer was greater than 7.6. Phenol was stored at 4 °C under an equal volume of 0.1 M Tris-HCl (pH 8.0). SEVAG was a mixture of chloroform and isoamyl alcohol (24:1 v/v). TE buffer contained 10 mM Tris-HCl (pH 8.0) and 1 mM Na_2EDTA (pH 8.0). Endostop solution (10X concentration) contained 50% glycerol (v/v), 0.1 M Na_2EDTA, pH 7.5, 1% sodium dodecyl sulfate (SDS) (w/v), 0.1% bromophenol blue (w/v), and 0.1% xylene cyanole FF (w/v) and was stored at 4 °C. Prior to use, 0.12 mL of DNase-free RNase was added to 1 mL of 10X Endostop

solution. DNase-free RNase was purchased from Roche or (10 mg mL^{-1}) was prepared by dissolving RNase in 10 mM Tris-Cl (pH 7.5) and 15 mM NaCl. DNase activity was inactivated by heating the solution at 100 °C for 15 min. Aliquots were stored at -20 °C.

PCR amplifications were carried out as described by Sambrook.[18] Each reaction (0.1 mL) contained 10 mM KCl, 20 mM Tris-Cl (pH 8.8), 10 mM (NH$_4$)$_2$SO$_4$, 2 mM MgSO$_4$, 0.1% Triton X-100, dATP (0.2 mM), dCTP (0.2 mM), dGTP (0.2 mM), dTTP (0.2 mM), template DNA, 0.5 μM of each primer, and 2 units of Platinum *Taq* HiFi or Pfu polymerase also have been used for PCR reaction with the reaction buffers provided. Initial template concentrations varied from 0.02 μg to 1.0 μg.

Large scale purification of plasmid DNA

In a 2 L Erlenmeyer flask, LB (500 mL) containing the appropriate antibiotics was inoculated from a single colony, and the culture was incubated in a gyratory shaker (250 rpm) for 14 h at 37 °C. DNA was purified using a Qiagen Maxi Kit or Midi Kit as described by the manufacturer. The purity of DNA isolated by this method was adequate for DNA sequencing.

Small scale purification of plasmid DNA

An overnight culture (5 mL) of the plasmid-containing strain was grown in LB containing the appropriate antibiotics.[18] Cells from 3 mL of the culture were collected in a 1.5 mL microcentrifuge tube by centrifugation. The resulting cell pellet was liquefied by vortexing (30 sec) and then resuspended in 0.1 mL of cold GETL solution into which lysozyme (5 mg mL^{-1}) had been added immediately before use. The solution was stored

on ice for 10 min. Addition of 0.2 mL of 1% sodium dodecyl sulfate (w/v) in 0.2 N NaOH was followed by gentle mixing and storage on ice for 5-10 min. To the sample was added 0.15 mL of cold KOAc solution. The solution was shaken vigorously and stored on ice for 5 min before centrifugation (15 min, 4 °C). The supernatant was transferred to another microcentrifuge tube and extracted with equal volumes of phenol and SEVAG (0.2 mL). The aqueous phase (approximately 0.5 mL) was transferred to a fresh microfuge tube, and DNA was precipitated by the addition of 95% ethanol (1 mL). The sample was left at room temperature for 5 min before centrifugation (15 min, room temperature) to collect the DNA. The DNA pellet was rinsed with 70% ethanol, dried, and redissolved in 50 -100 µL TE. DNA isolated from this method was used for restriction enzyme analysis, and the concentration was not determined by spectroscopic methods.

Determination of DNA concentration

The concentration of DNA in the sample was determined as follows. An aliquot (10 µL) of the DNA was diluted to 1 mL in TE and the absorbance at 260 nm was measured relative to the absorbance of TE. The DNA concentration was calculated based on the fact that the absorbance at 260 nm of a 50 µg mL^{-1} of plasmid DNA is 1.0.

DNA precipitation

DNA was precipitated by addition of 0.1 volume of 3 M NaOAc (pH 5.2) followed by thorough mixing and addition of 3 volumes of 95% ethanol. Samples were stored for at least 2 h at -78 °C. Precipitated DNA was recovered by centrifugation (15

min, 4 °C). To the DNA pellet was added 70% ethanol (100 µL), and the sample was centrifuged again (15 min, 4 °C). DNA was dried and redissolved in TE.

Restriction enzyme digestion of DNA

Restriction enzyme digests were performed using restriction enzyme buffers supplied by Invitrogen or New England Biolabs. A typical digest contained approximately 0.8 µg of DNA in 8 µL TE, 2 µL of restriction enzyme buffer (10X concentration), 1 µL of restriction enzyme, and TE to a final volume of 20 µL. Reactions were incubated at 37 °C for 1 h. Digests were terminated by addition of 2.2 µL of Endostop solution (10X concentration) and subsequently analyzed by agarose gel electrophoresis. When DNA was required for subsequent cloning, restriction digests were terminated by addition of 1 µL of 0.5 M Na_2EDTA (pH 8.0) followed by extraction of the DNA with equal volumes of phenol and SEVAG and precipitation of the DNA.

Agarose gel electrophoresis

Agarose gels were run in TAE buffer containing 40 mM Tris-acetate and 2 mM EDTA (pH 8.0). Gels typically contained 0.7% agarose (w/v) in TAE buffer. Higher concentrations of agarose (1%-2%) were used to resolve DNA fragments smaller than 1 kb. Lower concentrations of agarose (0.35%) were used to resolve DNA fragments larger than 10 kb. Ethidium bromide (0.5 µg mL^{-1}) was added to the agarose to allow visualization of DNA fragments over a UV lamp. The size of the DNA fragments were determined by using two sets of DNA standards: λ DNA digested with HindIII (23.1-kb, 9.4-kb, 6.6-kb, 4.4-kb, 2.3-kb, 2.0-kb, and 0.6-kb) and λ DNA digested with EcoRI and HindIII (21.2-kb, 5.1-kb, 5.0-kb, 4.3-kb, 3.5-kb, 2.0-kb, 1.9-kb, 1.6-kb, 1.4-kb, 0.9-kb,

147

0.8-kb, and 0.6-kb). Also 100 bp DNA Ladder (Invitrogen) was used to determine the size of small DNA fragements. The ladder consists of 15 blunt-ended fragments ranging in length from 100 to 1500 bp, at 100 bp increments, and an additional fragment at 2,072 bp.

Isolation of DNA from agarose

The band of agarose containing DNA of interest was excised from the gel while visualized with high wavelength UV and chopped thoroughly with a razor in a plastic weighing tray. The agarose was then transferred to a spin column consisting of a 500 µL microfuge tube packed tightly with glass wool and with an 18 gauge hole in its bottom. The spin column was then centrifuged for 5 min using a microcentrifuge to separate the DNA solution from the agarose. The DNA-containing aqueous phase collected after centrifugation were mixed with 3 M NaOAc and 95% ethanol. The DNA was precipitated as described previously and redissolved in TE.

Alternatively, the band of agarose containing DNA of interest was excised from the gel while visualized with high wavelength UV. Zymoclean Gel DNA Recovery Kit was used to isolate DNA from the agarose gel according to the protocol provided by the Zymo Research Company.

Treatment of vector DNA with calf intestinal alkaline phosphatase (CIAP)

Plasmid vectors digested with a single restriction enzyme were dephosphorylated to prevent self-ligation. Vector DNA after digestion was immediately combined in a total volume of 60 µL. To this sample was added 7 µL of dephosphorylation buffer (10X concentration, provided by enzyme supplier) and 3 µL of calf intestinal alkaline

phosphatase (3 units). The reaction was incubated at 37 °C for 1 h. The phosphatase was

inactivated by addition of 1 μL of 0.5 M Na2EDTA (pH 8.0) followed by heat treatment

(65 °C, 20 min). The sample was extracted with phenol and SEVAG (100 μL each) to

remove protein, and the DNA was precipitated as previously described and redissolved in

TE.

Treatment of DNA with Klenow fragment

DNA with recessed 3' termini was modified to blunt-ended fragment by treatment

with the Klenow fragment of *E. coli* DNA polymerase I. After the DNA (0.8-2 μg)

restriction digestion was completed in a 20 μL reaction, a solution (1 μL) containing each

of the desired dNTPs was added to provide a final concentration of 1 mM for each dNTP.

Addition of 1-2 units of the Klenow fragment to the reaction was followed by incubation

of the mixture at room temperature for 20-30 min. Since the Klenow fragment works

well in the common buffers used for restriction digestion of DNA, there was no need to

purify the DNA after restriction digestion and prior to filling recessed 3' termini. Klenow

reactions were quenched by heating the reaction at 70 °C for 20 min. DNA was

recovered Zymo Clean column kit.

Ligation of DNA

Alternatively, Fast-Link DNA Ligation Kit (Epicentre) was used for ligation of

insert DNA with cohesive or blunt ends into vectors with compatible cohevsive ends

according to the protocol provided by the manufacturer.

Preparation and transformation of competent cells

Competent cells were prepared using a procedure modified from Sambrook.[18] An aliquot (1 mL) from an overnight culture (5 mL) was used to inoculate 100 mL of LB (500 mL Erlenmeyer flask) containing the appropriate antibiotics. The cells were cultured in a gyratory shaker (37 °C, 250 rpm) until they reached the mid-log phase of growth (judged from the absorbance at 600 nm reaching 0.4-0.6). The culture was poured into a large centrifuge bottle that had been previously sterilized with bleach and rinsed with sterile water. The cells were collected by centrifugation (4 000g, 5 min, 4 °C) and the culture medium was discarded. All manipulations were carried out on ice during the remaining portion of the procedure. The cell pellet was washed with 100 mL of cold 0.9% NaCl (w/v) and then resuspended in 50 mL of cold 100 mM $CaCl_2$. The suspension was stored on ice for a minimum of 30 min and then centrifuged (4 000g, 5 min, 4 °C). The cell pellet was resuspended in 4 mL of cold 100 mM $CaCl_2$ containing 15% glycerol (v/v). Aliquots (0.25 mL) were dispensed into 1.5 mL microcentrifuge tubes and immediately frozen in liquid nitrogen. Competent cells were stored at -78 °C with no significant decrease in transformation efficiency over a period of six months.

Frozen competent cells were thawed on ice for 5 min before transformation. A small aliquot (1 to 10 μL) of plasmid DNA or a ligation reaction was added to the thawed competent cells (0.1 mL). The solution was gently mixed and stored on ice for 30 min. The cells were then heat shocked at 42 °C for 2 min and placed on ice briefly (1 min). LB (0.5 mL, no antibiotics) was added to the cells, and the sample was incubated at 37 °C (no agitation) for 1 h. Cells were collected in a microcentrifuge (30 s). If the transformation was to be plated onto LB plates, the cells were resuspended in a small

volume of LB medium (0.1 mL), and then spread onto plates containing the appropriate antibiotics. If the transformation was to be plated onto minimal medium plates, the cells was washed once with the same minimal medium. After resuspension in fresh minimal medium (0.1 mL), the cells was spread onto the plates. A sample of competent cells with no DNA added was also carried through the transformation procedure as a control. These cells were used to check the viability of the competent cells and to verify the absence of growth on selective medium.

Transformations were also performed by electroporation using electrocompetent cells. An aliquot (1 mL) from an overnight culture (5 mL) was used to inoculate 500 mL of 2×YT containing the appropriate antibiotics. The cells were cultured at 37 °C with shaking at 250 rpm. Once an absorbance of 0.6-0.8 at 600 nm was observed, the cells were kept on ice for 10 min and harvested ($3,000g$, 5 min, 4 °C). The cells were gently washed three times with sterile, cold water (450 mL once and 250 mL twice) and then resuspended in 100 mL sterile, ice-cold aqueous 10% glycerol (v/v). After centrifugation ($3,000g$, 5 min, 4 °C), the cells were resuspended in 1.5 mL sterile ice-cold aqueous 10% glycerol (v/v). Aliquots (0.1 mL) of electrocompetent cells were dispensed into 1.5 mL microfuge tubes, and immediately frozen in liquid nitrogen and stored at −78 °C.

The electroporation was performed in Bio-Rad Gene Pulser cuvettes with an electrode gap of 0.2 cm. The cuvettes were chilled on ice for 5 min prior to use. Electrocompetent cells were thawed in ice for 5 min, and 40 μL of thawed cells was added to the chilled cuvette. To this was added 1-10 μL of plasmid DNA (1 μg mL^{-1}), and the mixture was gently shaken. The Bio-Rad Gene Pulser was set at 2.5 kV, 25 μF and 200 Ω. The outside surface of the cuvette was wiped clean and it was placed in the

151

sample chamber. A single pulse was applied, the cuvette was removed, and 1 mL of freshly prepared SOC was added into it. The contents of the cuvette were transferred to a 15 mL sterile centrifugation tube. The cells were incubated at 37 °C for 1 h with shaking at 250 rpm. The transformed cells were plated in the same manner as in the transformation with chemically competent cells.

Purification of genomic DNA

Genomic DNA was purified using a method described by Pitcher.[19] Broth cultures (20 mL) were harvested at the end of the exponential growth phase by centrifugation (1 000g, 15 min, room temperature). A small cell pellet was obtained. The cells of Gram-positive species were resuspended in 100 μL of fresh lysozyme (50 mg/mL) in TE buffer and incubated at 37°C for 30 min. The Gram-negative species were resuspended in 100 μl of TE buffer without enzyme treatment and incubated at 37°C for 30 min. Cells were lysed with 0.5 mL 5 M guanidium thiocyanate (Sigma), 100 mM EDTA and 0.5% v/v sarkosyl (GES reagent), which was prepared as follows. Guanidium thiocyanate (60 g), 0.5 M EDTA at pH 8 (20 mL) and deionized water (20 mL) were heated at 65°C with mixing until dissolved. After cooling, 5 mL of 10% v/v sarkosyl were added, the solution was made up to 100 mL with deionized water, filtered through a 0.22-μm membrane and stored at room temperature.

Cell suspensions were vortexed briefly and checked for lysis (clear solution) after 5-10 min. The lysates were cooled on ice and 0.25 mL cold 7.5 M ammonium acetate was added with mixing on ice for 10 min. To this sample, 0.5 mL SEVAG was added, and the solution was mixed thoroughly. After centrifugation in a 1.5 mL Eppendorf tube (25 000g, 10 min, room temperature), supernatant fluids were transferred to Eppendorf

tubes and 0.54 volumes of cold 2-propanol was added. The tubes were inverted for 1 min to mix the solutions and the fibrous DNA precipitate was deposited by centrifugation (6 500g, 20 s, room temperature). Pellets of DNA were washed five times in 70% ethanol and dried at room temperature for 20 min. Genomic DNA was redissolved in 100 μL TE.

P1-mediated transduction

Transduction with P1 phage was carried out using a method modified from Miller.[20] P1 phage lysate was prepared by propagation of phage in the donor strain using the following procedure. Serial dilutions of P1 phage stock (0.1 mL, 10^{-1} to 10^{-5}) in LB were prepared in sterile test tubes (13 × 100 mm). An aliquot (0.1 mL, approximately 5 × 10^{8} cells) of an overnight culture of the donor strain was added to each tube. Sterile, molten soft agar (45 °C) was added to each tube. The contents of each tube were mixed and poured immediately onto a pre-warmed (37 °C) L plate, swirling gently to achieve uniform coverage of the plate. After the agar had solidified, the plates were incubated at 37 °C until confluent lysis had occurred (approximately 8 h). Because the multiplicity of infection is critical to phage generation, confluent lysis occurred on only one or two of the plates. L-Broth (4 mL) was added to these plates, which were then stored overnight at 4 °C to allow the phage particles to diffuse into the broth. The L-broth was collected from the plate and vortexed with several milliliters of $CHCl_3$ to make certain that all of the cells had lysed. The solution was centrifuged (2 000g, 5 min, room temperature) to separate the layers. Aqueous phage lysate was stored in 1.5 mL microfuge tubes over several drops of $CHCl_3$ at 4 °C.

Infection of the recipient strain with phage lysate proceeded as follows. Overnight culture (2 mL) of the recipient strain was centrifuged (microfuge, 30 s, 4 °C)

153

and the growth medium discarded. The cells were resuspended in 1 mL of 5 mM $CaCl_2$ and 100 mM $MgSO_4$ and shaken (200 rpm) at 37 °C for 15 min to promote aeration of the cells. In the meantime, 0.1 mL serial dilutions (10^0 to 10^{-3}) of phage lysate in LB were prepared in sterile microfuge tubes. An aliquot (0.1 mL) of aerated recipient cells was added to each of the phage dilutions, the samples were gently mixed and then incubated at 37 °C for 20 min without shaking. Sodium citrate (1 M, 0.2 mL) was added to each sample, and the cells were harvested (microfuge, 30s, room temperature) and resuspended in 0.2 mL of LB containing 100 mM sodium citrate. After incubation at 30 °C for 30 min, cells were again harvested (microfuge, 30 s, room temperature), resuspended in 0.1 mL of growth medium, and plated out onto appropriate agar plates.

Enzyme assays

After collected and resuspended in proper resuspension buffer, the cells were disrupted by two passages through a French pressure cell (SLM Aminco) at 16000 psi. Cellular debris was removed from the lysate by centrifugation (48 000g, 20 min, 4 °C). Protein was quantified using the Bradford dye-binding procedure.[21] A standard curve was prepared using bovine serum albumin. The protein assay solution was purchased from Bio-Rad.

Shikimate dehydrogenase assay in forward direction

Shikimate dehydrogenase was assayed using 3-dehydroshikimic acid as the substrate according to the procedure described by Coggins.[22] Lysate was prepared and protein concentrations were determined as previously mentioned. Cells were harvested and resuspended in 100 mM potassium phosphate buffer (pH 7.4), Na_2EDTA (1 mM) and

diethiothreitol (0.4 mM). Cellular lysate was diluted in 100 mM potassium phosphate buffer (pH 7.4). Assays (1 mL) contained potassium phosphate (100 mM, pH 7.0) buffer, 3-dehydroshikimic acid (2 mM), and β-NADPH (0.2 mM) sodium salt. Potassium phosphate, 3-dehydroshikimic acid, and β-NADPH solutions were mixed, and the spectrophotometer was zeroed. Addition of diluted lysate initiated the assay. The depletion of NADPH was monitored at 340 nm ($\varepsilon = 6{,}220$ M^{-1} cm^{-1}) for 60 seconds. One unit of shikimate dehydrogenase activity was defined as the formation of 1 μmol of NADP per minute at room temperature.

Shikimate dehydrogenase assay in reverse direction

Shikimate dehydrogenase was assayed using shikimic acid as the substrate according to the procedure described by Chaudhuri et al.[23] Lysate was prepared and protein concentrations were determined as previously mentioned. Cells were harvested and resuspended in a buffer containing Tris-HCl (100 mM, pH 7.5), Na_2EDTA (1 mM) and diethiothreitol (0.4 mM). Cellular lysate was diluted in 100 mM Tris-HCl (pH 9.0). Assays (1 mL) contained Tris-HCl (100 mM, pH 9.0), shikimic acid (4 mM), and β-NADP (2 mM) sodium salt. Tris-HCl, shikimic acid, and diluted lysate solutions were mixed, and the spectrophotometer was zeroed. Addition of β-NADP initiated the assay. The formation of NADPH was monitored at 340 nm ($\varepsilon = 6{,}220$ M^{-1} cm^{-1}) for 60 seconds. One unit of shikimate dehydrogenase activity was defined as the formation of 1 μmol of NADPH per minute at room temperature.

Quinate dehydrogenase assay

Quinate dehydrogenase was assayed using quinic acid according to the procedure described by Davis.[24] Lysate was prepared and protein concentrations were determined as previously mentioned. Cells were harvested and resuspended in a buffer containing 100 mM potassium phosphate (pH 7.6). Cellular lysate or purified enzyme was diluted in 100 mM potassium phosphate (pH 7.6). Diluted enzyme solution was treated with 1M KCN (1.0% vol/vol) and incubated at 4 °C for at least 10 min prior the continuous assay. Assay (1 mL) contained potassium bicarbonate (32 mM, pH 9.4), NAD^+ (0.32 mM) and clarified lysate. Addition of quinic acid (3.2 mM) initiated the assay. The formation of NADPH was monitored at 340 nm (ε = 6,220 M^{-1} cm^{-1}) for 60 seconds. One unit of quinate dehydrogenase activity was defined as the formation of 1 μmol of NADH per minute at room temperature.

Chapter two (experimental)

E. coli W3110 Δ*aroD*(new)::FRT-*cat*-FRT

The genomic *aroD* inactivation was generated by the methods described by Datsenko et al.[12] Linear DNA with an FRT-flanked chloramphenicol resistance gene was amplified by PCR from pKD3 using Platinum HiFi *Taq* DNA polymerase, with 5'- ATGAAAACCGTAACTGTAAAAGATCTCGTCATTGGTACGGGTGTAGGCTGG-AGCTGCTTC as the forward primer, and 5'- CCGGTAAATAACTCCAGATCGATCA-TATCAACCAGGCCGCCATATGAATATCCTCCTTAG as the reverse primer. The sequence underlined represent the homology arms, while the remainders are the priming sequences for hybridization to complementary sequences on the template plasmid pKD3.

The 1.2 kb PCR product was agarose gel purified and subsequently transformed into electrocompetent *E. coli* W3110/pKD46. The transformants were selected on an LB/Cm plate. Disruption of *aroD* was confirmed by PCR analysis using the following primers: 5'- GTTCACATTATGGACTGGC and 5'- AGAATTAGCGCACAGAGAC; and afforded 1.6 kbp fragment for mutant and 1 kbp for control strain *E. coli* W3110. Phenotype was confirmed by growth in the following plates: No growth on LB/Ap and M9/Glucose; growth on LB/Cm and M9/Glucose/Aromatics.

E. coli B *serA::aroB* Δ*aroD*(new)::FRT-*cat*-FRT

E. coli B *serA::aroB* Δ*aroD*(new)::FRT-*cat*-FRT was made from *E. coli* B *serA::aroB* by P1 phage-mediate transduction using *E. coli* W3110 Δ*aroD*(new)::FRT-*cat*-FRT as the donor strain. Colonies were plated on selective LB/Cm plates. The resulting colonies were screened for Δ*aroD*(new)::FRT-*cat*-FRT mutation by checking the growth on the following plates: No growth on LB/Ap, M9/Glucose, M9/Glucose/Serine, M9/Glucose/Aromatics; growth on LB/Cm and M9/Glucose/Aromatics/Serine. Additionally disruption of *aroD* gene was characterized by PCR analysis using following primers: 5'- GTTCACATTATGGACTGGC and 5'- AGAATTAGCGCACAGAGAC; and afforded 1.6 kbp fragment for mutant and 1 kbp for control strain *E. coli* B *serA::aroB*.

E. coli B *serA::aroB* Δ*aroD*(new)::FRT

The genomic antibiotic marker on *E. coli* KIT3 was excised by the method described by Posfai *et al.*[14] *E. coli* strain *E. coli* B *serA::aroB* Δ*aroD*(new)::FRT-*cat*-FRT was electroporated with plasmid pFT-A containing Flp recombinase gene, and

grown on LB plate containing 100 µg/mL ampicillin at 30 °C overnight. Next day single

colony was inoculated into LB/Ap liquid media and grown at 30 °C until OD_{600} reached

1-2. Overexpression of Flp recombinase was induced with 20 µg/mL (final

concentration) of chlorotetracycline and grown for additional 6 h at 30 °C. The loss of

plasmid pFT-A was due to temperature sensitive replicon and was carried by inoculating

(1:100 dilution) fresh LB liquid media with induced culture and growing overnight at 43

°C. Single colonies were obtained by streaking overnight culture on LB plate and

incubating at 37 °C. The loss of the antibiotic marker gene was verified by PCR analysis

using primers 5'- GTTCACATTATGGACTGGC and 5'- AGAATTAGCGCACA-

GAGAC; and afforded 0.5 kbp fragment for mutant and 1 kbp for control strain *E. coli* B

serA::aroB. Additionaly, phenotype was confirmed by the growth on the following

plates: no growth on LB/Ap, LB/Cm, M9/Glucose, M9/Glucose/Serine,

M9/Glucose/Aromatics; growth on LB and M9/Glucose/Aromatics/Serine.

Plasmid pJJ5.067

The *ydiB* insert with 31 bp upstream sequence was amplified from *E. coli* W3110

genomic DNA using the following primers: 5'-GG<u>GAATTC</u>CAATTAAGCATAG-

AGGTT and 5'-TCC<u>CCCGGG</u>TCAGGCACCGAACCCCATG. *Eco*RI and *Sma*I

restriction sequences (underlined nucleatides) were included to facilitate cloning,

respectively. Localization of the resulting 1-kb fragment into vector pKK223-3, which

had been previously incubated with *Eco*RI and *Sma*I followed by CIAP treatment,

afforded 5.6-kb plasmid pJJ5.067, where *ydiB* is transcribed from P_{tac} promoter.

Plasmid pJJ5.068

The construction of 5.7-kb plasmid pJJ4.150A started from amplification of $P_{tac}ydiB$ fragment from pJJ5.067 plasmid using the following primers: 5'-CG<u>GGTACC</u>GGAGCTTATCGACTGCACG and 5'- CG<u>GAATTC</u>TCAGGCACCGA-ACCCCAT. Plasmid pKD12.112 was digested with *KpnI/Bam*HI and treated with CIAP and liberated 3.2-kb $P_{tac}aroE$ *serA* fragment was separated from the plasmid by agarose gel. Resulted plasmid was ligated with 1.2-kb PCR product, which had been previously digested with *KpnI/Bam*HI and afforded plasmid pJJ5.068.

Plasmid pJJ5.069

Construction of pJJ5.069 began with pNR8.146A. A 3.8-kb *tktA, serA*-encoding fragment was liberated from pNR8.146A by digestion with *XbaI*. Insertion of the *tktA, serA* fragment into linerized pJJ5.068 with *XbaI* followed by CIAP treatment, yielded a 9.5-kb plasmid pJJ5.069.

Plasmid pJJ5.072

A 1.2-kb $aroF^{FBR}$-encoding fragment was liberated from pKD12.112 by digestion with *Eco*RI and was gel purified after Klenow treatment. Plasmid pJJ5.067 was linerized with *SmaI* and treated with CIAP followed by ligation with $aroF^{FBR}$ fragment, yielded a 6.8-kb plasmid pJJ5.072.

Plasmid pJJ5.073

A 3.8-kb *tktA, serA*-encoding fragment was liberated from pNR8.146A by digestion with *Xba*I followed by Klenow treatment. Insertion of the *tktA, serA* fragment into linerized pJJ5.072 with *Hind*III followed by Klenow and CIAP treatment, yielded a 10.6-kb plasmid pJJ5.073.

Chapter three (experimental)

E. coli BW25113 Δ*serA*::FRT-*kan*-FRT

The *E. coli* genomic *serA* inactivation was generated by the same protocol for generating *E. coli* W3110 Δ*aroD*(new)::FRT-*cat*-FRT. The FRT-flanked kanamycin gene was amplified from pKD4 using 5'- <u>TGACATGTGTCACGCTTTTACCAG-GCAATTGTCGATTGC</u>TGTGTAGGCTGGAGCTGCTTC as the forward primer, and 5'- <u>ACACAACGCATTGATCTGACTTTGATTTATTTTCTGGAGC</u>CATATGAATAT-CCTCCTTAG as the reverse primer. The sequence underlined represent the homology arms, while the remainders are the priming sequences for hybridization to complementary sequences on the template plasmid pKD4. The 1.6 kb PCR product was agarose gel purified and subsequently transformed into electrocompetent *E. coli* BW25113/pKD46. The transformants were selected on an LB/Kan plate. Disruption of *serA* was confirmed by PCR analysis using the following primers: 5'- ATTCTCTTCATTAAATTTGG and 5'- CGTAAATCCCCATTAAATAA; and afforded 1.7 kb DNA fragment for the mutant and 1.8 kb DNA fragment for the control strain BW25113. Phenotype was also confirmed by growth on selective plates: no growth on LB/Ap, M9/Glucose; growth on LB/Kan, M9/Glucose/Serine.

E. coli BW25113 Δ*serA*::FRT

The genomic antibiotic marker on *E. coli* BW25113 Δ*serA*::FRT-*kan*-FRT was excised by the method described by Cherepanov *et al.*[13] *E. coli* strain BW25113 Δ*serA*::FRT-*kan*-FRT was electroporated with plasmid pCP20 containing Flp recombinase gene, and grown on LB plate containing 100 µg/mL ampicillin at 30 °C overnight. The Flp recombinase excises the chloramphenicol gene flanked by FRT sites from the chromosome. After growth at 42 °C for one day in LB to cure BW25113 Δ*serA*::FRT-*kan*-FRT/pCP20 that has a temperature sensitive replication origin, ampicillin and kanamycin sensitivity were tested to verify loss of pCP20 and the antibiotic marker. The loss of the antibiotic gene marker was verified by PCR analysis using primers 5'- ATTCTCTTCATTAAATTTGG and 5'- CGTAAATCCCCATT-AAATAA; and afforded 0.2 kb DNA fragment for the mutant and 1.8 kb DNA fragment for the control strain BW25113. Phenotype was also confirmed by growth on selective plates: no growth on LB/Ap, LB/Kan and M9/Glucose; growth on LB and M9/Glucose/Serine.

E. coli BW25113 Δ*ydiB*::FRT-*kan*-FRT

The *E. coli* genomic *ydiB* (ORF) inactivation was generated by the same protocol for generating *E. coli* W3110 Δ*aroD*(new)::FRT-*cat*-FRT. The FRT-flanked kanamycin gene was amplified from pKD4 using 5'- <u>CGAATTGATTGGGTTGATGGCCTAT-CCTATCCGCCACAGT</u>GTGTAGGCTGGAGCTGCTTCG as the forward primer, and 5'- <u>CCTGTTTAACATATTCCAGAGGGAAATCTTTGCCAGTCCA</u>CATATGAATA-TCCTCCTTAG as the reverse primer. The sequence underlined represents the homology

arms, while the remainders are the priming sequences for hybridization to complementary sequences on the template plasmid pKD4. The 1.6 kb PCR product was agarose gel purified and subsequently transformed into electrocompetent *E. coli* BW25113/pKD46. The transformants were selected on an LB/Kan plate. Disruption of *ydiB* was confirmed by PCR analysis using the following primers: 5'- CGGAATTCATGGATGTTA-CCGCAAAATAC and 5'-CGGAATTCTCAGGCACCGAACCCCAT; and afforded 1.6 kb DNA fragment for the mutant and 0.9 kb DNA fragment for the control strain BW25113. Phenotype was also confirmed by growth on selective plates: No growth on LB/Ap; growth on LB/Kan.

E. coli JJ2*kan*

E. coli JJ*kan* was made from *E. coli* SP1.1 by P1 phage-mediate transduction using *E. coli* BW25113 Δ*ydiB*::FRT-*kan*-FRT as the donor strain. Colonies were plated on selective LB/Kan plates. The resulting colonies were screened for Δ*ydiB*::FRT-*kan*-FRT mutation by PCR analysis using following primers: 5'- CGGAATTCATGG-ATGTTACCGCAAAATAC and 5'-CGGAATTCTCAGGCACCGAACCCCAT; and afforded 1.6 kb DNA fragment for the mutant and 0.9 kb DNA fragment for the control strain SP1.1. Phenotype was also confirmed by growth on selective plates: No growth on LB/Ap, M9/Glucose, M9/Glucose/Serine, M9/Glucose/Aromatics; growth on LB/Cm, LB/Tc, LB/Kan and M9/Glucose/Aromatics/Serine. The *E. coli* SP1.1 Δ*ydiB*::FRT-*kan*-FRT was designated as JJ2*kan*.

E. coli JJ2

The genomic chloramphenicol marker was excised by the same protocol for generating *E. coli* BW25113 Δ*serA*::FRT. Thermal induction of the Flp recombinase in JJ2*kan*/pCP20 excised the kanamycin marker and afforded strain JJ2 (SP1.1 Δ*ydiB*::FRT). The loss of the antibiotic marker gene was verified by PCR analysis using primers 5'- CGGAATTCATGG-ATGTTACCGCAAAATAC and 5'-CGGAATTCTC-AGGCACCGAACCCCAT and afforded 0.2 kb DNA fragment for the mutant and 0.9 kb DNA fragment for the control strain SP1.1. Phenotype was also confirmed by growth on selective plates: No growth on LB/Ap, LB/Kan, M9/Glucose, M9/Glucose/Serine, M9/Glucose/Aromatics; growth on LB/Cm, LB/Tc, and M9/Glucose/Aromatics/Serine.

E. coli BW25113 Δ*ydiB*(H1, H2.2)::FRT-*kan*-FRT

The *E. coli* genomic *ydiB* inactivation was generated by the same protocol for generating *E. coli* W3110 Δ*aroD*(new)::FRT-*cat*-FRT. The FRT-flanked kanamycin gene was amplified from pKD4 using 5'- <u>ATGGATGTTACCGCAAAATACGAATTG-ATTGGGTTGATGGGTGTAGGCTGGAGCTGCTTCG</u> as the forward primer, and 5'- <u>TCGTCATATGCGGGTTATACACGCATTCAGTGACCAGAAG</u>CATATGAATATC-CTCCTTAG as the reverse primer. The sequence underlined represent the homology arms, while the remainders are the priming sequences for hybridization to complementary sequences on the template plasmid pKD4. The 1.6 kb PCR product was agarose gel purified and subsequently transformed into electrocompetent *E. coli* BW25113/pKD46. The transformants were selected on an LB/Kan plate. Disruption of *ydiB* was confirmed by PCR analysis using the following primers: 5'- CGGAATTCATGGATGTTA-CCGCAAAATAC and 5'-CGGAATTCTCAGGCACCGAACCCCAT; and afforded 2

kb DNA fragment for the mutant and 0.9 kb DNA fragment for the control strain BW25113. Phenotype was also confirmed by growth on selective plates: no growth on LB/Ap; growth on LB/Kan.

E. coli JJ2.2kan

E. coli JJ2.2kan was made from E. coli SP1.1 by P1 phage-mediate transduction using E. coli BW25113 ΔydiB(H1, H2.2)::FRT-kan-FRT as the donor strain. Colonies were plated on selective LB/Kan plates. The resulting colonies were screened for ΔydiB(H1, H2.2)::FRT-kan-FRT mutation by PCR analysis using following primers: 5'-CGGAATTCATGGATGTTACCGCAAAATAC and 5'-CGGAATTCTCAGGCAC-CGAACCCCAT; and afforded 2 kb DNA fragment for the mutant and 0.9 kb DNA fragment for the control strain SP1.1. Phenotype was also confirmed by growth on selective plates: No growth on LB/Ap, M9/Glucose, M9/Glucose/Serine, M9/Glucose/Aromatics; growth on LB/Cm, LB/Tc, LB/Kan and M9/Glucose/Aromatics/Serine. The E. coli SP1.1 ΔydiB(H1, H2.2)::FRT-kan-FRT was designated as JJ2.2kan.

E. coli JJ2.2

The genomic kanamycin marker was excised by the same protocol for generating E. coli BW25113 ΔserA::FRT. Thermal induction of the Flp recombinase in JJ2.2kan/pCP20 excised the kanamycin marker and afforded strain JJ2.2 (SP1.1 ΔydiB(H1, H2.2)::FRT). The loss of the antibiotic marker gene was verified by PCR analysis using primers 5'- CGGAATTCATGG-ATGTTACCGCAAAATAC and 5'-CGGAATTCTCAGGCACCGAACCCCAT and afforded 0.45 kb DNA fragment for the

mutant and 0.9 kb DNA fragment for the control strain SP1.1. Phenotype was also confirmed by growth on selective plates: no growth on LB/Ap, LB/Kan, M9/Glucose, M9/Glucose/Serine, M9/Glucose/Aromatics; growth on LB/Cm, LB/Tc and M9/Glucose/Aromatics/Serine.

E. coli JJ3cat

The *E. coli* genomic *aroK* inactivation was generated by the same protocol for generating *E. coli* W3110 Δ*aroD*(new)::FRT-*cat*-FRT. The FRT-flanked kanamycin gene was amplified from pKD3 using 5'- <u>ATGGCAGAGAAACGCAATATCTTT-CTGGTTGGGCCTATGGG</u>TGTAGGCTGGAGCTGCTTCG as the forward primer, and 5'- <u>CTTTCCAGCATGTGAATAATCTGGTTTGCAACCACTTTAG</u>CATATGAATA-TCCTCCTTAG as the reverse primer. The sequence underlined represent the homology arms, while the remainders are the priming sequences for hybridization to complementary sequences on the template plasmid pKD3. The 1.2 kb PCR product was agarose gel purified and subsequently transformed into electrocompetent *E. coli* RB791 *serA*::*aroB*/pKD46. The transformants were selected on an LB/Cm plate. Disruption of *aroK* was confirmed by PCR analysis using the following primers: 5'- GCTCT-AGATTTCCAGTGAGTAAACAGCC and 5'- GCTCTAGACCATAACGCGACATCC-ACCT; and afforded 1.7 kb DNA fragment for the mutant and 1 kb DNA fragment for the control strain RB791 *serA*::*aroB*. Phenotype was also confirmed by growth on selective plates: No growth on LB/Ap, M9/Glucose; growth on LB/Cm, M9/Glucose/Serine. The *E. coli* RB791 *serA*::*aroB* Δ*aroK*::FRT-*cat*-FRT was designated as JJ3*cat*.

E. coli JJ3

The genomic chloramphenicol marker was excised by the same protocol for generating *E. coli* BW25113 Δ*serA*::FRT. Thermal induction of the Flp recombinase in JJ3*cat*/pCP20 excised the chloramphenicol marker and afforded strain JJ3 (RB791 *serA*::*aroB* Δ*aroK*::FRT). The loss of the antibiotic marker gene was verified by PCR analysis using primers 5'- GCTCTAGATTTCCAGTGAGTAAACAGCC and 5'- GCTCTAGACCATAACGCGACATCCACCT and afforded 0.5 kb DNA fragment for the mutant and 1 kb DNA fragment for the control strain RB791 *serA*::*aroB*. Phenotype was also confirmed by growth on selective plates: No growth on LB/Ap, LB/Cm, M9/Glucose; growth on LB and M9/Glucose/Serine.

E. coli JJ4cat

The *E. coli* genomic *aroL* inactivation was generated by the same protocol for generating *E. coli* W3110 Δ*aroD*(new)::FRT-*cat*-FRT. The FRT-flanked kanamycin gene was amplified from pKD3 using 5'- <u>ATGACACAACCTCTTTT-TCTGATCGGGCCTCGGGGCTGTGG</u>TGTAGGCTGGAGCTGCTTCG as the forward primer, and 5'- <u>TCAACAATTGATCGTCTGTGCCAGGGCGCTGCGAATTTCA</u>CAT-ATGAATATCCTCCTTAG as the reverse primer. The sequence underlined represent the homology arms, while the remainders are the priming sequences for hybridization to complementary sequences on the template plasmid pKD3. The 1.2 kb PCR product was agarose gel purified and subsequently transformed into electrocompetent *E. coli* RB791 *serA*::*aroB*/pKD46. The transformants were selected on an LB/Cm plate. Disruption of *aroL* was confirmed by PCR analysis using the following primers: 5'- ACCTATTGGGGAAAACCCACG and 5'- TTAAGTATAGGCGCTCGAAAA; and

afforded 1.2 kb DNA fragment for the mutant and 0.6 kb DNA fragment for the control strain RB791 *serA::aroB*. Phenotype was also confirmed by growth on selective plates: no growth on LB/Ap, M9/Glucose; growth on LB/Cm, M9/Glucose/Serine. The *E. coli* RB791 *serA::aroB* Δ*aroL*::FRT-*cat*-FRT was designated as JJ4*kan*.

E. coli JJ4

The genomic chloramphenicol marker was excised by the same protocol for generating *E. coli* BW25113 Δ*serA*::FRT. Thermal induction of the Flp recombinase in JJ4*cat*/pCP20 excised the chloramphenicol marker and afforded strain JJ4 (RB791 *serA::aroB* Δ*aroL*::FRT). The loss of the antibiotic marker gene was verified by PCR analysis using primers 5'- CGGAATTCATGG-ATGTTACCGCAAAATAC and 5'- CGGAATTCTCAGGCACCGAACCCCAT and afforded 0.2 kb DNA fragment for the mutant and 0.6 kb DNA fragment for the control strain RB791 *serA::aroB*. Phenotype was also confirmed by growth on selective plates: no growth on LB/Ap, LB/Cm, M9/Glucose; growth on LB and M9/Glucose/Serine.

JJ5*cat*

E. coli JJ5*cat* was made from *E. coli* JJ3 by P1 phage-mediate transduction using *E. coli* JJ4*cat* as the donor strain. Colonies were plated on selective LB/Cm plates. The resulting colonies were screened for Δ*aroL*::FRT-*cat*-FRT mutation by PCR analysis using following primers: 5'- ACCTATTGGGGAAAACCCACG and 5'- TTAAGTAT-AGGCGCTCGAAAA; and afforded 1.2 kb DNA fragment for the mutant and 0.6 kb DNA fragment for the control strain RB791 *serA::aroB*. Colonies also were screened for Δ*aroK*::FRT mutation using following primers: 5'- GCTCTAGATTTCCAG-

167

TGAGTAAACAGCC and 5'- GCTCTAGACCATAACGCGACATCCACCT and afforded 0.5 kb DNA fragment for the mutant and 1 kb DNA fragment for the control strain RB791 *serA::aroB*. Phenotype was also confirmed by growth on selective plates: no growth on LB/Ap, M9/Glucose, M9/Glucose/Serine, M9/Glucose/Aromatics; growth on LB/Cm and M9/Glucose/Aromatics/Serine. The *E. coli* RB791 *serA::aroB* Δ*aroK*::FRT Δ*aroL*::FRT-*cat*-FRT was designated as JJ5*cat*. ·

JJ5

The genomic chloramphenicol marker was excised by the same protocol for generating *E. coli* BW25113 Δ*serA*::FRT. Thermal induction of the Flp recombinase in JJ5*cat*/pCP20 excised the chloramphenicol marker and afforded strain JJ5 (RB791 *serA::aroB* Δ*aroK*::FRT Δ*aroL*::FRT). The resulting colonies were screened for Δ*aroL*::FRT mutation by PCR analysis using following primers: 5'- ACCTATTGGGGAAAACCCACG and 5'- TTAAGTAT-AGGCGCTCGAAAA; and afforded 0.2 kb DNA fragment for the mutant and 0.6 kb DNA fragment for the control strain RB791 *serA::aroB*. Colonies also were screened for Δ*aroK*::FRT mutation using following primers: 5'- GCTCTAGATTTCCAG-TGAGTAAACAGCC and 5'- GCTCTAGACCATAACGCGACATCCACCT and afforded 0.5 kb DNA fragment for the mutant and 1 kb DNA fragment for the control strain RB791 *serA::aroB*. Phenotype was also confirmed by growth on selective plates: No growth on LB/Ap, LB/Cm, M9/Glucose, M9/Glucose/Serine, M9/Glucose/Aromatics; growth on LB and M9/Glucose/Aromatics/Serine.

Genomic DNA library of *Gluconobacter oxydans* IFO 3244

Genomic DNA of *G. oxydans* IFO3244 was isolated using genomic DNA isolation kit available from Qiagen. Genomic DNA was partially digested with *Bam*HI restriction endonuclease into approximately 0.5-10 kb DNA size. Genomic DNA library was ligated into pBluescrip SK (-) vector previously pretreated with *Bam*HI followed with CIAP. Ligation mixture was transformed into electrocompetent *E. coli* AB2834 and selected on M9/Glucose plate at 37 °C for 48 h. Plasmids from two colonies were isolated and designated as pBlue IFO3244 #1 and #2.

Plasmid pJJ5.151

This 5.8-kb plasmid was constructed by ligation the open reading frame (ORF) of *ydiN* into the *Eco*RI and *Pst*I (underlined nucleotides) site of pKK223-3. The *ydiN* ORF was amplified from *E. coli* W3110 genomic DNA using the following primers: 5'-CG<u>GAATTC</u>ATGTCTCAAAATAAGGCTT as the forward primer, and 5'-AA<u>CTGCAG</u>TTAACCTCTATGCTTAATTG as the reverse primer. Localization of the resulting 1.2-kb fragment into pKK223-3, which had been previously treated with *Eco*RI, *Pst*I followed by CIAP afforded pJJ5.151, where *ydiN* ORF is transcribed from P_{tac} promoter.

Plasmid pJJ5.164

The construction of 9.3-kb plasmid pJJ5.164 started from amplification of $P_{tac}ydiN$ fragment from pJJ5.151 plasmid using the following primers: 5'-ACGCGTCGACGGAGCTTATCGACTGCACG as the forward primer and 5'-GGCGGTCCGTTTAAGACAA as the reverse primer. Plasmid pKD12.112 was

linerized with *Sal*I and treated with Klenow followed by CIAP. Resulted linerized plasmid was ligated with 1.6-kb PCR product, which had been previously treated with Klenow.

Plasmid pJJ5.165

Plamsid pJJ5.164 was digested with *Xba*I restriction endonuclease and treated with Klenow followed by CIAP. A 2.2-kb *tktA*-encoding fragment was liberated from pNR8.146A by digestion with *Bam*HI and treated with Klenow. Insertion of the *tktA* fragment into linerized pJJ5.164 yielded a 11.5-kb plasmid pJJ5.165.

REFERENCES

1   Pittard, J.; Wallace, B. J. Distribution and function of genes concerned with aromatic biosynthesis in *Escherichia coli. J. Bacteriol.* **1966**, *91*, 1494-1508.

2   Li, K.; Mikola, M. R.; Draths, K. M.; Worden, R. M.; Frost, J. W. Fed-batch fermentor synthesis of 3-dehydroshikimic acid using recombinant *Escherichia coli. Biotechnol. Bioeng.* **1999**, *64*, 61-73.

3   Draths, K. M.; Knop, D. R.; Frost, K. M. Shikimic acid and quinic acid: replacing isolation from plant sources with recombinant biocatalysis. *J. Am Chem. Soc.* **1999**, *121*, 1603-1604.

4   Knop, D. R.; Draths, K. M.; Chandran, S. S.; Barker, J. L.; von Daeniken, R.; Weber, W.; Frost, J. W. Hydroaromatic equilibration during biosynthesis of shikimic acid. *J. Am. Chem. Soc.* **2001**, *123*, 10173-10182.

5   Brosius, J.; Holy, A. Regulation of ribosomal RNA promoters with a synthetic lac operator. *Proc. Natl. Acad. Sci. U.S.A.* **1984**, *81*, 6929-6933.

6   Bartolome, B.; Jubete, Y.; Martinez, E.; de la Cruz, F. Construction and properties of a family of pACYC184-derived cloning vectors compatible with pBR322 and its derivatives. *Gene* **1991**, *102*, 75-78.

7   Ran, N. Synthesis of aromatics and hydroaromatics from D-glucose via a native and a variant of the shikimate pathway. *Ph.D. Dissertation*, Michigan State University, **2004**.

8   LØbner-Olesen, A.; Marinus, M. G. Identification of the gene (*aroK*) encoding shikimic acid kinase-I of *Escherichia coli. J. Bacteriol.* **1992**, *174*, 525-529.

9   Yi, J.; Draths, K. M.; Li, K.; Frost, J. W. Altered glucose transport and shikimate pathway product yields in *E. coli. Biotechnol. Prog.* **2003**, *19*, 1450-1459.

10 Chandran, S. S.; Yi, J.; Draths, K. M.; von Daeniken, R.; Weber, W.; Frost, J. W. Phosphoenolpyruvate availability and the biosynthesis of shikimic acid. *Biotechnol. Prog.* **2003**, *19*, 808-814.

11 Chandran, S. S. Manipulation of the genes and enzymes of the shikimate pathway. *Ph.D. Dissertation.* Michigan State University, **2000**.

12 Datsenko, K.A.; Wanner, B.L. One-step inactivation of chromosomal genes in *Escherichia coli* K-12 using PCR products. *Proc. Natl. Acad. Sci. USA.* **2000**, *97*, 6640-6645.

13   Cherepanov, P. P.; Wackernagel, W. Gene disruption in *Escherichia coli*: TcR and KmR cassettes with the option of Flp-catalyzed excision of the antibiotic-resistance determinant. *Gene* **1995**, *158*, 9-14.

14   Posfai, G., Koob, M.D., Kirkpatrick, H.A., Blattner, F.R. Versatile insertion plasmids for targeted genome manipulations in bacteria: isolation, deletion, and rescue of the pathogenicity island LEE of the *Escherichia coli* O157:H7 genome. *J. Bacteriol.* **1997**, *179*, 4426-4428.

15   Jancauskas, J. Strategies for improving synthesis of 3-dehydroshikimic acid and shikimic acid from D-glucose. M.S. thesis. *Michigan State University*, **2006**.

16   Miller, J. H. *Experiments in molecular genetics*; Cold Spring Harbor Laboratory: Plainview, NY, 1972.

17   Yi, J.; Li, K.; Draths, K. M.; Frost, J. W. Modulation of phosphoenolpyruvate synthase expression increases shikimate pathway product yields in *E. coli*. *Biotechnol. Prog.* **2002**, *18*, 1141-1148.

18   Sambrook, J.; Fritsch, E. F.; Maniatis, T. *Molecular cloning: A laboratory manual*; Cold Spring Harbor Laboratory: Plainview, NY, 1990.

19   Pitcher, D. G.; Saunders, N. A.; Owen, R. J. Rapid extraction of bacterial genomic DNA with guanidium thiocyanate. *Lett. Appl. Microbiol.* **1989**, *8*, 151-156.

20   Miller, J. H. *A short course in bacterial genetics*; Cold Spring Harbor Laboratory: Plainview, NY, 1992.

21   Bradford, M. M. A Rapid and sensitive method for the quantitation of microgram quantities of protein utilizing the principle of protein-dye binding. *Anal. Biochem.* **1976**, *72*, 248-254.

22   Coggins, J. R.; Boocock, M. R.; Chaudhuri, S.; Lambert, J. M.; Lumsden, J.; Nimmo, G. A.; Smith, D. D. S. The *arom* multifunctional enzyme from *Neurospora crassa*. *Meth. Enzymol.* **1987**, *142*, 325-341.

23   Chaudhuri, S.; Anton, I. A.; Coggins, J. R. Shikimate dehydrogenase from *Escherichia coli*. *Methods Enzymol.* **1987**, *142*, 315-319.

24   Davis, B. D.; Gilvarg, C.; Mitsuhashi, S. Enzymes of aromatic biosynthesis: quinic dehydrogenase from *Aerobacter aerogenes*. *Methods Enzymol.* **1955**, *2*, 307-311.